

OPTIMIZING THE DETECTION OF CORTICOMUSCULAR
COHERENCE (CMC) WITH THE USE OF EEG AND EMG
RECORDINGS: APPLICATION FOR NORMAL SUBJECTS
AND PATIENTS

Katherina von Carlowitz-Ghori

OPTIMIZING THE DETECTION OF CORTICOMUSCULAR
COHERENCE (CMC) WITH THE USE OF EEG AND EMG
RECORDINGS: APPLICATION FOR NORMAL SUBJECTS
AND PATIENTS

vorgelegt von
Katherina von Carlowitz-Ghori, M.Sc.
geb. in Mainz

von der Fakultät IV - Elektrotechnik und Informatik
der Technischen Universität Berlin
zur Erlangung des akademischen Grades

Doktorin der Naturwissenschaften
- Dr. rer. nat. -

genehmigte Dissertation

Promotionsausschuss:

Vorsitzender: Prof. Dr. Benjamin Blankertz
Gutachter: Prof. Dr. Klaus-Robert Müller
Gutachter: Prof. Dr. Gabriel Curio
Gutachter: Dr. Vadim Nikulin
Gutachterin: Dr. Maria Herrojo Ruiz

Tag der wissenschaftlichen Aussprache: 08. Februar 2016

Berlin 2016

To my children

Abstract

The work of this thesis is centered around corticomuscular coherence (CMC), a neurophysiological phenomenon that refers to the phase synchronization between cortical and muscular activity. Aiming at improving the detection of CMC both in healthy subjects and in stroke patients, this thesis introduces the new method regression CMC (R-CMC) for the extraction of spatial filters that optimize the coherence. The R-CMC method thereby outperformed other conventional methods such as Laplacian filtering in terms of CMC amplitude measures and sensitivity with respect to recovering relevant sources. The thesis further provides empirical evidence against the full-wave EMG rectification, a commonly used but highly disputed pre-processing step in CMC analysis. Moreover, this thesis addresses basic neurophysiological questions in healthy subjects, such as the role of local and distal neuronal synchronization in corticospinal interaction. Here, it was shown that amplitude-envelope correlations may serve as a complementary measure of non-linear relationship. We also applied the R-CMC method in a clinical setting. In stroke patients, experiments were performed both directly after the stroke and 6 months later to obtain a CMC pattern at different stages of motor recovery and to identify cortical areas that are relevant for establishing a strong CMC. Building on the knowledge gained from offline recordings, CMC was used in the form of a neurofeedback, where online CMC was visualized enabling subjects to learn how to modify their CMC strength and thus voluntarily control the efficacy of corticomuscular interactions. The results contribute to neurophysiological understanding and open up new perspectives for clinical application by providing a basis for a novel motor rehabilitation approach in stroke patients: using CMC neurofeedback could allow associating CMC strength with certain motor commands, and thereby facilitating the process of motor recovery.

Zusammenfassung

Im Mittelpunkt dieser Arbeit steht die kortikomuskuläre Kohärenz (englisch corticomuscular coherence, Abk.: CMC), ein neurophysiologisches Phänomen, das sich auf die Phasensynchronisation zwischen kortikaler und muskulärer Aktivität bezieht. Mit dem Ziel, die Erkennung von CMC sowohl bei gesunden Probanden/innen als auch bei Schlaganfallpatienten/innen zu verbessern, stellt diese Arbeit die neue Methode regression-CMC (R-CMC) zur Extrahierung räumlicher Filter, die die Kohärenz optimieren, vor. Die R-CMC-Methode übertraf dabei andere übliche Methoden wie Laplace-Filter im Bezug auf CMC-Amplitudenwerte und Sensibilität bei der Wiederherstellung relevanter Quellsignale. Diese Arbeit liefert desweiteren empirische Hinweise gegen die Vollwellen-Rektifikation des EMG-Signals, ein weit verbreiteter und zugleich kontrovers diskutierter Schritt bei der Vorverarbeitung der Daten in der CMC-Analyse. Außerdem geht diese Arbeit auf grundsätzliche neurophysiologische Fragen bei gesunden Probanden/innen ein, wie die Rolle von lokaler und distaler Synchronisation bei der kortikomuskulären Interaktion. Hier wurde gezeigt, dass die Korrelation der Amplitudenhüllkurven ein ergänzendes Maß nonlinearer Zusammenhänge darstellen könnte. Die R-CMC-Methode wurde auch in klinischer Umgebung angewendet: Bei Schlaganfallpatienten/innen wurden Experimente sowohl direkt nach dem Schlaganfall als auch 6 Monate später durchgeführt, um ein CMC-Muster in verschiedenen Stadien der Wiedererlangung motorischer Fähigkeiten zu erhalten und die kortikalen Areale zu identifizieren, die relevant für die Erzeugung einer starken CMC sind. Basierend auf dem Wissen der offline-Messungen, wurde CMC in Form eines Neurofeedbacks angewendet, bei dem CMC online visualisiert wurde, sodass Probanden/innen in der Lage waren, die Stärke ihrer CMC zu beeinflussen und damit die Effizienz kortikomuskulärer Interaktion willentlich zu steuern. Die Ergebnisse tragen zum neurophysiologischen Verständnis bei und eröffnen neue Perspektiven zur klinischen Anwendung, indem sie eine Grundlage für einen neuartigen Rehabilitationsansatz bei Schlaganfallpatienten/innen bieten: CMC-Neurofeedback könnte es ermöglichen, die CMC-Stärke

mit bestimmten motorischen Befehlen in Verbindung zu bringen und dabei den Prozess der motorischen Genesung zu erleichtern.

Acknowledgments

It is a great pleasure to thank my advisers, colleagues, friends and family who accompanied and supported me on the long road to this dissertation. This dissertation would not have been possible without them. I know this list cannot be complete. Many more people who I do not mention gave me inspiration, support and encouragement during the past years.

First of all, I am truly grateful to Vadim Nikulin for the exceptional support and guidance throughout these years. I could greatly benefit from his knowledge, ideas and encouragement. Furthermore, I would like to thank Gabriel Curio for his support, advice and inspiring discussions, which often provided a new angle of view. I am particularly thankful for the opportunity to work on the project on neuroscience and media in Bonn, where I gained new experiences outside research. I would like to show my gratitude to Klaus-Robert Müller for his advice and supervision. Many thanks also to Maria Herrojo Ruiz, who agreed to be an external referee.

I want to extend my thanks to the members of the Neurophysics group who had been amazing colleagues. I am especially grateful to Zübeyir Bayraktaroglu who I worked with in the CMC project for sharing his experience. Thank you Friederike Hohlefeld, Gunnar Waterstraat, Tommaso Fedele, Natalie Schaworonkow, Irene Sturm, Bartosz Telenczuk, Jewgeni Kegeles, Manfred Gugler, Florian Losch, Birgit Nierula and Dominik Koller for helping with experiment preparations and for engaging science and not-science related conversations during and between coffee and lunch breaks.

Finally, I would like to thank my parents for their unconditional support, my husband Adnan Ghori for being by my side and our two sons for many little and great moments of joy.

Contents

1. Introduction	1
1.1. Outline of the Thesis	2
1.2. Scientific Contributions	4
1.3. List of all publications	6
2. Background	8
2.1. Neurophysiological basis of corticomuscular coherence	9
2.1.1. Control of voluntary muscle movement	9
2.2. Synchronization as binding mechanism over distance	12
2.2.1. Coherence and phase synchronization	12
2.2.2. Amplitude dynamics	15
2.3. Factors influencing CMC strength and frequency	18
2.3.1. Effects of motor behavior and cognition	18
2.3.2. Afferent mechanisms	19
2.3.3. Developmental changes	21
2.3.4. CMC in stroke and other movement disorders	22
2.4. Functional role of CMC	22
2.5. Further methodological aspects of analysis	24
2.5.1. Rectification of surface EMG as pre-processing step	24
2.5.2. Principal Component Analysis	26
2.5.3. Spatial filters and patterns	28
2.5.4. Multiple Linear Regression	29
3. Methodology for optimal detection of CMC and Rectification	34
3.1. Update on the EMG-rectification debate	45
3.2. Limitations and outlook	46

4. Amplitude modulation in cortico-spinal interaction	49
4.1. Limitations and outlook	60
5. CMC in stroke	61
5.1. Limitations and outlook	72
6. Neurofeedback on the basis of CMC	74
6.1. Limitations and outlook	87
7. Summary and Conclusion	90
8. Bibliography	94
List of Figures	108
A. Experimental setup	111

The phenomenon of corticomuscular coherence (CMC)¹ is a well established neurophysiological measure which relates to the coupling between cortical activity and motor neuron firing (Conway et al., 1995). CMC occurs (mostly) within the beta-frequency range during sustained muscle contraction but is absent during the movement phase (Kilner et al., 2000; Riddle and Baker, 2006); it can be measured using electroencephalography (EEG) or magnetoencephalography (MEG) and electromyography (EMG) to access cortical and muscle activity, respectively. Figure 1.1 gives an example of such a CMC spectrum obtained with EEG/EMG.

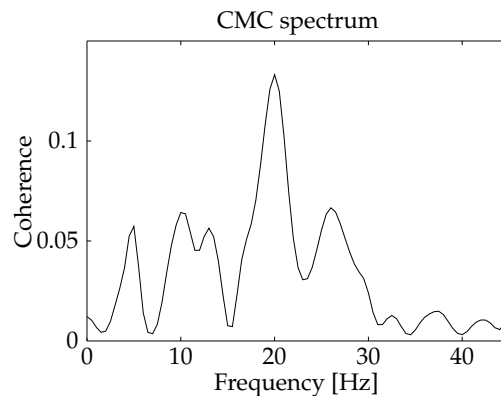


Figure 1.1.: Coherence spectrum peaking around 20 Hz. Signals were measured between EEG (channel C3) and EMG (channel on the APB muscle) during sustained contraction of the right thumb.

While its general importance in fine motor control is widely accepted (e.g. Baker, 2007), the underlying neurophysiological mechanisms leading to the formation of CMC remain largely unknown. A better understanding of CMC and its functional role could

¹within the included papers *corticomuscular coherence* is also spelled *cortico-muscular coherence* or referred to as *EEG-EMG coherence*

also contribute to an improvement of therapy in clinical conditions where CMC is altered. This relates to e.g. stroke where many patients suffer from a persistent motor dysfunction such as motor paresis (Rathore et al., 2002). Our knowledge on neuroplasticity in the motor system could be improved by identifying the functional relevant contribution of reorganized cortical areas as measured by CMC. Elucidating mechanisms related to motor disabilities would help developing better rehabilitation approaches and support motor recovery after stroke.

Although, CMC has been quite extensively studied in healthy people, its role in stroke recovery is less explored. The description of CMC behavior in stroke, particular at acute stage, is crucial for the understanding of CMC. Its proper description thereby benefits from methods optimized for its detection. Optimal detection relates also to the question whether to apply the controversially discussed pre-processing step of EMG rectification. In addition, measures of non-linear relationships can complement our knowledge of corticospinal interaction. Building on the knowledge of CMC behavior in stroke recovery, one can develop new rehabilitation approaches to support the recovery process. Here, neurofeedback could provide an interesting tool that allows the access to one's own brain activity and manipulate it in order to facilitate the recovery process.

1.1. Outline of the Thesis

Chapter 2 provides the background for the following chapters which are assigned to one publication each. Besides the neurophysiological basis, this chapter includes the theoretical signal processing and machine learning foundations of coherence estimation and other methodological aspects of relevance for the subsequent chapters. Moreover, it gives a comprehensive overview of the phenomenon of CMC including influencing factors, functional role and neuropathological conditions.

A fundamental factor of the project is to optimally detect CMC in offline analysis as well during real-time CMC-neurofeedback. Chapter 3 introduces the newly developed procedure regression corticomuscular coherence (R-CMC) for the extraction of spatial filters which allow to obtain the maximized coherence between cortical and muscle activity. The method was published in '*Optimal imaging of cortico-muscular coherence through a novel regression technique based on multi-channel EEG and un-rectified EMG*' (Bayraktaroglu et al., 2011). Another important aspect of this publication is related to the current dispute in CMC research, namely the use of EMG rectification. Traditionally, the EMG signal is rectified before coherence analysis. However until recently its justification was neither thoroughly tested experimentally nor theoretically. In Bayraktaroglu et al.

(2011), the effect of EMG rectification on CMC estimation was examined with experimental data comparing different approaches including the R-CMC method.

In addition, to exploring phase-locking between cortical and muscle activity, Chapter 4 of this thesis aimed at studying how local neuronal interaction in the motor cortex can be reflected in the local activity at the spinal cord (as indirectly measured on the basis of muscle activity). In *'It is not all about phase: Amplitude dynamics in corticomuscular interactions'* (Bayraktaroglu et al., 2013) the correlation of amplitude modulations between beta oscillations in the sensorimotor cortex and the hand muscle was investigated. These amplitude dynamics might convey additional information on how local neuronal dynamics at the cortical and spinal cord levels relate to each other.

There are only a few stroke-related CMC studies, which were all performed at the chronic stage, mostly at least one year after the stroke when many compensatory processes already took place. Longitudinal CMC studies following stroke patients from acute to chronic period could provide new insight into the temporal evolution of corticomuscular interaction after stroke and add to the understanding of mechanisms underlying motor recovery. In Chapter 5, the study *'Corticomuscular coherence in acute and chronic stroke'* (von Carlowitz-Ghori et al., 2014) examined for the first time the changes in the dynamics of corticomuscular interaction both at acute and early chronic stage of stroke.

On the basis of the experiments for offline CMC detection, the aim was to develop a paradigm for online CMC monitoring which could be used as a visual neurofeedback in a novel rehabilitation approach for motor recovery. It is not known whether (without changing motor output parameters) CMC can be voluntarily modified by intrinsically learning to associate the CMC strength with a certain activation pattern using mental imagery. In *'Voluntary control of corticomuscular coherence through neurofeedback: a proof-of-principle study'* (von Carlowitz-Ghori et al., 2015), Chapter 6, we show that healthy people are able to voluntarily modify their CMC strength using neurofeedback independent of motor output parameters.

The final Chapter 7 provides a summary of the papers and their relation to each other and a conclusion of this thesis.

The experimental setup was only slightly varied between the series of studies; for illustrative purposes additional pictures of the setup are provided in Appendix A.

1.2. Scientific Contributions

Objectives The work of this thesis is driven by the following main objectives which are also depicted in Figure 1.2:

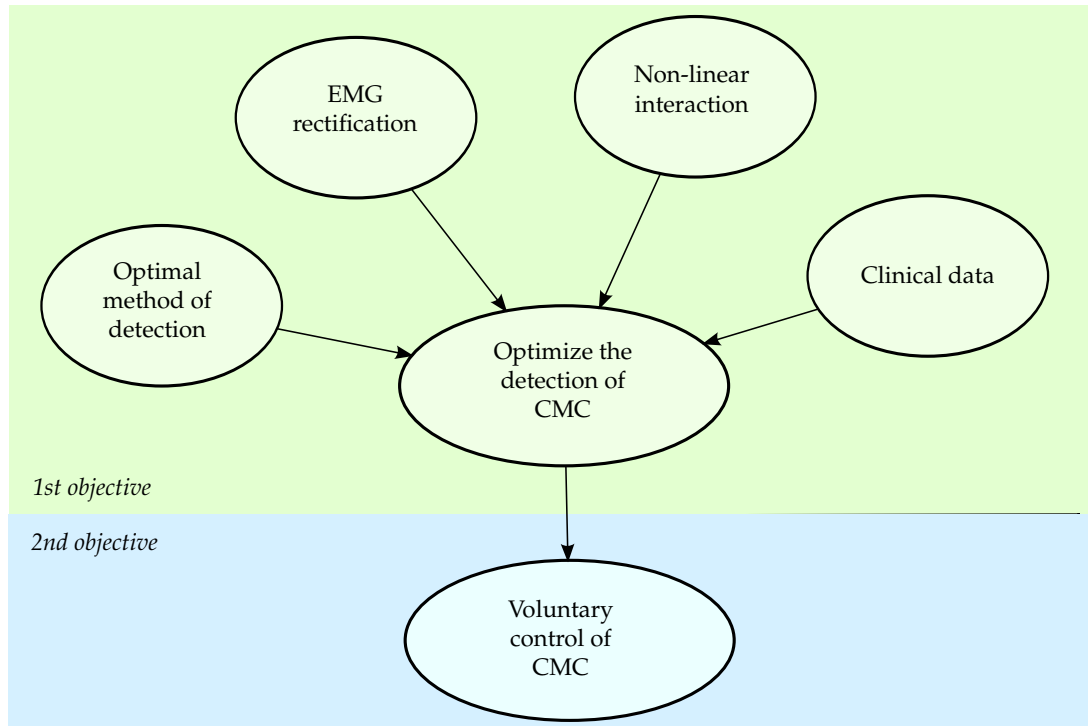


Figure 1.2.: Objectives

1. Optimize the detection of CMC. This objective was fundamental to all four publications of this thesis and comprised
 - An appropriate method to improve the detection of CMC first offline and later also online for instantaneous feedback.
 - Empirically addressing the dispute of EMG rectification as pre-processing step
 - Testing for the existence of non-linear relationships in corticospinal interactions.
 - The inclusion of clinical (stroke) data to gain knowledge about CMC behavior in motor recovery.

2. Voluntarily control CMC. This thesis aimed at showing the feasibility of CMC manipulation by means of mental strategies, i.e. in a neurofeedback paradigm. This objective was subject to the last paper.

Achievements The current thesis is submitted as cumulative work and based on the following publications in peer-review journals:

- I) Bayraktaroglu, Z., von Carlowitz-Ghori, K., Losch, F., Nolte, G., Curio, G., and Nikulin, V. V. (2011). Optimal imaging of cortico-muscular coherence through a novel regression technique based on multi-channel EEG and un-rectified EMG. *NeuroImage*, 57(3):1059-1067. (Chapter 3), doi: 10.1016/j.neuroimage.2011.04.071
- II) Bayraktaroglu, Z., von Carlowitz-Ghori, K., Curio, G., and Nikulin, V. V. (2013). It is not all about phase: Amplitude dynamics in corticomuscular interactions. *NeuroImage*, 64:496-504. (Chapter 4), doi: 10.1016/j.neuroimage.2012.08.069
- III) von Carlowitz-Ghori, K., Bayraktaroglu, Z., Hohlefeld, F. U., Losch, F., Curio, G., and Nikulin, V. V. (2014). Corticomuscular coherence in acute and chronic stroke. *Clinical Neurophysiology*, 125(6):1182-1191. (Chapter 5), doi: 10.1016/j.clinph.2013.11.006
- IV) von Carlowitz-Ghori, K., Bayraktaroglu, Z., Waterstraat, G., Curio, G., Nikulin, V. V. (2015). Voluntary control of corticomuscular coherence through neurofeedback: A proof-of-principle study in healthy subjects. *Neuroscience*, 290:243-254. (Chapter 6), doi: 10.1016/j.neuroscience.2015.01.013

For paper I, the first two authors conducted experiments, analysis was performed by the first author, I contributed with ideas and discussion to study design and manuscript. The subjects of paper II were largely identical with subjects in paper I, analysis was performed by the first author, I contributed with ideas and discussion to study design and manuscript.

The healthy subjects in paper III were largely identical with the subjects of the papers I and II, both first authors conducted the experiments in stroke patients and performed analysis, I wrote the manuscript.

For paper IV, I designed the study, performed measurements and analysis, and wrote the manuscript, co-authors contributed with ideas and discussion to study design and manuscript, the third author helped with experiment preparation.

1.3. List of all publications

The following list contains all publications (co-)authored by me.

Journal articles

1. von Carlowitz-Ghori, K. M. B., Hohlefeld, F. U., Bayraktaroglu, Z., Curio, G., and Nikulin, V. V. (2011). Effect of complete stimulus predictability on P3 and N2 components: an electroencephalographic study. *Neuroreport*, 22(9):459-463
2. Bayraktaroglu, Z., von Carlowitz-Ghori, K., Losch, F., Nolte, G., Curio, G., and Nikulin, V. V. (2011). Optimal imaging of cortico-muscular coherence through a novel regression technique based on multi-channel EEG and un-rectified EMG. *NeuroImage*, 57(3):1059-1067.
3. Bayraktaroglu, Z., von Carlowitz-Ghori, K., Curio, G., and Nikulin, V. V. (2013). It is not all about phase: Amplitude dynamics in corticomuscular interactions. *NeuroImage*, 64:496-504.
4. von Carlowitz-Ghori, K., Bayraktaroglu, Z., Hohlefeld, F. U., Losch, F., Curio, G., and Nikulin, V. V. (2014). Corticomuscular coherence in acute and chronic stroke. *Clinical Neurophysiology*, 125(6):1182-1191.
5. von Carlowitz-Ghori, K., Bayraktaroglu, Z., Waterstraat, G., Curio, G., Nikulin, V. V. (2015). Voluntary control of corticomuscular coherence through neurofeedback: A proof-of-principle study in healthy subjects. *Neuroscience*, 290:243-254.

Contribution to conferences

1. Bayraktaroglu, Z., von Carlowitz-Ghori, K., Curio, G., Losch, F., Nolte, G., Nikulin, V. V. (2011). Rectification of surface EMG impairs cortico-muscular coherence estimation, DGKN, Münster, Germany.
2. Bayraktaroglu, Z., von Carlowitz-Ghori, K., Losch, F., Nolte, G., Curio, G., Nikulin, V. V. (2011). Rectification of EMG reduces cortico-muscular coherence: multichannel EEG study. ECCN, Rome, Italy.
3. Bayraktaroglu, Z., von Carlowitz-Ghori, K., Curio, G., Nikulin, V. (2012). Amplitude dynamics in corticospinal interactions. DGKN, Köln, Germany.

4. von Carlowitz-Ghori, K., Bayraktaroglu, Z., Hohlefeld, F. U., Losch, F., Curio, G., and Nikulin, V. V. (2014). Corticomuscular Coherence in Acute and Chronic Stroke. DGKN, Berlin, Germany.
5. von Carlowitz-Ghori, K., Bayraktaroglu, Z., Waterstraat, G., Curio, G., Nikulin, V. V. (2014). Neurofeedback based on corticomuscular coherence. HBMO, Hamburg, Germany.

Background 2

In 1995, Conway et al. (1995) were the first to demonstrate the phenomenon of CMC in a systematic study with human subjects using MEG and EMG. Further studies in humans followed using (whole-scalp) MEG (Salenius et al., 1997), EEG (Halliday et al., 1998) and local field potential (LFP) recordings in monkeys (Baker et al., 1997).

CMC relates to the synchronization between muscle activity and the activity over the (contralateral) sensorimotor cortex. There is a clear distinction between sources relating to hand and foot; for different upper limb muscles there were no differences in spatial location detectable (Salenius et al., 1997). Some studies found phase lags between cortex and muscle that were in agreement with the conduction velocity from cortex to muscle (Salenius et al., 1997) while other studies did not (Riddle and Baker, 2005).

CMC occurs predominantly in the beta frequency range (13-30 Hz) during isometric contraction but some healthy subjects show CMC also in the alpha frequency band (Mima et al., 1999; Ushiyama et al., 2011b). In contrast, CMC in the gamma-band was assigned a different functional significance (See Section 2.3.1 for more details). CMC shows both a large within-subject variability (Pohja et al., 2005) and between-subject variability (Ushiyama et al., 2011b). Particularly the strength of CMC can vary substantially between different days; the peak frequency is more stable (Pohja et al., 2005). Interestingly, there seems to be no effect of handedness (Schoffelen et al., 2011; von Carlowitz-Ghori et al., 2011). However, several behavioral and cognitive factors can influence CMC strength and frequency which are reviewed in Section 2.3.1.

While CMC is broadly seen as a mechanism of the motor system that plays a role in fine motor control, its exact functional role remains unclear (more details on potential roles will be given in section 2.4).

2.1. Neurophysiological basis of corticomuscular coherence

2.1.1. Control of voluntary muscle movement

Voluntary interaction with the environment is one of the main functions of the brain. The motor cortex which is situated in the frontal lobe of the cerebral cortex, plays a critical role in planning, control and execution of voluntary movement. Here the abstract plan of action is converted to motor commands. To perform the movement accurately, external sensory information has to be continuously integrated (Kalaska and Rizzolatti, 2012; Dum and Strick, 2002; Rizzolatti and Luppino, 2001). In primates, voluntary movement is mediated by direct, monosynaptic projections from the motor cortex onto motor neurons in the spinal cord enabling skillful hand and relatively independent finger movement control. These motor neuron fibers, of which 30-40% originate in the primary motor cortex, form the major descending pathway for voluntary motor activity, the corticospinal tract, also called the pyramidal tract. In the medulla oblongata, most descending fibers cross to the opposite side at the pyramidal decussation; about 10% of the fibers remain uncrossed until the spinal cord (Amaral, 2012; Lemon, 2008).

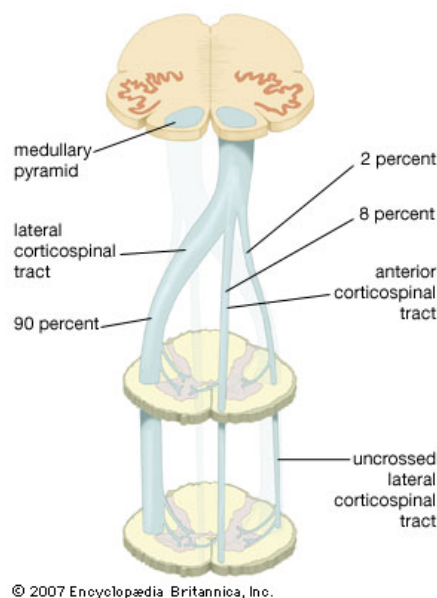


Figure 2.1.: Pyramidal decussation and the formation of the corticospinal tract in the spinal cord. Retrieved from <http://www.britannica.com/EBchecked/media/48418/The-decussation-of-the-medullary-pyramids-and-the-formation-of>

From motor unit firing to surface EMG Muscle activity is regulated by the recruitment of motor units. A motor unit (MU) denotes a motor neuron and the group of muscle fibers it innervates and constitutes the basic functional unit for the control of movement. The number of innervated fibers can vary substantially with muscle type and function; the smaller the number, the finer the control that can be achieved by varying the number of activated MUs. The force exerted by a muscle depends (not only) on the number of activated MUs (Burke, 1975; Enoka and Pearson, 2012; Monti et al., 2001). When a motor neuron generates an action potential (AP), neurotransmitters are released leading to an action potential in the muscle fibers. The action potentials in all fibers of a MU occur almost simultaneously adding to extracellular currents which sum up to generate a field potential. Most contractions involve the activation of many MUs, whose currents produce signals that can be detected by surface electromyography (EMG), i.e. an electrode placed on the skin (see Figure 2.2 for an example of an EMG signal during voluntary muscle contraction). EMG signals essentially consist of the superimposed motor unit action potentials (MUAPs). The timing and amplitude of EMG signal therefore reflects the activation of muscle fibers by the motor neurons (Enoka and Pearson, 2012).

Besides the number activated MUs, MU firing rates modulate the strength of muscle contraction. The rates at which a MU fires ranges between 6-35 Hz (Freund, 1983); only in certain cases and for a short time firing rates up to 50 Hz are reached (Mima and Hallett, 1999a).

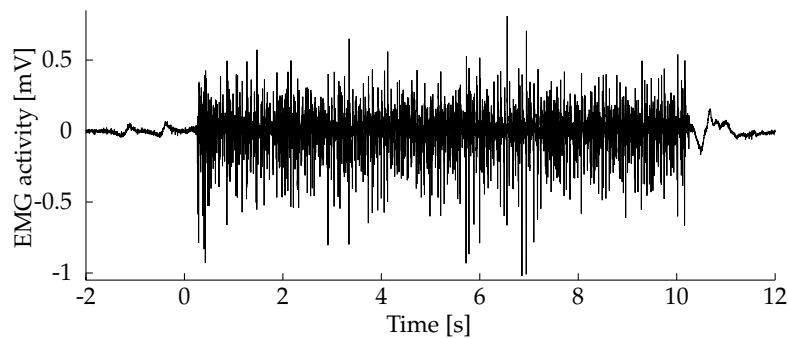


Figure 2.2.: EMG signal during voluntary muscle contraction in the interval around 0-10 s

Oscillatory activity in the sensorimotor cortex Oscillatory or rhythmic activity can be observed with EEG or MEG and subserves important functions in the brain. Ongoing oscillations are traditionally subdivided into five frequency bands: delta (0.5-3.5

2. Background

Hz), theta (4-7 Hz), alpha (8-12 Hz), beta (13-30 Hz) and gamma (30-70 Hz), as displayed in Fig. 2.3. Oscillatory activity in these different frequency bands are thought to have distinct physiological roles and have been assigned to specific perceptual, sensorimotor or cognitive operations.

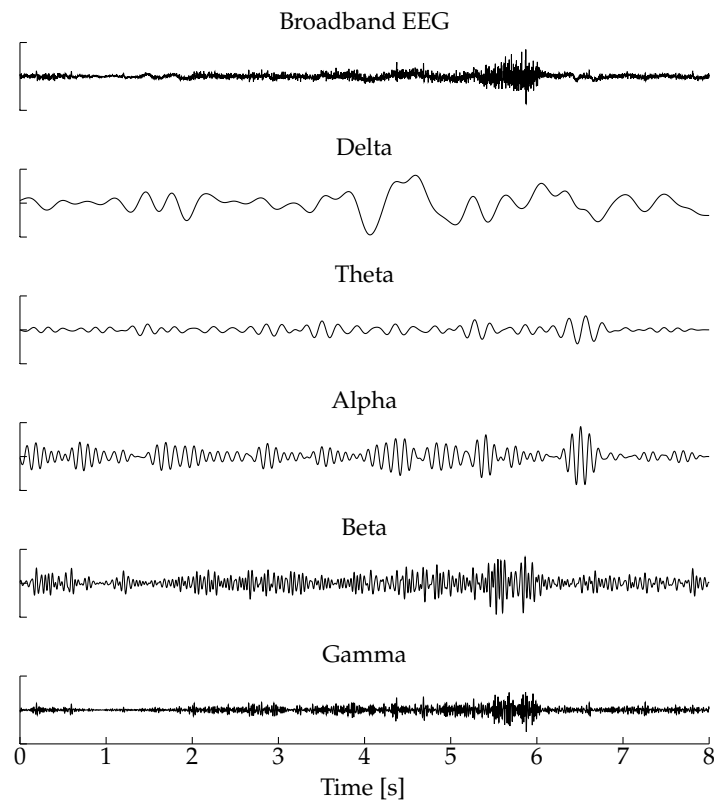


Figure 2.3.: Frequency bands of the EEG signal. From the top down: the original signal; the signal after digital filtering with bandpass filters 0.5–3.5 Hz (delta), 4–7 (theta), 8–12 Hz (alpha), 13–30 (beta) and 30–70 Hz (gamma).

Beta-band oscillations have been linked to motor functions being pronounced during steady contractions, especially during periods of holding directly following phasic movements and they are attenuated by voluntary movements (Baker, 2007; Baker et al., 1997). Interestingly they are also inhibited by motor imagery (Schnitzler et al., 1997; De Lange et al., 2008), which is of particular relevance for brain-computer interfaces (BCIs). While beta rhythms, which are observed in all parts of the motor system, have been related to a steady motor state, during the preparation and the actual execution

of movements, faster rhythms in the gamma-band are predominating. Therefore, beta oscillations were suggested to be an 'idling' rhythm, a resting state of the neurons in the motor area (Pfurtscheller et al., 1996). More recently, however, Engel and Fries (2010) promoted the idea of beta oscillations as active process to maintain the existing motor set while preventing neuronal processing of new movements. Further, the authors suggest a similar functional role of beta-band activity also in cognitive processing. At the same time, abnormal enhancement of beta-band activity would result in a abnormal persistence of the current state, as it is the case in Parkinson's disease, leading to a declined flexible behavior and cognitive control. It remains unclear through which mechanisms, beta-band oscillations inhibit changes and promote the maintenance of the current motor set (Engel and Fries, 2010).

2.2. Synchronization as binding mechanism over distance

Synchronization of neural oscillatory activity is thought to reflect functional communication between spatially separate regions (Gray et al., 1989) and was suggested to be a basic mechanism for brain integration that mediates the formation of dynamic links over multiple frequency bands (Varela et al., 2001). Oscillations at different frequencies might enable dynamic interactions across neuronal populations over different spatial dimensions: while gamma-band interactions are prevalent in relatively local synchronization, interactions in beta-band involve more distant structures (Kopell et al., 2000). The following section 2.2.1 gives the mathematical definition of coherence and aspects of phase synchronization; the functional role of synchronization in corticospinal interactions is then discussed in Section 2.4.

2.2.1. Coherence and phase synchronization

Coherence is a measure of linear coupling between two time signals: two waves are coherent if they have a constant phase difference, see Figure 2.4. Coherence analysis is widely used in neurophysiology where coherence between two signals originating from two different spatial locations is interpreted as functional connection between them.

Coherence or magnitude-squared coherence between two time series $x(t)$ and $y(t)$ is an extension of the Pearson's correlation coefficient in the frequency domain.

If $F_x(\omega)$ and $F_y(\omega)$ are the (complex) Fourier transforms of the signals x and y , then the

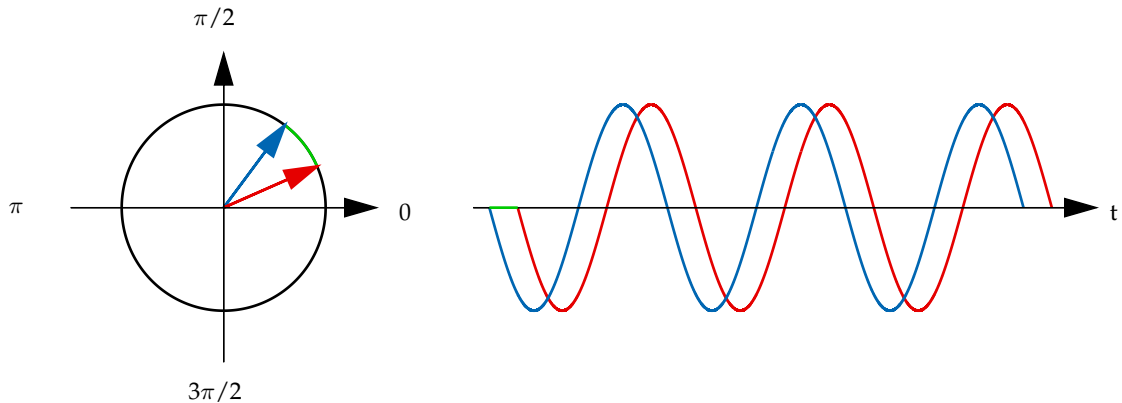


Figure 2.4.: Coherence of two signals. The blue oscillatory signal precedes the red one by a constant phase shift (marked in green). Note that this illustration is simplified: the phase lag does not allow to draw any conclusion on which signal is the leading one.

cross-spectrum is defined as:

$$S_{xy}(\omega) = \langle F_x(\omega)F_y^*(\omega) \rangle \quad (2.1)$$

where * denotes complex conjugation and $\langle \rangle$ the expectation value.

Coherence is defined as the crosspectrum $S_{xy}(\omega)$ normalized by the autospectra $S_{xx}(\omega)$ and $S_{yy}(\omega)$ of the two signals x and y, respectively:

$$Coh_{xy}(\omega) = \frac{|S_{xy}(\omega)|^2}{S_{xx}(\omega)S_{yy}(\omega)} \quad (2.2)$$

Values of coherence always satisfy $0 \leq Coh_{xy}(\omega) \leq 1$ reflecting the consistency of the phase difference between the two signals at a given frequency ω ; 0 corresponds to randomly changing phase shifts and 1 to a constant phase shift indicating perfect linear correlation (as in Figure 2.4). Note that this ideal case does usually not occur in coherence analysis of neurophysiological data: Coherent signals always jitter around a constant phase difference as displayed in Figure 2.5 showing the example of corticospinal interaction. Reasons for coherence values always being < 1 may be due to additive noise and desynchronization between processes.

In practice, to obtain a meaningful coherence estimate and to reduce variance, spectra are usually calculated by averaging over the windowed periodograms for subsegments of equal length, i.e. Welch's periodogram method (Welch, 1967). Without averaging,

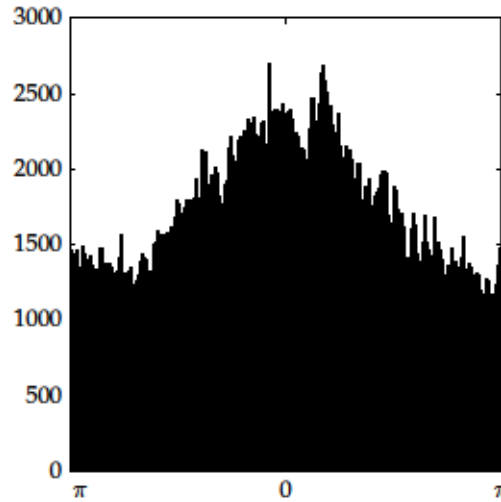


Figure 2.5: Distribution of phase difference between EEG and EMG processes

coherence would result in 1 for all frequencies.

Generally, coherence is regarded as a measure of phase synchronization in the analysis of brain activity. However, coherence depends also on the signal-to-noise ratio (SNR), i.e. in practice, coherence analysis has the advantage to give stronger weight to signals with better SNR.

Within paper II (Chapter 4) also the phase synchronization index (SI) (Rosenblum et al., 2001), quantifying the distribution of phase difference as illustrated in Figure 2.5, is calculated which does not take amplitudes into account. In practice however, coherence and phase synchronization were shown to give similar results (Mezeiová and Paluš, 2012).

When the signals x_ω and y_ω are bandpass-filtered signals around the frequency ω and $\Theta(t) = \phi_x(t) - \phi_y(t)$ is the phase difference between x_ω and y_ω (phases are extracted with Hilbert transform, see Section 2.2.2) at time t with the total number of samples T and the imaginary unit j , then SI is estimated as:

$$SI = \frac{1}{T} \left| \sum_{t=1}^T e^{j\Theta(t)} \right| \quad (2.3)$$

where $0 \leq SI \leq 1$; 0 and 1 corresponding to absent and perfect phase synchronization, respectively.

Effect of volume conduction on coherence estimation Coherence between two signals does not necessarily show the presence of synchronization between two sources (Rosenblum et al., 2001; Nolte et al., 2004). Due to volume conduction brain activity originating from one single source can be measured at many channels. This may lead to the detection of spurious brain connectivity. As an alternative to examining connectivity in source space, Nolte et al. (2004) proposed to use the imaginary part of coherency to study true brain interactions. They show that for different signals originating from the same source the imaginary part of (complex) coherency is necessarily zero since artifactual coherence due to volume conduction occurs with zero phase lag (Grosse and Brown, 2005; Nolte et al., 2004). The real-valued function of coherence is the magnitude squared of the complex coherency $Coh_{xy}(\omega) = |C_{xy}(\omega)|^2$, thus coherency is defined as

$$C_{xy}(\omega) = \frac{S_{xy}(\omega)}{\sqrt{S_{xx}(\omega)S_{yy}(\omega)}} \quad (2.4)$$

Note that the terms *coherence* and *coherency* are not defined consistently and are also used interchangeably. Coherence may further refer to the absolute (but not squared) value of coherency $Coh_{xy}(\omega) = |C_{xy}(\omega)|$. In all publications of this thesis, coherence is employed as given in Equation 2.2.

For spatially remote sources such as cortex and muscle, the detection of spurious connectivity is generally less of an issue; artifactual contamination from e.g. scalp muscle activity can quite easily be identified. Mima and Hallett (1999b), however, found that re-referencing to a common electrode led to a spurious coherence peak in the case of corticospinal interaction, possibly due to volume conduction.

2.2.2. Amplitude dynamics

Amplitude (or power) and phase are generally independent measures of oscillatory signals although cortical dynamics may lead to a relationship between them. While the amplitude of an analytic signal is the length of a vector in a complex plane, phase is the angle in the same plane (see Figure 2.6). Consequently, length and angle can change independently of each other; the two measures provide information about different aspects of the underlying processes. While the amplitude of cortical activity is typically associated with local synchronization (see Figure 2.7), phase synchronization reflects locking of spatially remote neuronal activities (Varela et al., 2001).

In paper II (Bayraktaroglu et al., 2013, Chapter 4) the amplitude-envelope of beta oscillations are used as a measure of local cortical and spinal cord synchronization and the

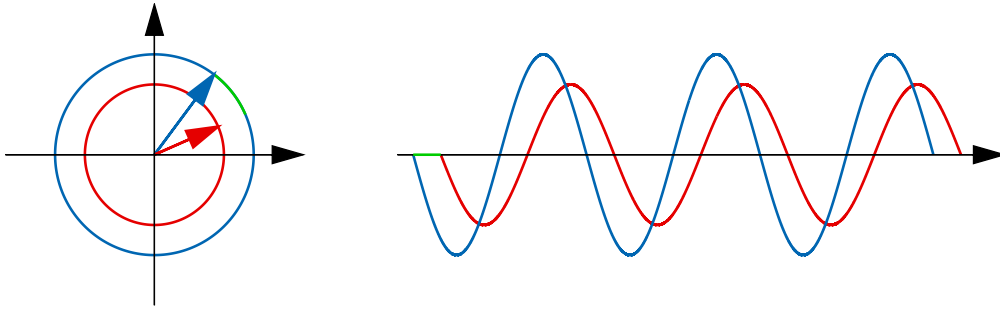


Figure 2.6.: Amplitude and phase of signals correspond to the length and angle of a vector, respectively. The two measures constitute two aspects of a process and can change independently of each other.

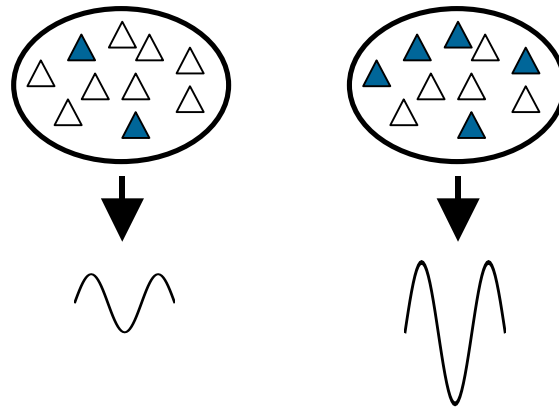


Figure 2.7.: Local synchronization influences the signal amplitude: the more neurons are active at a time the larger is the amplitude of the signal. Triangles represent neurons; filled triangles indicate active neurons.

relationship between the amplitude-envelope correlation and CMC is investigated. In contrast to coherence, which measures linear coupling, amplitude-envelope correlation relates to the measurement of non-linear relationships.

By means of the Hilbert transform, the amplitude envelope of a signal can be calculated (see Figure 2.8). The Hilbert transform $\mathcal{H}[x(t)]$ of function $x(t)$ is defined as

$$\mathcal{H}[x(t)] = \tilde{x}(t) = \frac{1}{\pi} p.v. \int_{-\infty}^{\infty} \frac{x(y)}{t-y} dy \quad (2.5)$$

where p.v. denotes the Cauchy principal value. Alternatively, the Hilbert transform of

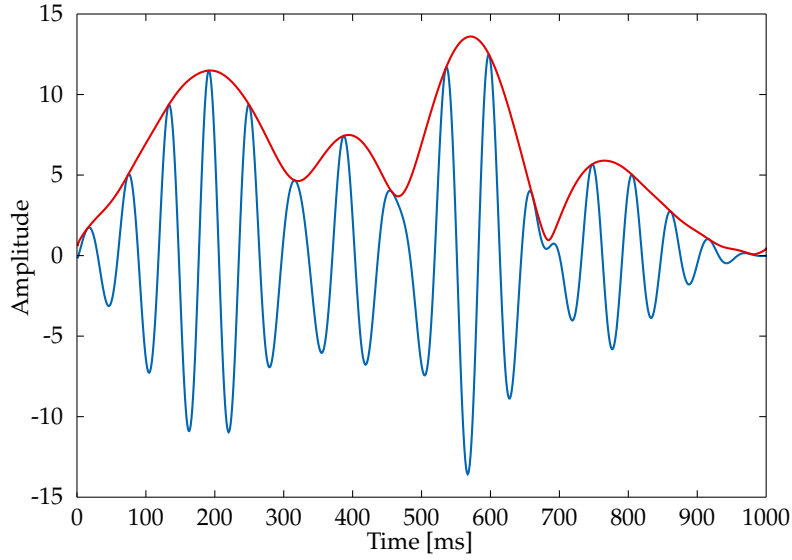


Figure 2.8.: Amplitude envelope of an analytic signal

$x(t)$ can be written as the convolution of $x(t)$ with the signal $1/\pi t$:

$$\mathcal{H}[x(t)] = \tilde{x}(t) = x(t) * \frac{1}{\pi t} \quad (2.6)$$

This envelope detection method involves creating the analytic signal using the Hilbert transform. An analytic signal is a complex measure, where the real part is the original signal and the imaginary part is the Hilbert transform of the original signal:

$$\psi = x(t) + j\tilde{x}(t) = A(t)e^{j\phi(t)} \quad (2.7)$$

The instantaneous amplitude $A(t)$ of the signal $x(t)$ is defined as the magnitude of the analytic signal:

$$A(t) = \sqrt{x^2(t) + \tilde{x}^2(t)} \quad (2.8)$$

where $\tilde{x}(t)$ is the Hilbert transform of the signal $x(t)$.

The instantaneous phase of the signal can be obtained by:

$$\phi(t) = \arctan \frac{\tilde{x}(t)}{x(t)} \quad (2.9)$$

Note that only for narrow-band signals the instantaneous amplitude $A(t)$ corresponds to the envelope of $x(t)$ (Rosenblum et al., 2001; Boashash, 1992).

2.3. Factors influencing CMC strength and frequency

2.3.1. Effects of motor behavior and cognition

Since 1995 factors influencing (beta-band) CMC have been investigated extensively. The magnitude of CMC was shown to be unaffected by changes in the force level for low to moderate forces, i.e. for force levels up to about 60% of maximum voluntary contraction (MVC) (Brown et al., 1998; Mima et al., 1999). However, CMC strength was found to be influenced by a range of other parameters related to fine motor control. CMC showed a task-dependent modulation (Baker et al., 1999): it was present only during the steady hold phase while it is abolished during the ramp phase. The magnitude of CMC increased with better motor performance (Witte et al., 2007). Further, a compliant object, i.e. when subjects move a lever against a spring-like load, yielded a larger CMC magnitude than a simple isometric contraction (Kilner et al., 2000; Riddle and Baker, 2006) which was due to the digit displacement rather than the compliance of the object as such (Riddle and Baker, 2006). CMC was shown to increase after (short-term) motor learning/adaptation and CMC even became visible due to motor learning in subjects who previously did not present CMC (Mendez-Balbuena et al., 2012; Perez et al., 2006). Besides, CMC-modulation was reported to be influenced by muscle fatigue, the results were however controversial. While some studies found increased CMC (Ushiyama et al., 2011a; Tecchio et al., 2006), others report that CMC decreased (Yang et al., 2009; Siemionow et al., 2010) due to muscle fatigue. The discrepancy may be explained by the task which included sustained contraction with maximal (Tecchio et al., 2006) or submaximal (Yang et al., 2009; Ushiyama et al., 2011a) force until exhaustion or intermittent handgrip contractions (Siemionow et al., 2010) or by the involved muscle.

Moreover, CMC peaks can also occur in other frequency ranges than beta. In some healthy people, CMC can be found in alpha frequency range; alpha-band CMC has however not been attributed any other functional meaning than CMC in beta frequency range. In contrast, gamma CMC has been linked to different motor behavior, in particular dynamic force output. While steady-state isometric contraction is associated with CMC in the beta frequency range, periodically-modulated dynamic force output leads to a shift of the dominant CMC peak to the high beta/low gamma frequency range (30-45 Hz) (Omlor et al., 2007). Omlor et al. (2007) concluded that during dynamic force the corticospinal oscillation mode of the sensorimotor system shifts towards the higher gamma frequencies to rapidly integrate visual and somatosensory information required to produce the appropriate motor command. Gamma-band CMC was not influenced

by the amplitude of the dynamic force (Andrykiewicz et al., 2007); it could however not always be identified as a peak distinct from beta CMC at different low levels of dynamic force (Chakarov et al., 2009). In addition, Salenius et al. (1996) demonstrated CMC at 40 Hz for one subject performing slow movements. Moreover, for very strong contractions, i.e. 80% of MVC, Mima et al. (1999) detected CMC within the gamma frequency range, however, only in a few subjects. The topographical distribution of beta-band CMC during weak contractions differed from gamma-band CMC during strong contraction suggesting a different neuronal origin of beta and gamma CMC.

Besides influences of motor-related behavior, CMC has also been shown to be affected by motor-unrelated, cognitive processes such as attention, cognitive effort and anticipation. Divided attention due to a secondary task led to decreased CMC strength (Kristeva-Feige et al., 2002; Safri et al., 2007). In contrast, CMC strength increased when cognitive effort was required to ignore a visual distractor (Safri et al., 2006, 2007). Moreover, Schoffelen et al. (2005, 2011) demonstrated that gamma-band CMC could be selectively modulated by cognitive demands, i.e., by the subjects' expectation of performing a movement. The gamma-CMC modulation occurred during a period of isometric contraction prior to the anticipated change in movement; CMC in beta frequency range remained unaffected. In contrast to Mima et al. (1999), the authors report a very similar topography for beta-band and gamma-band CMC which suggests the involvement of the same or spatially highly overlapping neuronal groups. Taken together, these studies give evidence that CMC is not a purely motor-related phenomenon but can be modulated by cognitive demands.

2.3.2. Afferent mechanisms

It has been suggested that CMC may not solely originate from cortical output pathways but also involve feedback afferent pathways (Baker, 2007).

Indeed, some studies indicated that an alteration of somatosensory inputs affected coherence. Intermuscular (EMG-EMG) coherence was shown to be decreased by digital nerve anesthesia blocking cutaneous input (Fisher et al., 2002). At the same time, however, also task performance was markedly reduced which has been related to a decrease in coherence strength (Witte et al., 2007, see also section 2.3.1). Note that EMG-EMG coherence may give comparable information about descending cortical drives as corticomuscular coupling (Grosse et al., 2003; Grosse and Brown, 2005) since it is at least partially of cortical origin (Kilner et al., 1999). Riddle and Baker (2005) employed a paradigm which increased the peripheral motor conduction time by cooling the arm.

2. Background

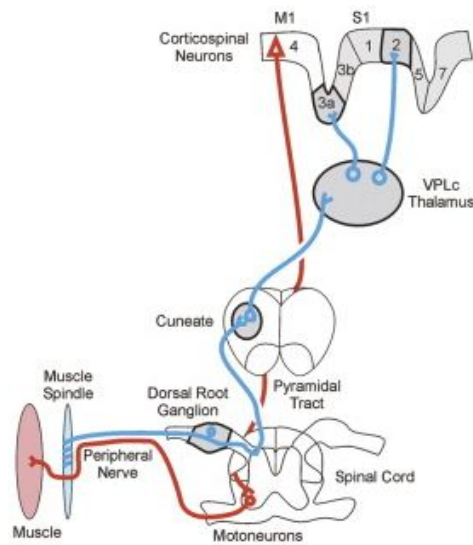


Figure 2.9.: Ascending (blue) and descending (red) pathways possibly mediating CMC. While the cortical output pathway (red) alone has been shown to be sufficient for the generation of CMC, feedback from the periphery might form an additional route which at least might have an modulatory effect on CMC. The picture has been retrieved from Baker (2007)

As a result, the delay calculated from the coherence phase increased twice as much as one would expect from just a change of the efferent pathway indicating afferent feedback pathways may contribute to the generation of CMC. Another study (Pohja and Salenius, 2003) found CMC to be reduced under temporary sensory deafferentiation; the peak frequency remained unchanged. Further evidence comes from the case of a deafferented patient who showed reduced EMG-EMG coherence while task performance under visual control was comparable to controls (Kilner et al., 2004). These studies demonstrate an effect on CMC strength by manipulation of peripheral input. As CMC is however only reduced and not abolished, an afferent feedback loop cannot be essential for the generation of corticomuscular synchrony. The efferent motor information alone is sufficient to establish beta-band CMC. The study conducted by Gerloff et al. (2006) supports this view: in the brain-lesioned patients, primary motor and somatosensory cortex could be clearly differentiated due to a relocation of the primary motor cortex to the other hemisphere. The authors found no contribution of the primary somatosensory cortex to beta CMC indicating that beta-range CMC represents efferent drive from the primary motor and not reafferent feedback processing. For the same deafferented patient as studied by Kilner et al. (2004), Patino et al. (2008) reported the absence of gamma CMC during dynamic force task; instead CMC remained

in the beta frequency range. During the static isometric force condition, beta CMC was comparable to controls. For both task conditions, the patient showed marked deficits in performance. The authors conclude that controlling dynamic force output poses a more complex task which makes proprioceptive information mandatory for the generation of gamma-band CMC. At the same time, when afferent feedback is absent, CMC in the beta-band can operate in an efferent motor mode to maintain a steady motor output during static and dynamic force.

2.3.3. Developmental changes

Several studies have examined CMC at different stages of development and aging (Graziadio et al., 2010; Kamp et al., 2011; Kanazawa et al., 2014; James et al., 2008). During the time from early development until adolescence, CMC magnitude was found to increase with age (Kanazawa et al., 2014; Graziadio et al., 2010) despite EEG power in alpha and beta frequency range showing the opposite trend (Graziadio et al., 2010). In newborns, CMC magnitude in the beta frequency range correlated with postnatal age (Kanazawa et al., 2014) which implies a relationship between beta CMC and neural maturation during neonatal development. In addition this could be an indication of corticomuscular communication beginning to develop, a process which may facilitate sensory-motor integration and activity-dependent development (Kanazawa et al., 2014). Besides lower amplitudes, CMC in newborns also showed larger variation in peak frequencies compared to young children or adults which Kanazawa et al. (2014) attributed to the immature corticomuscular functional connectivity during the developmental stage. Young children (4-12 years) more often showed multiple peaks with a broad spread of frequencies including alpha frequencies compared to young adults (Graziadio et al., 2010). Topographical CMC distributions and power changes were further indicative of larger, more distributed cortical networks being activated and relates to more non-specific cortical activation in children. In early adulthood, CMC was then characterized by a single peak within the beta frequency range (Graziadio et al., 2010). In contrast to younger and older age groups, the amplitude of CMC in young adults inversely correlated with motor performance. In adults (22-77 years), Kamp et al. (2011) found CMC frequency to be negatively and CMC amplitude to be positively correlated with age. For the age groups above 40 years there was however no difference in CMC frequency. Yet, there was a trend of CMC amplitude to be higher in elderly (58-77 years) compared to middle-aged people (41-55 years). Kamp et al. (2011) suggested that increased coherence amplitude might denote a compensatory mechanism to maintain

isometric contraction. Graziadio et al. (2010), however, found no difference in CMC amplitude when comparing elderly (>55 years) with young adults (20-35 years). Yet, as for children, peak frequencies were again more broadly spread and multiple peaks occurred more often, which the authors related to a breakdown of recurrent inhibition. They further found that a greater deviation from 23 Hz corresponded to poorer motor performance. The authors assumed that networks become less tuned including breakdown in their integration which may be likely to contribute to a decrement in motor control.

Age effects had to be considered for paper III (von Carlowitz-Ghori et al., 2014, Chapter 5) where stroke patients were compared to a healthy control group including middle-aged to elderly subjects.

2.3.4. CMC in stroke and other movement disorders

It is important to understand the functional coupling between cortical commands and the consequential muscle activation in movement disorders in order to add to the understanding of underlying mechanisms and aid in restoring normal motor function. CMC can be used as a tool to identify and characterize changes in functional coupling related to motor deficits. CMC alterations have been reported in a number of motor disorders including stroke (Mima et al., 2001; Braun et al., 2007; Fang et al., 2009; Meng et al., 2009; Graziadio et al., 2012; Rossiter et al., 2013), various types of tremor (Raethjen et al., 2002; Caviness et al., 2006; Raethjen et al., 2013) or myoclonus¹ of Parkinson's disease (Caviness et al., 2003).

The optimized detection of CMC in acute and chronic stroke was one topic of this thesis. The abovementioned CMC studies in stroke were only performed at chronic stage, i.e. from about one year post-stroke. The reported results regarding CMC amplitude changes on the ipsilesional and contralesional side varied; interhemispheric differences in CMC peak frequencies were not reported. The results of these studies will be discussed in more detail within paper III (von Carlowitz-Ghori et al., 2014, Chapter 5) of this thesis.

2.4. Functional role of CMC

There is substantial evidence that corticospinal synchronization evolves not just from cortical signals being transmitted to the muscle.

¹quick involuntary muscle contraction (jerk)

Studies suggest a bidirectional connectivity in the corticomuscular system: in addition to the efferent pathway, an afferent feedback loop may allow the ongoing motor activity being modulated by the sensory feedback signals (Riddle and Baker, 2005; Pohja and Salenius, 2003; Campfens et al., 2013). As already discussed in Section 2.3.2, CMC strength can be manipulated by peripheral input. While the afferent pathway might not be essential for establishing CMC, it still suggests that CMC does not simply arise from the propagation of cortical activity to the muscle.

Moreover, some studies demonstrated a dissociation between CMC and the power of beta oscillations. The sedative Diazepam, which has inhibitory effects (GABA_A receptor agonist), slightly reduced beta-CMC amplitude while the power of beta oscillations doubled (Baker and Baker, 2003). In contrast, the opposite reaction was caused by administering the antiepileptic drug Carbamazepine, which inhibits sustained repetitive firing (blocker of voltage-gated sodium channels in the axon): beta-CMC amplitude increased whereas beta power and also CMC frequency remained unchanged (Riddle et al., 2004). Similarly, also a dissociation between power and CMC in the gamma-band frequency range has been reported (Schoffelen et al., 2005). As discussed in Section 2.2.2 power and coherence are generally independent measures: While the power is associated with local synchrony, coherence between distant sources is not necessarily reflected in amplitude. For a further discussion of this issue, please be referred to paper II (Bayraktaroglu et al., 2013, Chapter 4).

CMC is likely to reflect functional connectivity within the motor system, in particular efferent commands from the cortex to muscle (Kanazawa et al., 2014). Generally, beta-band CMC is considered to be of some importance for fine motor control. As it is however absent during the movement itself, it is presumably not crucial for motor performance. MacKay (1997) proposed the idea that descending oscillations could function as a motor 'test pulse' (MacKay 1997) such that sensorimotor areas of the brain would be informed of current muscle conditions. Another complimentary idea suggested that beta-band oscillations could act to 'recalibrate' the sensorimotor system by providing updated information following a movement (Baker, 2007). Schoffelen et al. (2005) hypothesized that coherence is as mechanism of effective corticospinal interaction: In a simple reaction-time task, the subjects' readiness to respond was closely correlated with the strength of gamma-band CMC. The authors conclude that (gamma-band) CMC may contribute to an effective corticospinal interaction and shortened reaction times. They speculate that in general, selective coherence could be a mechanism for regulating the efficiency of input. Gamma-band CMC may further function to provide rapid integration of attention resources and afferent mechanisms (Lattari et al., 2010).

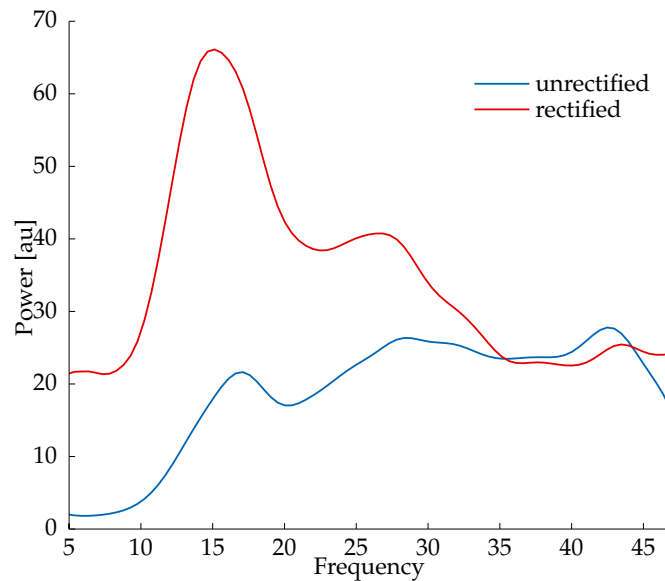


Figure 2.10.: Effect of rectification on EMG power spectrum. Rectification led to an increased peak at about 15 Hz

2.5. Further methodological aspects of analysis

2.5.1. Rectification of surface EMG as pre-processing step

The full-wave rectification of the EMG signal, i.e. taking the absolute value of the signal, has been widely applied as pre-processing procedure prior to CMC estimation. EMG rectification results in a shift of the EMG power spectrum towards lower frequencies which correspond to the MU firing rate (Myers et al., 2003, see also Section 2.1.1). This effect is illustrated in Figure 2.10 where rectification led to an increased peak at about 15 Hz in the EMG power spectrum; the figure closely resembles e.g. Figure 4 by Myers et al. (2003). Due to the shift in the power spectrum, EMG rectification was concluded to enhance MU firing rate information while suppressing frequency contents related to the MUAP wave shape.

Despite the routine use of rectification, the rationale behind this step had for a long time hardly received any attention. Recently however, the applicability of EMG rectification has been challenged (Neto and Christou, 2010) starting a still ongoing debate (Boonstra, 2010; Halliday and Farmer, 2010; Stegeman et al., 2010; Christou and Neto,

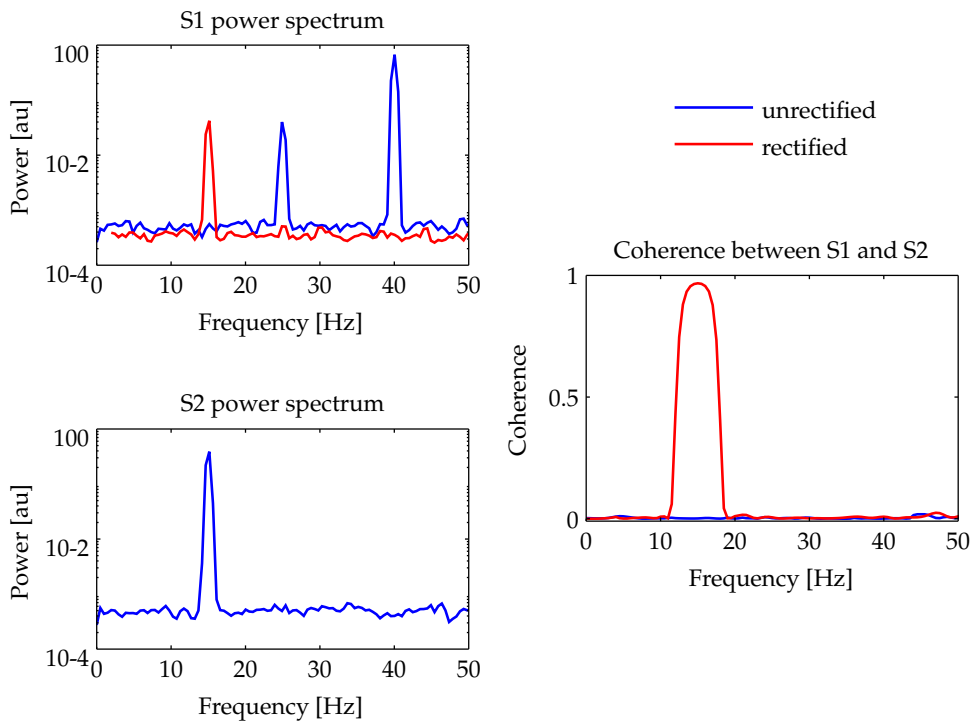


Figure 2.11.: Rectification of an amplitude-modulated signal. The left hand side shows the power spectra of the simulated signals S1 and S2. Signal S1 is an amplitude-modulated signal plus additive noise, the frequency of the carrier wave is 40 Hz and the modulation frequency 15 Hz. The modulating signal is a time-shifted version of S2. Only after rectification, the 15-Hz peak is visible in the power spectrum. The (unmodulated) signal S2 has a frequency of 15 Hz. On the right hand side, the coherence spectrum shows a peak at 15 Hz only after the rectification of S1.

2010; Bayraktaroglu et al., 2011; Boonstra and Breakspear, 2012; McClelland et al., 2012; Ward et al., 2013; Farina et al., 2013; Dakin et al., 2014; McClelland et al., 2014; Farmer and Halliday, 2014).

The full-wave rectification provides an approximation of the signal envelope (Myers et al., 2003). As noted by Boonstra (2010), amplitude modulations of higher frequency contents, which may result from periodic input to the MU pool, can be retrieved by rectification. Amplitude modulation is only visible in the Fourier spectrum with but not without rectification (or Hilbert/wavelet transform), as illustrated on the left-hand side of Figure 2.11. When the frequency of the second signal corresponds to the frequency of the amplitude modulation, coherence is also only detectable after rectification (see right-hand side of Figure 2.11).

Arguing against rectification, McClelland et al. (2012) pointed out that rectification constitutes a non-linear step and should therefore not be applied in coherence analysis which detects linear coupling. Rectification was shown to distort the frequency content (Neto and Christou, 2010) and introduce a frequency dependency (Stegeman et al., 2010).

EMG rectification is one focus of this thesis as part of paper I (Bayraktaroglu et al., 2011, Chapter 3) At the time when paper I was prepared for publication, studies largely addressed the issue from a theoretical viewpoint (Myers et al., 2003; Neto and Christou, 2010; Stegeman et al., 2010). Paper I provided experimental evidence against the rectification of the EMG signal as it resulted in a significant reduction of the coherence peak. The issue of EMG rectification continues to be highly debated. More recently, studies have been conducted providing further evidences both in favor (Boonstra and Breakspear, 2012; Ward et al., 2013; Farina et al., 2013; Dakin et al., 2014) and against (McClelland et al., 2012) EMG rectification. Therefore, I will update the reader on these more recent findings in Section 3.1.

2.5.2. Principal Component Analysis (PCA)

Principal component analysis (PCA) (Pearson, 1901; Jolliffe, 2002) is a popular multivariate technique in machine learning for feature extraction and data analysis/reduction which aims at explaining the data by a linear combination of uncorrelated variables, the *principal components*.

By this linear transformation the data is projected into a new coordinate system where the principal components are the coordinate axes; the first principal component thereby accounts for the largest variance in the data, the second principal component being orthogonal to the first component accounts for the most of the remaining variation and so forth. A simple two-dimensional example is given in Figure 2.12.

Due to volume conduction, the same sources in the brain may be recorded at several scalp EEG channels resulting in a correlation of EEG signals. By removing redundancies, i.e collinearity among variables/EEG signals, in the data, PCA allows to reduce dimensions while keeping most of the information.

Given a data set of EEG signals $x(t) = (x_1(t), x_2(t) \dots x_n(t))^T$ where n is the number of EEG channels, the principal components can be determined by the eigenvalue decomposition of the $(n \times n)$ covariance matrix Σ derived from the data.

This is done by finding the eigenvectors e_i and their associated eigenvalues λ_i of Σ such that

2. Background

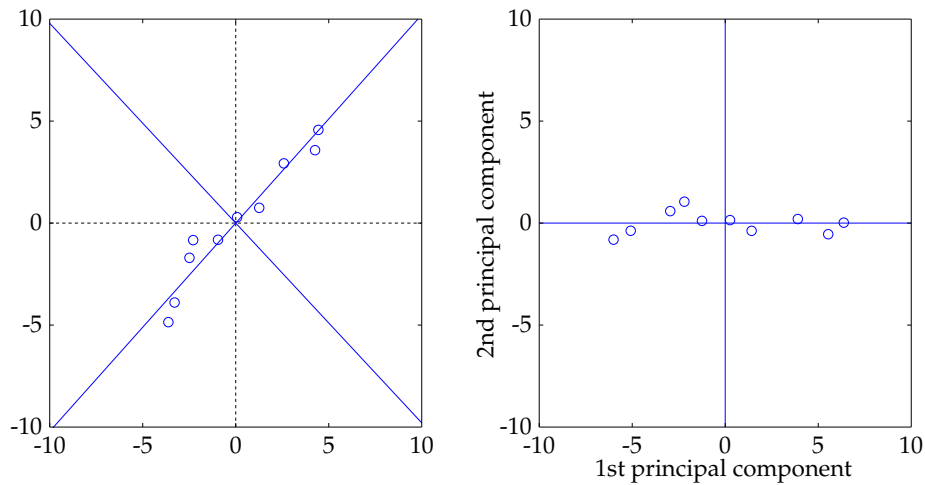


Figure 2.12.: Two-dimensional example of the PCA procedure. The left hand shows the original data and the corresponding principal components (blue). On the right hand side, the data was projected into a new coordinate system with the two principal components as axes; the 1st principal component accounts for the vast majority of variation in the data.

$$\Sigma e_i = \lambda e_i, i = 1, 2, \dots, n \quad (2.10)$$

If the eigenvectors are sorted according to their eigenvalues (= variances) in descending order, then the first eigenvector (with the largest eigenvalue) is the first principal component. For dimension reduction, a number of k components can be selected ($k \leq n$) that account for the desired amount of variability in the data, typically above 95%. The data is then projected into the new coordinate system:

$$m(t) = x(t)V \quad (2.11)$$

where V is the $n \times k$ matrix containing the k selected eigenvectors.

Figure 2.13 illustrates how dimensions are reduced by PCA on an example of EEG signals. In contrast to e.g. Independent Component Analysis (ICA) which find statistically independent components, PCA is unlikely to produce components which reflect source signals.

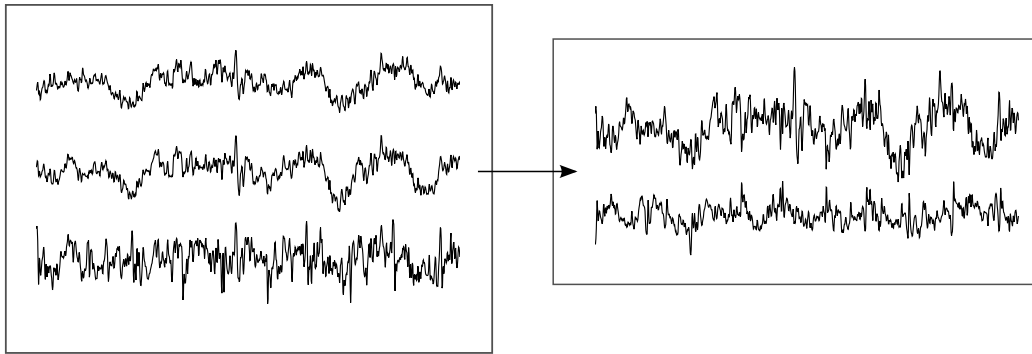


Figure 2.13.: Dimension reduction of EEG signals by PCA. The left hand side shows the original signals; the right hand side shows the projected data which has been reduced by one dimension, i.e. two of the three eigenvectors had been selected.

2.5.3. Spatial filters and patterns

Generally, EEG signals provide only a low spatial resolution. Due to volume conduction, information is spread over several channels. Therefore, spatial filters are applied as pre-processing step in order to improve the SNR of relevant EEG activity. In the context of BCI, spatial filters can serve to optimize the discrimination between two conditions; one of the most popular algorithms for classification in motor-imagery BCI is e.g. the Common Spatial Pattern (CSP) approach or variants of it (Koles, 1991; Ramoser et al., 2000; Blankertz et al., 2008; Tomioka et al., 2006) which aims to find spatial filters that maximize the difference in variance between the two conditions.

In CMC analysis, Laplacian filters (Hjorth, 1975) are commonly applied (Mima and Hallett, 1999b; Sağlam et al., 2008). Laplacian filters are basic spatial filters based on the fixed sensor position: for each channel, the signals of the neighboring channels are subtracted (see Figure 2.14). They act as spatial high-pass filter amplifying localized activity. More advanced filters are individually optimized for the specific neurophysiological measure such as the R-CMC method (Chapter 3) introduced in this thesis for optimizing the detection of CMC. Results obtained with Laplacian filtering will be shown in comparison. The R-CMC method is based on Multiple Linear Regression which is described in section 2.5.4.

The weights of spatial filters which serve to extract the relevant EEG activity cannot be interpreted as neurophysiologically meaningful, i.e. a stronger weight does not need to correspond to a larger contribution to the process and vice versa. In contrast, spatial patterns reflect how the strength of activity is topographically distributed and therefore

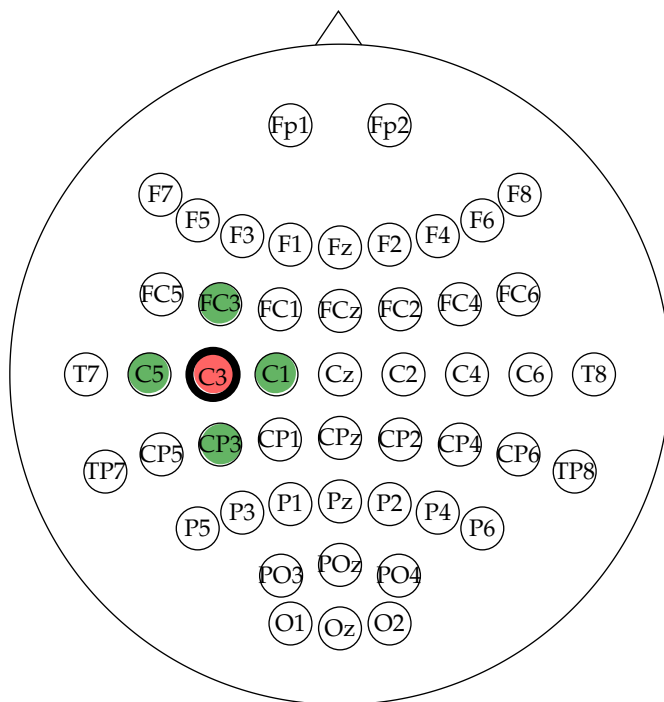


Figure 2.14.: Laplacian spatial filter. From the signal of each channel (red), the signals of the neighboring channels (green) are subtracted.

allow for an interpretation of the origin of the neural processes (for a detailed elaboration on this issue see Haufe et al., 2014). Figure 2.15 shows filter and pattern in comparison.

The R-CMC method employs an approach by Parra et al. (2002) to derive the pattern (of CMC activity) from the spatial filter: for a $(n \times t)$ data matrix X (for n channels and t time samples) and the optimized filter weights b , the spatial pattern P can be calculated as

$$P = \frac{Xv}{v^T v} \quad (2.12)$$

where the component v results from the projection of the data by the weights $v = (b^T X)^T$. The pattern P represents the coupling between the activity of component v and the sensor-space data.

2.5.4. Multiple Linear Regression

Multiple linear regression is one of the most widely used predictive models in the field of machine learning. The procedure, which requires only minimal computational effort,

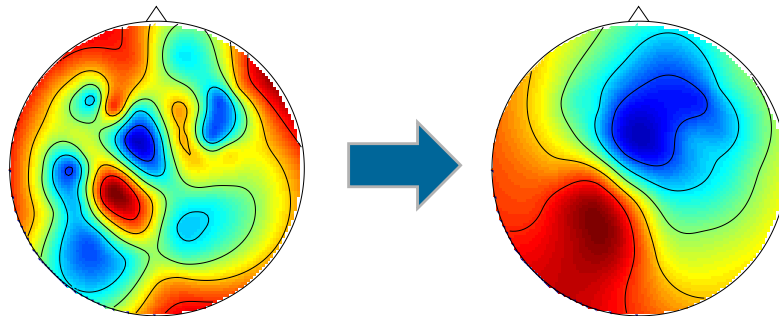


Figure 2.15.: Spatial filters and patterns. The left hand side shows a spatial filter which serves to improve the SNR of relevant activity. The right hand side displays the corresponding spatial pattern (of CMC activity). Only the pattern is neurophysiologically interpretable.

models the relationship between one dependent/response variable or regressand and several independent/predictor variables or regressors. Figure 2.16 shows an example of multiple linear regression for two independent variables. In the case of only one predictor, the method is referred to as simple linear regression.

For a target variable y and n predictor variables x_1, x_2, \dots, x_n , the multiple linear regression model can be described as

$$\hat{y} = \beta_0 + \beta_1 x_1 + \beta_2 x_2 + \dots + \beta_n x_n + \epsilon \quad (2.13)$$

where \hat{y} is the estimated value of y , $\beta_1, \beta_2, \dots, \beta_n$ are the regression coefficients, β_0 is the intercept and ϵ is a random variable (noise).

The model parameters can be estimated by the least-square criterion which minimizes the sum of squared residuals, i.e. the squared deviation of the estimated from the observed values

$$\sum_{i=1}^n (y_i - X\beta)^2 \quad (2.14)$$

where X is a matrix containing the predictor variables and β a vector containing the unknown regression parameters.

The matrix solution of this minimization problem is given by the least-square estimator b of the parameters

$$b = (X^T X)^{-1} X^T y \quad (2.15)$$

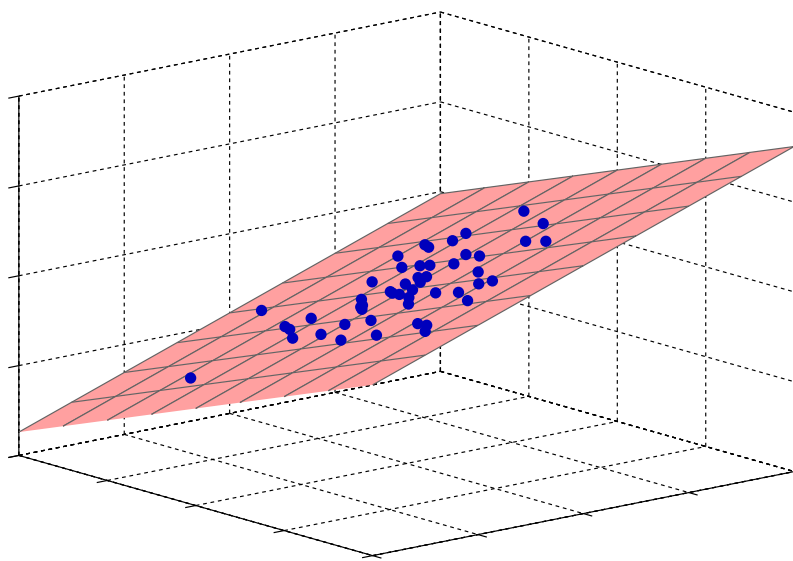


Figure 2.16.: Example of multiple linear regression with two independent variables where a plane is fit to the data such that the (squared) distances between the data points and the plane is minimized.

The goodness of fit of the multiple linear regression model can be measured by the coefficient of determination usually denoted as R^2 or r^2

$$R^2 = 1 - \frac{SS_{res}}{SS_{tot}} \quad (2.16)$$

where SS_{res} is the explained and SS_{tot} the total variance, i.e. R^2 indicates the explained variability of the model. The coefficient of determination is such that $0 \leq R^2 \leq 1$; the larger the value, the better the model fits to the data.

Collinearity One issue of multiple linear regression analysis is *collinearity* (or *multi-collinearity*) which occurs when two or more predictor variables are highly intercorrelated. For perfect collinearity, the matrix X does not have full rank and $X^T X$ becomes singular; therefore $(X^T X)^{-1}$ does not exist; as a result there is no unique solution. Perfect collinearity e.g. due to duplicates in the data is easily eliminated. In practice, high but not perfect collinearity tends to be more of an issue. Though there exists a unique solution ($X^T X$ is invertible), high collinearity makes the parameter estimates less stable: the estimates may change drastically upon slight variations in the data and are therefore little accurate. The problem of collinearity is illustrated in Figure 2.17. The fitted plane is not well supported by the data points. See in contrast Figure 2.16 where the predictor variables are uncorrelated.

Regularization Regularization refers to techniques that can be applied to prevent overfitting which reduces the predictability of the model. For multidimensional data, overfitting can occur due to the number of parameters being too high relative to the amount of data. Further, regularization allows to restrict the impact of outliers/strong noise (Müller et al., 2003). Common regularization methods for linear models are Ridge Regression (Hoerl and Kennard, 1970) and Lasso (Tibshirani, 1996) which constrain the size of the estimated regression coefficients. At the same time, regularization may introduce a bias to the model. The regularization parameters, which can be adjusted using cross-validation, are therefore chosen such that they provide a trade-off between bias of the model and variance of estimates.

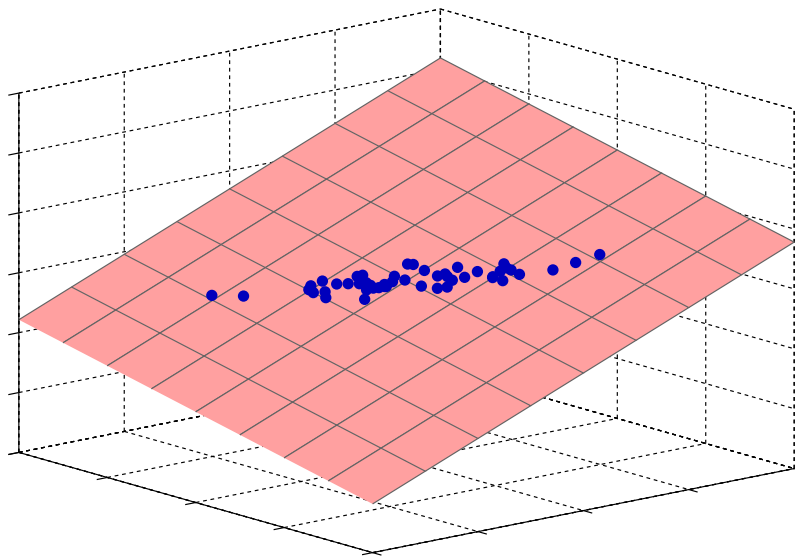


Figure 2.17: Example of collinearity. The fitted plane is not well supported: little changes in the data could have a large effect on the parameter estimates. In contrast, Figure 2.16 shows an example where the plane is well supported by the data points.

Methodology for optimal detection of CMC and Rectification

3

This chapter introduces the method Regression CMC (R-CMC) in comparison to other methods commonly used for CMC analysis. The method allows the extraction of spatial filters that optimize the detection of CMC. Thereby also differences concerning EMG rectification could be detected (see below) which emphasizes the importance of improving CMC detection. Due to the positive results, the R-CMC method was also used for CMC analysis of the remaining three publications of this thesis. Some parameters have been varied, particularly in the last publication on CMC-based neurofeedback (Chapter 6) where the method is adjusted for online presentation. While the technical details of the method will be extensively introduced within the following publication, the flowchart of Figure 3.1 is meant to provide a schematic overview of the method.

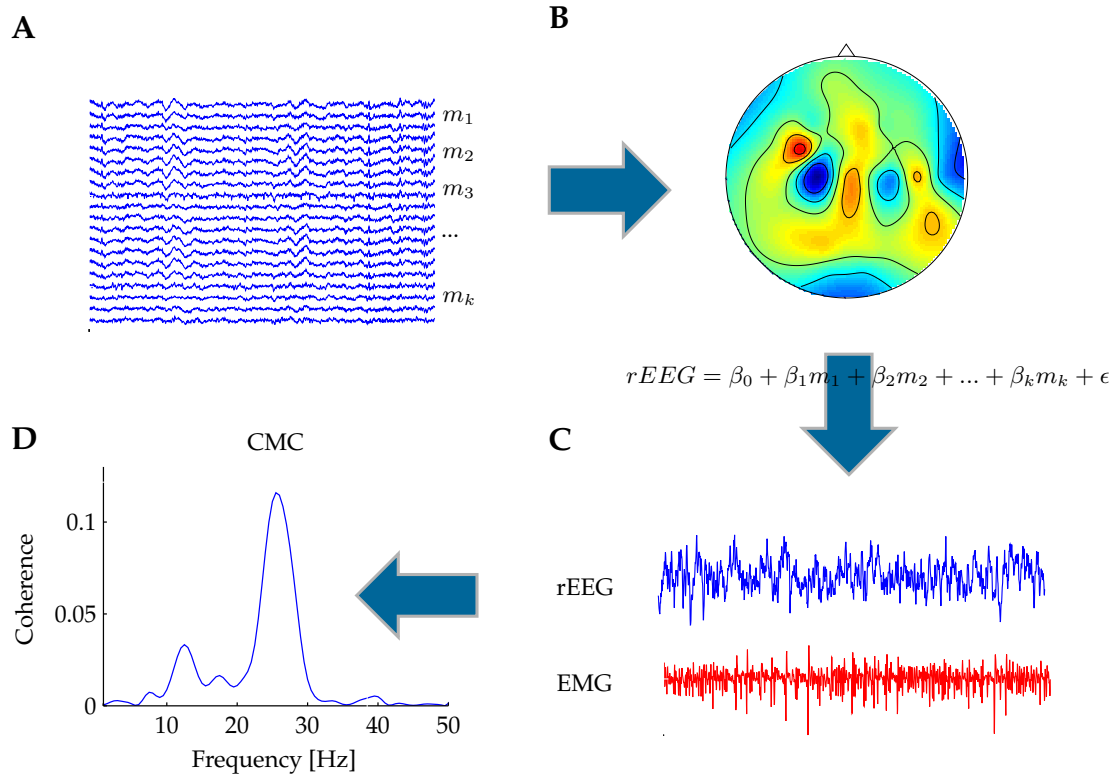
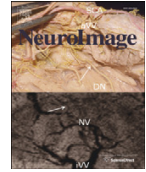


Figure 3.1.: R-CMC method. For the bandpass-filtered EEG signals (A) the linear combination of channels with specific weights is found which best explain the EMG signal. The regression coefficients serve as spatial filters (B) to project the EEG signals resulting in one projected signal rEEG and the EMG signal (C). Coherence is the calculated between the two signals (D).



Optimal imaging of cortico-muscular coherence through a novel regression technique based on multi-channel EEG and un-rectified EMG

Zubeyir Bayraktaroglu ^{a,b,*}, Katherina von Carlowitz-Ghori ^a, Florian Losch ^a, Guido Nolte ^c, Gabriel Curio ^{a,b,d}, Vadim V. Nikulin ^{a,b,d}

^a Neurophysics Group, Department of Neurology, Charité - University Medicine, Berlin, Germany

^b Center for Stroke Research Berlin (CSB), Charité - University Medicine, Berlin, Germany

^c Fraunhofer Institute FIRST, Berlin, Germany

^d Bernstein Center for Computational Neuroscience, Berlin, Germany

ARTICLE INFO

Article history:

Received 9 February 2011

Revised 28 April 2011

Accepted 30 April 2011

Available online 7 May 2011

Keywords:

Coherence

Neuronal oscillations

EEG

EMG

Synchronization

ABSTRACT

Cortico-muscular coherence (CMC) reflects interactions between muscular and cortical activities as detected with EMG and EEG recordings, respectively. Most previous studies utilized EMG rectification for CMC calculation. Yet, recent modeling studies predicted that EMG rectification might have disadvantages for CMC evaluation. In addition, previously the effect of rectification on CMC was estimated with single-channel EEG which might be suboptimal for detection of CMC. In order to optimally detect CMC with un-rectified EMG and resolve the issue of EMG rectification for CMC estimation, we introduce a novel method, Regression CMC (R-CMC), which maximizes the coherence between EEG and EMG. The core idea is to use multiple regression where narrowly filtered EEG signals serve as predictors and EMG is the dependent variable. We investigated CMC during isometric contraction of the abductor pollicis brevis muscle. In order to facilitate the comparison with previous studies, we estimated the effect of rectification with frequently used Laplacian filtering and C3/C4 vs. linked earlobes. For all three types of analysis, we detected CMC in the beta frequency range above the contralateral sensorimotor areas. The R-CMC approach was validated with simulations and real data and was found capable of recovering CMC even in case of high levels of background noise. When using single channel data, there were no changes in the strength of CMC estimated with rectified or un-rectified EMG – in agreement with the previous findings. Critically, for both Laplacian and R-CMC analyses EMG rectification resulted in significantly smaller CMC values compared to un-rectified EMG. Thus, the present results provide empirical evidence for the predictions from the earlier modeling studies that rectification of EMG can reduce CMC.

© 2011 Elsevier Inc. All rights reserved.

Introduction

Oscillatory neuronal activity in the beta frequency range (15–30 Hz) has been shown to be important for the movement control (Baker et al., 1999; Donoghue et al., 1998; Murthy and Fetz, 1992; Penfield, 1954). Particularly, cortico-muscular coherence (CMC) in the beta range has been hypothesized to underlie a mechanism through which the cortex is able to achieve fine motor control (Baker, 2007; Jackson et al., 2002; Schnitzler et al., 2000). In its essence, CMC shows how electrical cortical and muscle activities are correlated at a specific frequency range. CMC during isometric muscle contractions was demonstrated by both non-invasive MEG (Conway et al., 1995; Salenius et al., 1997) and EEG

recordings (Baker and Baker, 2002; Graziadio et al., 2010; Halliday et al., 1998; Kristeva-Feige, et al., 2002; Mima and Hallett, 1999) in healthy subjects and confirmed with intracortical local field potential (LFP) recordings in monkeys (Baker et al., 1997). CMC is diminished during a movement and appears predominantly during periods of isometric contraction following the movement (Kilner et al., 2000; Riddle and Baker, 2006) and reaches its maximum peak in the beta frequency range (16–32 Hz) over the primary sensorimotor cortices contralateral to the innervated limb (Salenius et al., 1997; Tsujimoto et al., 2009; Witham et al., 2010). Across studies CMC magnitude ranges between 0.02 and 0.2 (Conway et al., 1995; Riddle and Baker, 2005; Salenius and Hari, 2003). CMC peak frequency, spectral distribution and magnitude show task, attention and age related modulations (Graziadio et al., 2010; Kristeva-Feige et al., 2002; Riddle and Baker, 2006).

In the present study we aimed at elucidating the issue of EMG rectification for CMC calculation. Using simulations, Neto and Christou (2010) showed that rectification impairs estimation of EMG activity. Moreover, a recent modeling study (Stegeman et al., 2010) predicted that EMG rectification should lower CMC values. In contrast, an earlier

Abbreviations: CMC, cortico-muscular coherence; R-CMC, regression cortico-muscular coherence; PCA, principal component analysis.

* Corresponding author at: Department of Neurology, Charité - Universitätsmedizin Berlin, Neurologie, AG Neurophysik, Hindenburgdamm 30, 12203 Berlin, Germany. Fax: +49 30 8445 4264.

E-mail address: zuebeyir.bayraktaroglu@charite.de (Z. Bayraktaroglu).

empirical study (Yao et al., 2007) using EEG signals derived from electrode C3 (referenced to linked mastoids) found no significant CMC differences when using either rectified or un-rectified EMG signals. Neuronal activity recorded by a single EEG channel represents a superposition of multiple sources which might obscure specific cortical oscillations engaging neurons in the spinal cord. An obvious step in dealing with such superposition is to use spatial filters for sharpening the sensorimotor oscillations. In this study, we utilized a novel approach on the basis of multiple regression for the optimal detection of cortico-muscular interactions. Such optimization allows reduction of irrelevant neuronal oscillations and background noise which might impair CMC estimation and obscure possible differences between rectified and un-rectified EMG. In addition, we also used Laplacian filtering which is commonly used in CMC studies (Andrykiewicz et al., 2007; Graziadio et al., 2010; Mima and Hallett, 1999; Sağlam et al., 2008) to verify the notion that spatial high-pass filtering is indeed required for the demonstration of the rectification effects. Since EMG rectification is a standard preprocessing step in many CMC studies, the present results have direct implications for the interpretation of oscillatory control of muscle activity.

Methods

Subjects

We studied 10 healthy volunteers (9 males and 1 female), and mean age was 46 ± 10.8 (mean \pm SD). Subjects were without any history of neurological or psychiatric disorders. The experimental protocol was approved by the Institutional Review Board of Charité, Berlin, and the subjects gave their written informed consent prior to the experiments. All subjects were right-handed according to the Edinburg Handedness Inventory (Oldfield, 1971) and had normal or corrected to normal vision.

Paradigm

We have chosen a digit displacement paradigm including manipulation of a compliant object which requires the subject to move the levers against a load and then hold. Previous studies reported that the coherence was smaller when the task involved an isometric condition rather than a compliant condition (Kilner et al., 2000; Riddle and Baker, 2006).

Subjects were seated in a comfortable chair; arms were rested on the chair handles, forearms flexed at 60° and hands were pronated. The task required pressing a spring-loaded lever with the left or right thumb at 0.5 N force. The force level was measured with a Honeywell Load Sensor (FSG15N1A). Visual feedback for the force level was provided on a computer screen as a horizontal bar of a varying lateral extent proportional to the exerted force. A cross in the center of the screen served as an eye-fixation point. The displacement of the spring-loaded lever was ~ 3.5 cm.

The task was performed with each hand separately and the hand order was counter-balanced between the subjects. One hundred trials were recorded for each hand in four blocks. The subjects were instructed to reach the desired force level as fast as possible after a single tone and hold it constant until a double tone. Each trial lasted 9 s in total (5 s active and 4 s rest). There were sixty seconds of rest between the blocks.

Data acquisition

EEG and EMG data were recorded with BrainAmp MR plus (Brain Products, Germany) amplifiers, filtered in the frequency range 0.015–250 Hz and sampled at 1000 Hz. Voltage resolution for EEG and EMG channels was 0.1 μ V and 0.5 μ V, respectively.

EEG

During the acquisition, EEG was referenced to physically linked earlobes and recorded with an EEG cap (61 electrodes, EasyCap™) where electrodes had a higher density between frontal and parietal areas over the sensorimotor cortex. As verified empirically, physically linked-earlobes did not lead to the distortion of voltage topographies (Gonzalez Andino et al., 1990). Ag/AgCl sintered ring electrodes 12 mm in diameter were used (EasyCap GmbH, Germany). Ocular artifacts were recorded with two electrodes placed on the right zygomatic and supraorbital processes.

EMG

Six EMG electrodes were placed over the thenar side of each hand and EMG was recorded from the Abductor Pollicis Brevis (APB) muscle. Ag/AgCl sintered electrodes 4 mm in diameter were used. The skin surface was abraded with NuPrep (Weaver and Co., CO, USA) before electrode application. The electrode-skin conductive contact was established with Ten20 electrode paste (Weaver and Co., CO, USA) and the electrodes were secured to the skin with adhesive medical tape.

An EMG reference electrode was placed on the styloid process of the ulnar bone and a ground electrode on the inner surface of wrist at the midline. Ag/AgCl sintered electrodes 12 mm in diameter were used as reference and ground.

Analysis

All data and statistical analyses were performed offline in MATLAB (Mathworks Inc., MA, USA) environment with custom written functions.

Data preprocessing

The analysis was focused on the stable hold period of the task, in which the strongest coherent activity in beta band has been shown before (Baker et al., 1997; Kristeva et al., 2007; Riddle and Baker, 2006). This period corresponded to the post-stimulus interval between 2000 and 5000 ms after the start tone. The data were visually inspected for the presence of strong abrupt force changes in the hold period. If the force output deviated from 0.5 ± 0.1 N range, the epoch was discarded. After artifact rejection 207 ± 34.32 s and 201.3 ± 41.22 s of data were utilized for the analysis of the left and right hand tasks, respectively.

Regression – cortico-muscular coherence (R-CMC)

Our novel R-CMC method employs two steps: dimension reduction and multiple linear regression with the delay optimization.

Dimension reduction

Since coherence is analogous to the calculation of correlation in a narrow frequency band, we found it useful to perform the following calculations in the time domain. When fitting a regression model to the data, the number of variables (in our case number of EEG channels) is an important factor. In order to avoid collinearity of the predictors (EEG from different channels) and to make the estimation of covariance matrices more robust, we first reduced the number of dimensions with Principal Component Analysis. We start with the measurement matrix \mathbf{M} of size $l \times n$ where l is the number of time samples and n is the number of channels. We then proceed with band-pass filtering each column/channel in \mathbf{M} in the specific frequency band around a frequency f (the band is defined as $f \pm 2$ Hz) creating the matrix \mathbf{M}_f . The columns in matrix \mathbf{M}_f are centered to have a zero mean.

Next, we estimate the time-averaged covariance matrices for \mathbf{M}_f :

$$\mathbf{C}_f = \frac{\mathbf{M}_f^T \mathbf{M}_f}{l} \quad (1)$$

where l is the number of samples. Then, we calculate orthogonal basis by finding eigenvectors \mathbf{e}_i and eigenvalues λ_i of the matrix \mathbf{C}_f such that:

$$\mathbf{C}_f \mathbf{e}_i = \lambda_i \mathbf{e}_i, i = 1, 2, 3 \dots n. \quad (2)$$

Let \mathbf{P}_f be the matrix containing first k eigenvectors as columns. The number k is selected to account for 99% of variability in the data. We then project our original data into a new coordinate system:

$$\mathbf{T}_f = \mathbf{M}_f \mathbf{P}_f. \quad (3)$$

Multiple linear regression

R-CMC is based on multiple linear regression, which finds linear combination of all input variables (EEG activity) maximally explaining the EMG activity. This in turn translates into the maximization of linear correlation/coherence between EEG and EMG activities (see below). The R-CMC procedure was performed separately for each of the six EMG electrodes.

Let \mathbf{g} be the vector containing EMG activity which is filtered around the same frequency f as in the case of EEG. The linear model for EMG can then be expressed as:

$$\mathbf{g} = \beta_1 \mathbf{t}_{f1} + \beta_2 \mathbf{t}_{f1} + \dots + \beta_k \mathbf{t}_{fk} + \boldsymbol{\varepsilon} \quad (4)$$

where \mathbf{t}_{fi} are columns in the \mathbf{T}_f matrix and $\boldsymbol{\varepsilon}$ is a random variable (noise).

In a matrix form Eq. (4) can be written as:

$$\mathbf{g} = \mathbf{T}_f \boldsymbol{\beta} + \boldsymbol{\varepsilon}. \quad (5)$$

We estimate $\boldsymbol{\beta}$ by minimizing the difference between the observed and the modeled data

$$\mathbf{b} = \arg \min_{\boldsymbol{\beta}} \|\mathbf{g}_\tau - \mathbf{T}_f \boldsymbol{\beta}\| \quad (6)$$

where $\|\cdot\|$ indicates L2 norm and τ indicates a time-delayed EMG signal in the range of $-\tau_{\max}$ to τ_{\max} , where τ_{\max} is defined according to the center frequency f of the band-pass filter (see below for further details on “Delay optimization”).

The least-squares solution to Eq. (6) is:

$$\mathbf{b} = \left(\mathbf{T}_f^T \mathbf{T}_f \right)^{-1} \mathbf{T}_f^T \mathbf{g}_\tau. \quad (7)$$

Here we also explain why minimization in Eq. (6) leads to the maximization of correlation.

Recall that the coefficient of determination (R^2 value) is defined as:

$$R^2 \equiv 1 - \frac{SS_{res}}{SS_{tot}} \quad (8)$$

where SS_{res} is the residual sum of squares related to Eq. (6) and SS_{tot} is the total variance of the regressand (EMG activity). The coefficient of correlation R is then simply obtained by taking a square root of R^2 (the sign of the correlation is irrelevant). Since SS_{tot} depends only on the EMG values, R^2 value can be maximized through the decrease in SS_{res} , which is achieved in Eq. (6).

\mathbf{T}_f data is then projected using \mathbf{b} , leading to:

$$\mathbf{y} = \mathbf{T}_f \mathbf{b}. \quad (9)$$

Delay optimization

Since the interactions between cortex and muscle are not instantaneous, a certain delay τ is expected between the activities at these two levels. In order to take into account this delay EEG and EMG data were band-pass filtered with 2 Hz steps and 4 Hz bandwidth at center frequencies f between 10 and 34 Hz using a Butterworth filter of 4th order. The filtered EMG signal was shifted relative to EEG between $-\pi (-\tau_{\max})$ and $+\pi (\tau_{\max})$ with $\pi/6$ steps. Separately for each EMG electrode and delay, a multiple regression was performed and the coherence, corresponding to the best EMG channel and delay was selected for further analysis. The coherence across segments was estimated as:

$$Coh_{g,y} = \frac{|\mathbf{s}_{g,y}|^2}{|\mathbf{s}_g|^2 |\mathbf{s}_y|^2} \quad (10)$$

where \mathbf{s}_g and \mathbf{s}_y are complex Fourier transforms for EMG and projected EEG data (y), respectively, and $\mathbf{s}_{g,y}$ is a cross-spectrum. For the calculation of the Fourier transforms, the data was divided into 500 ms non-overlapping segments and windowed with a Hanning window.

Localization of coherent activity

We employed an approach proposed by Parra et al. (2002) for the calculation of patterns from the spatial filter \mathbf{b} . For \mathbf{T}_f data (related to PCA components), the pattern \mathbf{p}_{PCA} can be calculated as:

$$\mathbf{p}_{PCA} = \frac{\mathbf{T}_f^T \mathbf{y}}{\mathbf{y}^T \mathbf{y}}. \quad (11)$$

Thus \mathbf{p}_{PCA} can be considered as a coupling/correlation of projected \mathbf{y} vector with the EEG activity in matrix \mathbf{T}_f .

Next we have to obtain the final pattern \mathbf{p}_{EEG} taking into account previous PCA decomposition:

$$\mathbf{p}_{EEG} = \mathbf{P}_f \mathbf{p}_{PCA}. \quad (12)$$

For further analysis and delay optimization we excluded components with \mathbf{p}_{EEG} patterns showing abnormal activity such as the presence of mosaic like high-frequency spatial frequencies or strong activity at the temporal or frontal edges of the patterns (a typical indication for the presence of the scalp muscle activity). After obtaining \mathbf{p}_{EEG} patterns one can perform localization of neuronal sources with different inverse modeling methods. In the present study we used the sLORETA algorithm (Pascual-Marqui, 2002) to localize neuronal sources related to the specific patterns \mathbf{p}_{EEG} corresponding to the strongest cortico-muscular coherence and mapped these sources using the standard MNI305 head (Collins et al., 1994). For comparative purposes, sLORETA maps were normalized by dividing the power in each voxel by the sum of power from all voxels.

Un-rectified and rectified EMG activity

As mentioned earlier R-CMC was estimated for raw EMG activity filtered around different frequencies f as in the case of EEG (see above). In addition to this R-CMC was also calculated for rectified EMG. In this case, EMG was high-pass filtered at 10 Hz, band-stop filtered at 50 Hz and rectified. Then the R-CMC procedure was applied to the rectified EMG as in the case of raw EMG.

Cortico-muscular coherence assessed with Laplacian filtering

Laplacian filtering of EEG for CMC estimation has been used frequently (Andrykiewicz et al., 2007; Graziadio et al., 2010; Mima and Hallett, 1999; Sağlam et al., 2008). In addition to the R-CMC method, we estimated coherence between Laplacian-filtered EEG for both rectified and un-rectified EMG data. The Laplacian-based coherence was calculated on the same data epochs as in the case of R-CMC analysis. The Laplacian filtering of 61 channels resulted in 22 Laplacian derivations. CMC with Laplacian filtering was estimated for each of six EMG channels and for rectified and un-rectified EMG. The highest coherence values in the frequency range 13 to 33 Hz over the hemisphere opposite to the performing hand were selected for the further analysis.

Cortico-muscular coherence on the basis of EEG with linked-earlobes as a reference

For the replication of earlier results (Yao et al., 2007), we also calculated the coherence between channels C3/C4 and the EMG channel located over the belly of APB muscle. Cortico-muscular coherence was calculated for both rectified and un-rectified EMG data.

Significance of coherence

The confidence limit (CL) for the coherence obtained on the basis of Laplacian filtering and linked ear-lobe approach can be estimated as proposed by Rosenberg et al. (1989),

$$CL_{\gamma} = 1 - \left[1 - \frac{\gamma}{100} \right]^{\frac{1}{N-1}} \quad (13)$$

where γ is the significance level set to 5%, N is the number of epochs, and CL is a confidence limit above which the coherence is significant. For the coherence obtained with R-CMC approach, we used permutation tests (Hesterberg et al., 2005). For this procedure, we repeated all the steps of R-CMC such as PCA, multiple regression and delay optimization but EMG segments were shuffled with respect to the EEG data. For each permutation, we obtained a specific coherence value and altogether 500 permutations were performed. The significance was determined as percentage of coherence values exceeding the coherence value corresponding to unpermuted data.

Simulations

We tested CMC with Laplacian and R-CMC methods in the presence of strong background noise and interfering oscillatory activity. We simulated EEG recordings for 61 channels, which were fitted to the outermost layer of the standard Montreal Neurological Institute (MNI) head (Evans et al., 1994). The head model was based on a three compartment realistic volume conductor and was used for calculation of EEG forward solutions (Nolte and Dassios, 2005). The source of coherent activity was modeled as a single tangential cortical dipole placed at the primary hand motor area in the pre-central gyrus of the right hemisphere. The sources of beta oscillations were generated by band-pass filtering white noise in the 18–22 Hz frequency range. The coherent EMG activity was a time-shifted version of the cortical oscillations with the addition of white noise. The resulting original coherence between cortical source and EMG activity was ~ 0.14 . Note that for these simulations rectification of EMG is not relevant because R-CMC anyway works with band-pass filtered data which is obtained with or without rectification. This simulation addresses the ability of R-CMC to obtain spatial filters which maximize coherence between EMG and the extracted neuronal source. For the generation of background noise, we used 500 uncorrelated dipoles with random orientation and distribution on

the cortex. The noise sources had $1/f$ type spectra. Additionally, we simulated an interfering uncorrelated dipole with either equal or 20 times stronger amplitude than the amplitude of CMC source. This dipole had the same frequency and location as CMC dipole, but different orientation (thus also leading to different scalp patterns, Fig. 8). The simulated data was 90 s long and sampled at 1000 Hz. The SNR of the CMC source was set to 0.05. The SNR was calculated as the ratio between the mean variance across channels for the projected dipole and the mean variance of additive $1/f$ noise (produced by all noise dipoles) in the center frequency of the coherent source.

The error between the original pattern and the pattern recovered by R-CMC was calculated according to:

$$Err = 1 - \frac{|a_{or}^T a_r|}{\|a_{or}\| \cdot \|a_r\|} \quad (14)$$

where a_{or} is the original simulated pattern and a_r is a pattern recovered by R-CMC.

Results

Performance

The subjects were able to keep the required force level during the active period of the trials. The trials, which exceeded ± 0.1 N of the desired force in the analyzed period (2000 to 5000 ms), were removed from the analysis. On average, the subjects were able to stay within $\pm 12.5\%$ of the required force level. Fig. 1 shows an example of motor performance for one subject.

PCA components

The number of PCA components (explaining 99% of variance) ranged from 19 to 36 (mean \pm SD: 25.9 ± 4.8) which translates to 41 to 69% decrease in the number of channels.

Cortico-muscular coherence

Single-channel analysis (linked earlobes as a reference)

An example of the coherence spectrum for one subject is presented in Fig. 2. The mean and the standard error of the mean for the coherence, calculated for rectified and un-rectified EMG, are shown in

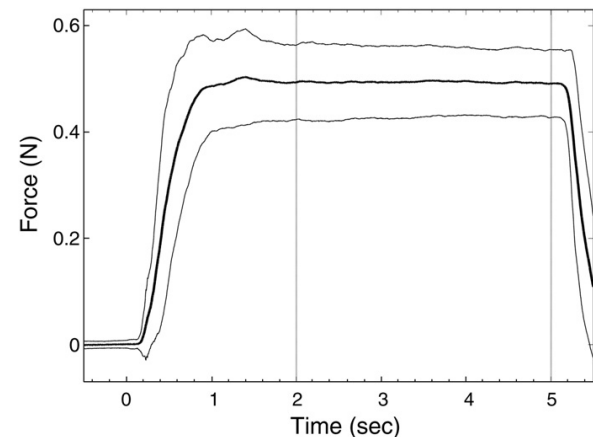


Fig. 1. Force output during task performance. Bold and thin lines show mean \pm SD for one typical subject. The vertical lines at 2 and 5 s mark the analyzed period. The force was measured in N (Newtons).

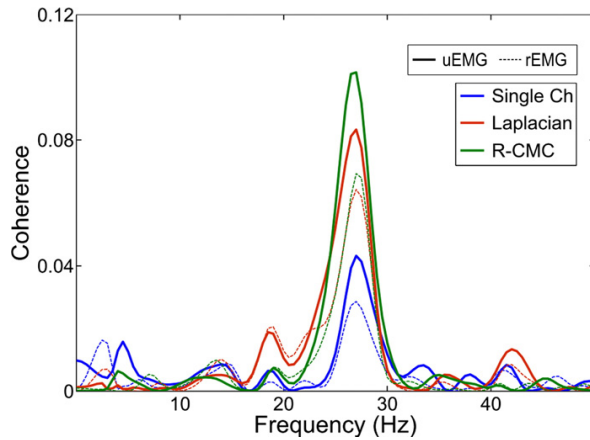


Fig. 2. CMC spectra calculated for single channel, Laplacian-filtered and R-CMC using rectified (rEMG) and un-rectified (uEMG) EMG data in a typical subject. Thick and thin lines correspond to un-rectified and rectified EMG, respectively.

Fig. 3. There was no significant difference between the strength of CMC related to rectified or un-rectified EMG ($p > .05$; a confidence interval for two-tailed paired t -test at 95% (CI): $[-0.070\ 0.008]$). The mean frequency of the coherence peaks for the single-channel analysis is shown in Fig. 4. There were no significant differences between the peak frequencies related to rectified vs. un-rectified EMG ($p > .05$; CI: $[-0.505\ 1.076]$).

Laplacian filtering

The maximum of the coherence values in the beta range (13 to 33 Hz) was found in the hemisphere contralateral to the performing hand. The mean and standard error of the coherence for rectified and un-rectified EMG are shown in Fig. 3. The statistical analysis showed that the coherence was smaller when being based on rectified EMG compared to the un-rectified EMG ($p < .05$; CI: $[0.005\ 0.023]$). The coherence spectrum for a representative subject is shown in Fig. 2. Topographical distributions of the coherence values for the Laplacian filtering are shown in Fig. 5. Note that the number of electrode

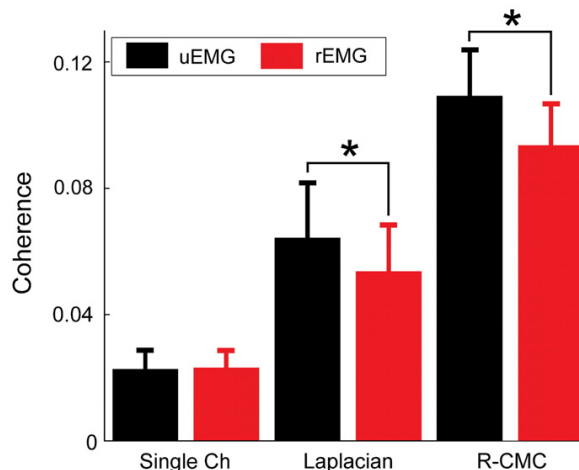


Fig. 3. Comparison of CMC values from three analysis methods when using rectified (rEMG) and un-rectified (uEMG) EMG. The error bars indicate standard error of the mean. The analysis was based on data across all subjects and left/right hand performances (* paired t -test, $p < 0.05$).

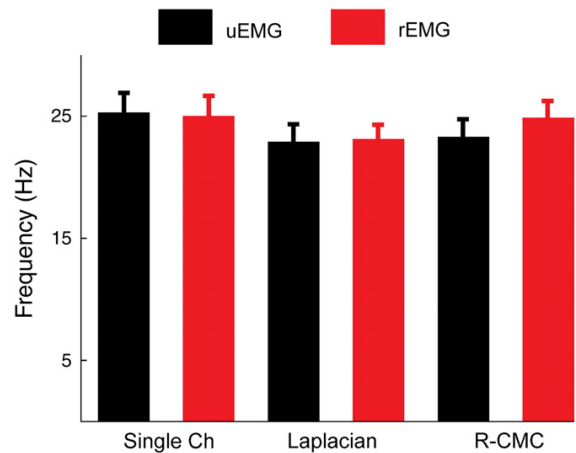


Fig. 4. CMC peak frequencies estimated by the three different analysis methods.

locations is limited to 22 Laplacian derivations. The mean frequency of the coherence peaks for the Laplacian analysis is shown in Fig. 4. There were no significant differences between the peak frequencies related to rectified vs. un-rectified EMG ($p > .05$; CI: $[-2.615\ 2.187]$).

R-CMC

Fig. 2 shows a characteristic enhancement of coherence spectrum at beta frequency for R-CMC in comparison to single-channel and Laplacian-filtered data. Corresponding spatial topographies, obtained with the R-CMC procedure for the un-rectified EMG (Fig. 6A), are shown in Fig. 6B. Note the pronounced contralateral activations with respect to the left or right hand performance. The strongest coherence peak was at about 27 Hz.

The mean values of the coherence for R-CMC approach with rectified and un-rectified EMG are shown in Fig. 3. For all the extracted components it was possible to show the presence of significant peaks in the coherence spectrum when using the permutation procedure. The R-CMC method showed that there was a significant effect of EMG rectification. In agreement with the data from the Laplacian filtering, coherence based on the R-CMC approach was smaller by about 14.4% for the rectified than un-rectified EMG ($p < .05$; CI: $[.006\ .026]$). The mean frequency of the coherence peaks for R-CMC analysis is shown in Fig. 4. There were no significant differences between peak frequencies related to rectified vs. un-rectified ($p > .05$; CI: $[-4.180\ 1.038]$).

To determine the cortical sources corresponding to the patterns obtained with the R-CMC method, we used sLORETA (Pascual-Marqui, 2002). Fig. 6C shows sLORETA solutions for the individual topography presented in Fig. 6B on average MNI head. Fig. 7 shows also a grand-average of sLORETA solutions across all subjects. For this grand-average, the voxels for each individual subjects were normalized by the sum of activity in all voxels (for a given subject). The results of the source reconstruction revealed the presence of the strongest activity in the contralateral sensorimotor cortex with a maximum in the precentral gyrus – corresponding to motor cortex.

Simulations

Fig. 8 presents the simulation results. Fig. 8B, shows that when the amplitude of an interfering source is weak both R-CMC and Laplacian methods detect peaks in the simulated frequency range, yet they are much weaker for the Laplacian approach. In the presence of a strong interfering source only the R-CMC approach recovered a clear and significant (permutation tests) peak. No significant peaks were detected with Laplacian filtering. Importantly, for both high and low

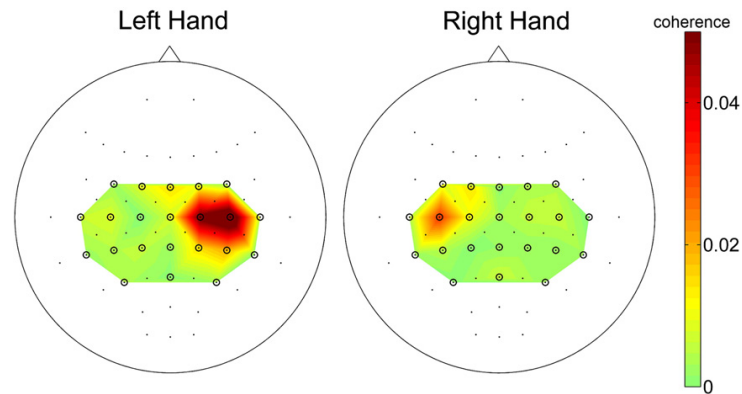


Fig. 5. The topographical distribution of CMC values estimated at 22 Laplacian derivations during left and right hand tasks from one typical subject. Locations of electrodes are marked with black points and Laplacian derivations (where CMC was calculated) are encircled.

amplitudes of the interfering source R-CMC errors in the recovery of the original patterns were quite small ($Err < 0.1$, Eq. (14)).

Discussion

In this study we presented and tested a novel method for CMC analysis based on multiple linear regression (R-CMC) which finds the spatial projection for EEG data maximizing the coherence between cortical and muscle activities. R-CMC and Laplacian filtering provided new insights on the contested necessity to rectify EMG for CMC analysis. Below we elaborate on the specific points of the study.

Estimation of CMC based on multiple regression

R-CMC is based on the idea of finding the linear combination of multiple EEG signals best explaining EMG. When finding a spatial filter (regression coefficients) one can use all EEG channels, which makes R-CMC distinctly different from other frequently used estimates of local EEG activity such as bipolar and Laplacian filtering. In the present study in order to reduce over-fitting and multi-collinearity between the predictor variables, we used PCA as a pre-processing step. Multi-collinearity occurs when the predictors, included in the regression model, are strongly correlated with each other, which often occurs in EEG recordings due to the volume

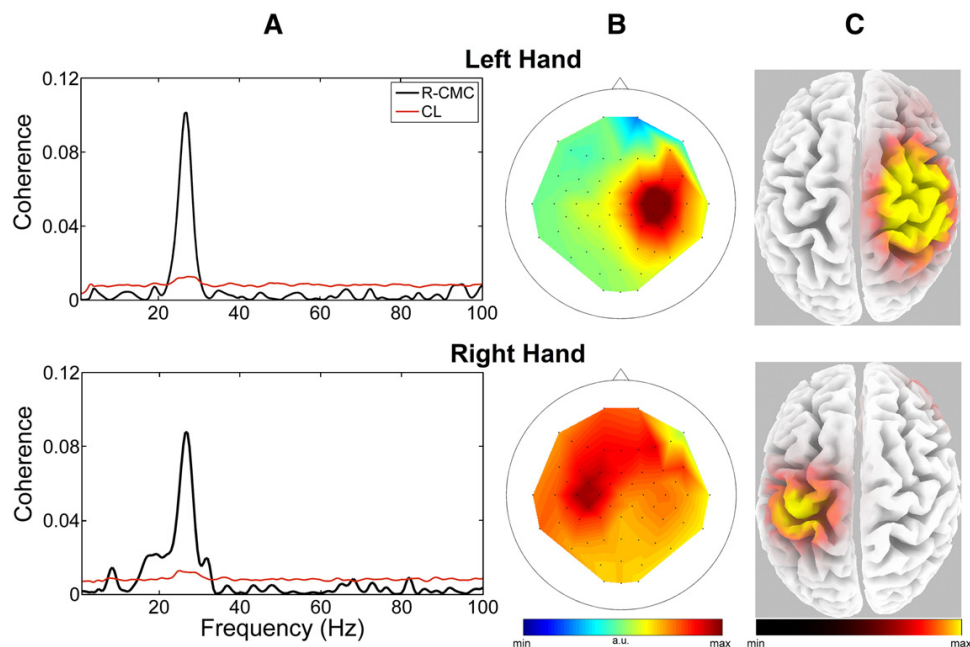


Fig. 6. R-CMC analysis for left and right hand performances of a typical subject (upper and lower panels, respectively). A) CMC spectrum. B) Scalp distribution of the component extracted with R-CMC, and C) cortical sources for the topography presented in B. CL: upper limit of the confidence limit (mean + 1.96 standard deviation of the shuffled data), a.u. – arbitrary units.

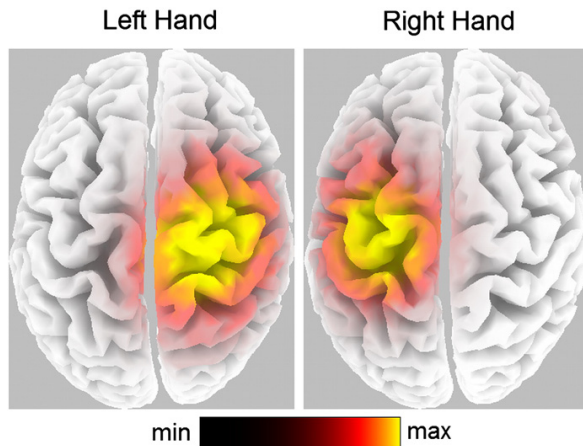


Fig. 7. Cortical sources of the coherent activity estimated with sLORETA. The normalized source maps were averaged across 7 subjects.

conduction. In case of multi-collinearity the covariance matrix tends to be singular, with the mean values not being very different across different analysis techniques. This indicates that similar neurophysiological processes were detected by all three types of CMC approaches. However, advantageously R-CMC allows recovery of the EEG topographies related to the cortical sources coherent with muscle activity. This in turn allows reconstructing neuronal sources with inverse modeling,

e.g., the sLORETA algorithm, which showed that the R-CMC topographies were modeled best by neuronal sources located at contralateral sensorimotor areas, with strongest activity in the pre-central gyrus corresponding to motor cortex. This finding is in agreement with previous studies where inverse modeling was used for localization of sensorimotor oscillations synchronous with muscle activity (Gross et al., 2001; Salenius et al., 1997; Schoffelen et al., 2008). Even using standard MNI template, we obtained functionally meaningful results for the location of the coherent cortical activity. This is due to the fact that sLORETA has low spatial resolution and thus, smoothes differences in individual locations of cortical sources between subjects providing approximate “center of gravity” localization.

R-CMC is different from approaches related to CMC estimation based on single channel (Yao et al., 2007), bipolar (Graziadio et al., 2010; Riddle and Baker, 2005), or Laplacian derivations (Mima and Hallett, 1999). In case of single channels the major drawback is that the recorded activity represents a massive superposition of the signals from multiple sources of beta oscillations, thus not allowing studying activity from specific cortical areas. Bipolar and Laplacian derivations act as spatial high-pass filters and partially alleviate the superposition problem. However, since these techniques do not take into account information from EMG, they can filter out neuronal oscillations contributing to CMC. Alternatively, beamformer techniques proved useful for CMC estimation (Gross et al., 2001; Schoffelen et al., 2008), yet they require massive statistical testing performed for each voxel. In addition, for very accurate results, at least in the case of EEG, beamforming requires detailed (e.g., MRI-based) information about the brain conductivity, which is not always available.

EMG rectification and CMC

EMG rectification and CMC

Farmer et al. (1993) estimated coherence between individual motor unit pairs of the same or separate intrinsic hand muscles and demonstrated a significant association between motor unit firings in

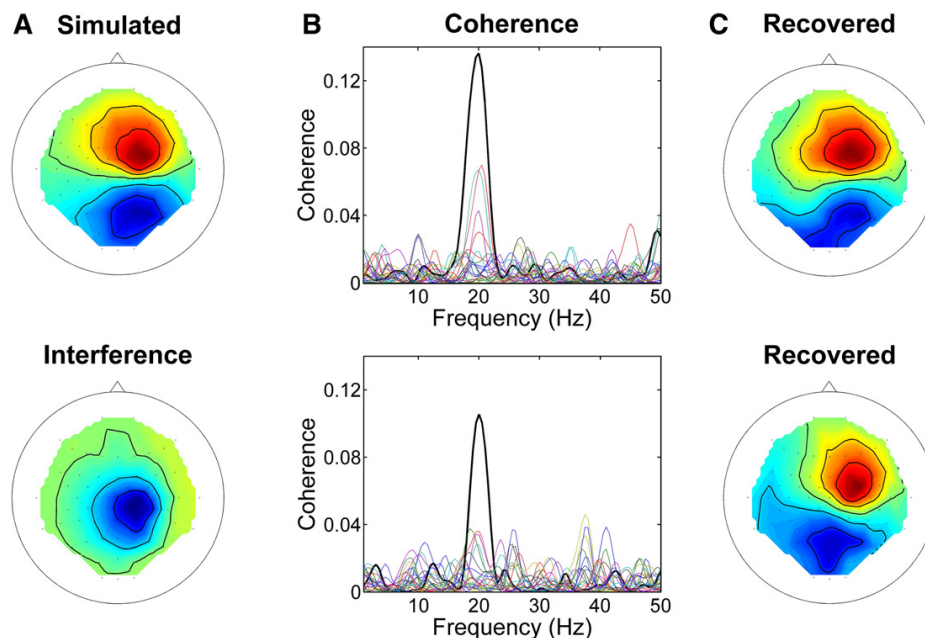


Fig. 8. A. Original patterns for the simulated CMC source (top) and a strong interfering source (bottom). B. Coherence spectra for the conditions in which the interfering source was equal (top) and 20 times stronger (bottom) than the CMC source. The thick black line represents the coherence spectrum estimated by the R-CMC approach and the colored lines represent coherence spectra estimated by Laplacian filtering at different EEG derivations. C. The patterns recovered by R-CMC in the presence of the equal (top) and 20 times stronger (bottom) interfering source, the recovery errors for the patterns were 0.033 and 0.092, respectively.

the 1–12 Hz and 16–32 Hz ranges. By comparing recordings from healthy subjects, and patients with peripheral and central lesions, they concluded that the synchronization between motor units at 16–32 Hz was a result of central input rather than peripheral afferent pathways. Conway et al. (1995) supported this hypothesis and demonstrated for the first time the existence of CMC between MEG and rectified surface EMG. Only in a separate paper, Halliday et al. (1995) stated that the surface EMG is rectified in order to remove waveform artifacts. Although it has been recognized that it is difficult to interpret a rectified EMG signal, the authors stated the rationale behind EMG rectification as an approach to enhance detectability of motor unit action potential (MUAP) timing, and for this reason limited their analysis to the frequency range below 50 Hz. Although these low frequencies are related to MUAP firing rate, EMG signals are usually high pass filtered and rectified in order to shift the spectral power from higher frequencies (mostly related to MUAP shape) towards the lower frequency range as shown by Myers et al. (2003) and Neto and Christou (2010).

Although rectification has been widely used as pre-processing step, its effect on CMC was explicitly addressed for the first time by Myers et al. (2003) who validated the hypothesis of Halliday et al. (1995) in a simulation study. They suggested that enhancing MUAP timing by rectification could also make coherence more visible but they did not confirm this idea with empirical data.

Yao et al. (2007) studied the effect of rectification empirically, using EEG and MEG recordings. They confirmed that rectification improved the identification of motor unit firing rates in the EMG power spectrum; nevertheless, there was no difference in coherence estimates between rectified and un-rectified signals. Notably, this conclusion might be limited by suboptimal spatial filtering, which we discuss below.

In the present study, we utilized single-channel, Laplacian filtering and R-CMC in order to address the effect of EMG rectification on CMC. For single channel data we found no significant changes in CMC strength when comparing rectified to un-rectified EMG, thus reconfirming the results of Yao et al. (2007). On the contrary, for both Laplacian and R-CMC methods EMG rectification resulted in significantly decreased coherence values compared to the un-rectified EMG. Such reduction has been suggested by recent simulation study (Stegeman et al., 2010). In a detailed modeling study, Stegeman et al. (2010) showed that the transmission of central rhythmic activity to EMG relates directly to the spectral content of EMG and the coupling strength between alpha motor neurons and EMG is not frequency dependent in a relatively broad frequency range. On the other hand, EMG rectification resulted in a frequency dependence of the spectral content of EMG with respect to the varying central rhythms. Moreover, EMG rectification significantly attenuated the coherence between the alpha-motor neuron pool and EMG. In addition, Neto and Christou (2010) showed in their modeling study that the power spectrum of un-rectified EMG correctly detects changes in the oscillatory input, while the power spectrum of rectified EMG did not. These results from Stegeman et al. (2010) and Neto and Christou (2010) indicate that EMG rectification could strongly impair the estimation of CMC, which indeed was observed in the present study.

We provide the following explanation for why Laplacian filtering and the new R-CMC method are superior for the detection of EMG rectification effects on CMC compared to single-channel results as reported here and in Yao et al. (2007). Laplacian and R-CMC methods act as spatial high-pass filters thus eliminating interference from other CMC-irrelevant neuronal sources. The latter are usually adding up to neuronal activity directly related to CMC. Such superposition of EEG activity from multiple sources leads in turn to smaller CMC values. In case of excessive amounts of such additive undesirable activity, a “floor” effect might occur when the true CMC is so heavily affected/reduced by the irrelevant neuronal activity that there might be simply no possibility to see differences in CMC strength with or

without EMG rectification. Indeed, our analysis revealed that the smallest CMC values were obtained for the single channel data (Fig. 3). As we have shown in our simulation, Laplacian filtering is susceptible to interfering sources and thus, the R-CMC approach provides a safety margin for dealing with interfering sources. For datasets with exceedingly high levels of interfering sources (both neuronal and extra-neuronal origin, e.g. from scalp muscles) the use of only Laplacian filtering can miss the effects of EMG rectification as in the case of the single-channel approach. Therefore, methods more robust than Laplacian filtering (e.g., beamformers or R-CMC) should be used.

In conclusion, we have developed a novel method for CMC detection based on multiple regression. The method maximizes CMC and allows the extraction of EEG topographies, which can be used for an inverse localization of neuronal sources. In agreement with previous predictions from modeling studies, both R-CMC and Laplacian filtering provided converging evidence suggesting that CMC can be reduced for rectified EMG.

Acknowledgments

Z.B., V.V.N, and G.C. were supported by the Center for Stroke Research Berlin, and V.V.N and G.C. were additionally supported by the Berlin Bernstein Center for Computational Neuroscience.

References

- Andrykiewicz, A., Patino, L., Naranjo, J.R., Witte, M., Hepp-Reymond, M.-C., Kristeva, R., 2007. Corticomuscular synchronization with small and large dynamic force output. *BMC Neurosci.* 8, 101.
- Baker, S.N., 2007. Oscillatory interactions between sensorimotor cortex and the periphery. *Curr. Opin. Neurobiol.* 17 (6), 649–655.
- Baker, M.R., Baker, S.N., 2002. The effect of diazepam on motor cortical oscillations and corticomuscular coherence studied in man. *J. Physiol.* 546 (3), 931–942.
- Baker, S.N., Olivier, E., Lemon, R.N., 1997. Coherent oscillations in monkey motor cortex and hand muscle EMG show task-dependent modulation. *J. Physiol.* 501 (1), 225–241.
- Baker, S.N., Kilner, J.M., Pinches, E.M., Lemon, R.N., 1999. The role of synchrony and oscillations in the motor output. *Exp. Brain Res.* 128 (1–2), 109–117.
- Collins, D.L., Neelin, P., Peters, T.M., Evans, A.C., 1994. Automatic 3D intersubject registration of MR volumetric data in standardized Talairach space. *J. Comput. Assist. Tomogr.* 18 (2), 192–205.
- Conway, B.A., Halliday, D.M., Farmer, S.F., Shahani, U., Maas, P., Weir, A.I., Rosenberg, J.R., 1995. Synchronization between motor cortex and spinal motoneuronal pool during the performance of a maintained motor task in man. *J. Physiol.* 489 (3), 917–924.
- Donoghue, J.P., Sanes, J.N., Hatsopoulos, N.G., Gaál, G., 1998. Neural discharge and local field potential oscillations in primate motor cortex during voluntary movements. *J. Neurophysiol.* 79 (1), 159–173.
- Evans, A.C., Kamber, M., Collins, D.L., MacDonald, D., 1994. An MRI-based probabilistic atlas of neuroanatomy. In: Shorvon, S., et al. (Ed.), *Magnetic Resonance Scanning and Epilepsy*. Plenum, New York, pp. 263–274.
- Farmer, S.F., Bremner, F.D., Halliday, D.M., Rosenberg, J.R., Stephens, J.A., 1993. The frequency content of common synaptic inputs to motoneurons studied during voluntary isometric contraction in man. *J. Physiol.* 470 (1), 127–155.
- Gonzalez Andino, S.L., Pascual Marqui, R.D., Valdes Sosa, P.A., Biscay Lirio, R., Machado, C., Diaz, G., Figueredo Rodriguez, P., Castro Torrez, C., 1990. Brain electrical field measurements unaffected by linked earlobes reference. *Electroencephalogr. Clin. Neurophysiol.* 75 (3), 155–160.
- Graziadio, S., Basu, A., Tomasevic, L., Zappasodi, F., Tecchio, F., Eyre, J.A., 2010. Developmental tuning and decay in senescence of oscillations linking the corticospinal system. *J. Neurosci.* 30 (10), 3663–3674.
- Gross, J., Kujala, J., Hämäläinen, M., Timmermann, L., Schnitzler, A., Salmelin, R., 2001. Dynamic imaging of coherent sources: studying neural interactions in the human brain. *PNAS* 98 (2), 694–699.
- Halliday, D.M., Rosenberg, J.R., Amjad, A.M., Breeze, P., Conway, B.A., Farmer, S.F., 1995. A framework for the analysis of mixed time series/point process data-theory and application to the study of physiological tremor, single motor unit discharges and electromyograms. *Prog. Biophys. Mol. Biol.* 64 (2–3), 237–278.
- Halliday, D.M., Conway, B.A., Farmer, S.F., Rosenberg, J.R., 1998. Using electroencephalography to study functional coupling between cortical activity and electromyograms during voluntary contractions in humans. *Neurosci. Lett.* 241 (1), 5–8.
- Hesterberg, T., Moore, D.S., Monaghan, S., Clipson, A., Epstein, R., 2005. Bootstrap methods and permutation tests. In: Moore, D.S., McCabe, G.P. (Eds.), *Introduction to the Practice of Statistics*, 5th edition. W.H. Freeman, New York.
- Jackson, A., Spinks, R.L., Freeman, T.C.B., Wolpert, D.M., Lemon, R.N., 2002. Rhythm generation in monkey motor cortex explored using pyramidal tract stimulation. *J. Physiol.* 541 (3), 685–699.

- Kilner, J.M., Baker, S.N., Salenius, S., Hari, R., Lemon, R.N., 2000. Human cortical muscle coherence is directly related to specific motor parameters. *J. Neurosci.* 20 (23), 8838–8845.
- Kristeva, R., Patino, L., Omlor, W., 2007. Beta-range cortical motor spectral power and corticomuscular coherence as a mechanism for effective corticospinal interaction during steady-state motor output. *Neuroimage* 36 (3), 785–792.
- Kristeva-Feige, R., Fritsch, C., Timmer, J., Lücking, C.-H., 2002. Effects of attention and precision of exerted force on beta range EEG-EMG synchronization during a maintained motor contraction task. *Clin. Neurophysiol.* 113 (1), 124–131.
- Mima, T., Hallett, M., 1999. Electroencephalographic analysis of cortico-muscular coherence: reference effect, volume conduction and generator mechanism. *Clin. Neurophysiol.* 110 (11), 1892–1899.
- Murthy, V.N., Fetz, E.E., 1992. Coherent 25- to 35-Hz oscillations in the sensorimotor cortex of awake behaving monkeys. *PNAS* 89 (12), 5670–5674.
- Myers, L.J., Lowery, M., O'Malley, M., Vaughan, C.L., Heneghan, C., St Clair Gibson, A., Harley, Y.X.R., Sreenivasan, R., 2003. Rectification and non-linear pre-processing of EMG signals for cortico-muscular analysis. *J. Neurosci. Methods* 124 (2), 157–165.
- Neto, O.P., Christou, E.A., 2010. Rectification of the EMG signal impairs the identification of oscillatory input to the muscle. *J. Neurophysiol.* 103 (2), 1093–1103.
- Nolte, G., Dassios, G., 2005. Analytic expansion of the EEG lead field for realistic volume conductors. *Phys. Med. Biol.* 50, 3807–3823.
- Oldfield, R.C., 1971. The assessment and analysis of handedness: the Edinburgh inventory. *Neuropsychologia* 9 (1), 97–113.
- Pascual-Marqui, R.D., 2002. Standardized low-resolution brain electromagnetic tomography (sLORETA): technical details. *Methods Find. Exp. Clin. Pharmacol.* 24D, 5–12.
- Parra, L., Alvino, C., Tang, A., Pearlmutter, B., Yeung, N., Osman, A., Sajda, P., 2002. Linear spatial integration for single-trial detection in encephalography. *Neuroimage* 17 (1), 223–230.
- Penfield, W., 1954. Mechanisms of voluntary movement. *Brain* 77 (1), 1–17.
- Riddle, C.N., Baker, S.N., 2005. Manipulation of peripheral neural feedback loops alters human corticomuscular coherence. *J. Physiol.* 566 (2), 625–639.
- Riddle, C.N., Baker, S.N., 2006. Digit displacement, not object compliance, underlies task dependent modulations in human corticomuscular coherence. *Neuroimage* 33 (2), 618–627.
- Rosenberg, J.R., Amjad, A.M., Breeze, P., Brillinger, D.R., Halliday, D.M., 1989. The Fourier approach to the identification of functional coupling between neuronal spike trains. *Prog. Biophys. Mol. Biol.* 53 (1), 1–31.
- Sağlam, M., Matsunaga, K., Murayama, N., Hayashida, Y., Huang, Y.-Z., Nakanishi, R., 2008. Parallel inhibition of cortico-muscular synchronization and cortico-spinal excitability by theta burst TMS in humans. *Clin. Neurophysiol.* 119 (12), 2829–2838.
- Salenius, S., Hari, R., 2003. Synchronous cortical oscillatory activity during motor action. *Curr. Opin. Neurobiol.* 13 (6), 678–684.
- Salenius, S., Portin, K., Kajola, M., Salmelin, R., Hari, R., 1997. Cortical control of human motoneuron firing during isometric contraction. *J. Neurophysiol.* 77 (6), 3401–3405.
- Schnitzler, A., Gross, J., Timmermann, L., 2000. Synchronised oscillations of the human sensorimotor cortex. *Acta Neurobiol. Exp.* 60 (2), 271–287.
- Schoffelen, J.-M., Oostenveld, R., Fries, P., 2008. Imaging the human motor system's beta-band synchronization during isometric contraction. *Neuroimage* 41 (2), 437–447.
- Stegeman, D.F., van de Ven, W.J.M., van Elswijk, G.A., Oostenveld, R., Kleine, B.U., 2010. The alpha-motoneuron pool as transmitter of rhythmicities in cortical motor drive. *Clin. Neurophysiol.* 121 (10), 1633–1642.
- Tsujimoto, T., Mima, T., Shimazu, H., Isomura, Y., 2009. Directional organization of sensorimotor oscillatory activity related to the electromyogram in the monkey. *Clin. Neurophysiol.* 120 (6), 1168–1173.
- Witham, C.L., Wang, M., Baker, S.N., Nelson, R.J., 2010. Corticomuscular coherence between motor cortex, somatosensory areas and forearm muscles in the monkey. *Neuroscience* 4, 38.
- Yao, B., Salenius, S., Yue, G.H., Brown, R.W., Liu, J.Z., 2007. Effects of surface EMG rectification on power and coherence analyses: an EEG and MEG study. *J. Neurosci. Methods* 159 (2), 215–223.

3.1. Update on the EMG-rectification debate

After publication of the current paper, the very active debate on EMG rectification continued (Boonstra and Breakspear, 2012; McClelland et al., 2012; Farina et al., 2013; Ward et al., 2013; Dakin et al., 2014; McClelland et al., 2014; Farmer and Halliday, 2014; Negro et al., 2015). Boonstra and Breakspear (2012) suggested that the effect of rectification may depend on the heterogeneity of MUAP shapes. The simulation data was supported by experimental recordings of intermuscular coherence in subjects standing quietly. The authors concluded that in heterogeneous MUAP populations rectification improved coherence because the common drive, which has been canceled out, was recovered by rectification. Further, Ward et al. (2013) found rectification to be advantageous at very low force levels, i.e. finger extension against gravity. At higher force levels there was no difference for rectified and raw EMG signal. Aiming at elucidating the issue when to rectify or not, the degree of amplitude cancellation was accounted for the effectiveness of rectification in extracting common oscillatory inputs (Farina et al., 2013; Negro et al., 2015): rectification was identified as advantageous when the level of amplitude cancellation was low. The level of amplitude cancellation changes with contraction level, fatigue, or across subjects and muscles making comparisons across conditions that differ in the level of cancellation complicated. At the same time, such a dependency on amplitude cancellation was not found using the raw EMG signal. In line with the amplitude-cancellation hypothesis, the advantageous effect of rectification at low force levels (Ward et al., 2013) can be attributed to little amplitude cancellation (Farina et al., 2013). The hypothesis also explains the observation by Boonstra and Breakspear (2012): the uniformity of MUAP shapes influences the degree of cancellation. Thereby, the amplitude cancellation is maximal when shapes all are the same and decreases with increasing heterogeneity of the shapes. Adding to their previous study (Farina et al., 2013), Negro et al. (2015) concluded that rectification is beneficial for studying low frequency oscillations (delta and alpha frequency bands) with short-duration action potentials and low level of amplitude cancellation. However, as also McClelland et al. (2014) pointed out, it may be difficult to tell whether a change in coherence is due to a genuine physiological change or the variable effect of rectification. Further, Negro et al. (2015) noted that rectification may distort the estimation of common synaptic inputs at beta and gamma frequency bands. However, these are the frequency bands where CMC is generally studied.

In conclusion, several cases where EMG full-wave rectification might be beneficial have been identified by the abovementioned studies. They presented simulations to predict

empirical results (Boonstra and Breakspear, 2012) and supported them with theoretical framework (Farina et al., 2013; Negro et al., 2015). However, the non-linear step of rectification does have a very complex effect on the signal leading to a distortion of the frequency content of the signal. The effectiveness of rectification depends on a range of factors including the force level and the frequency band at which coherence is studied. In consequence, the effect of rectification becomes inconsistent which is particularly problematic when comparing conditions where those factors differ.

In addition, some papers find no negative effect of rectification, e.g. at slightly higher force levels (Ward et al., 2013). However, paper I shows that this might be due to the method used to detect coherence. Methods like R-CMC that employ spatial filtering may be more sensitive to detect differences that are otherwise buried by a superposition of unrelated cortical sources (this point is more extensively discussed in paper I). Thus, to safeguard against potentially unpredictable effects, in many cases the use of the unrectified EMG signal may be the preferential choice. Consequently, the general statement of paper I rather arguing against rectification is not to be reinterpreted in view of studies published afterwards. There could however be additional cases where rectification may prove beneficial. Therefore, in new paradigm settings it may be appropriate to compare results from both analyses. Nevertheless, it remains interesting that despite rectification being a non-linear step with complex, unpredictable effects on the frequency content, the obtained peak frequencies of CMC are very similar for the rectified and unrectified EMG signal.

3.2. Limitations and outlook

The current paper presented a new method for the extraction of spatial filters optimizing CMC detection. The method is based on multiple linear regression taking all EEG channels into account at a time. In addition, the topography of CMC-related activity can be retrieved which allows for source localization. Furthermore, the paper provided empirical evidence that EMG rectifications impairs CMC estimation as it had been predicted from simulation studies.

Sensitivity of the method The paper compared the results of the R-CMC method to those obtained from Laplacian filtering which has spatially fixed weights (see also Section 2.5.3). The R-CMC method individually optimizes the channel weights resulting in CMC peak amplitudes that were significantly larger. One potential problem of such

optimization is overfitting which will be discussed in the next section.

Yet, in simulations, where background noise was very strong, R-CMC could still reliably detect coherence and thereby outperformed Laplacian filtering. Nevertheless, in empirical data, some subjects still remained where CMC could not be detected using the R-CMC method. One explanation is that these people simply do not have CMC. However, at least in some of these subjects, this may also be due to a great day-to-day variability (Pohja et al., 2005; von Carlowitz-Ghori et al., 2015): on some days CMC may be detectable and on others not. Thus, these cases offer the possibility to enhance the detectability of CMC. The method SPoC (Dähne et al., 2014) allows to extract neuronal components whose power highly correlate with a target variable. However, sample tests did not indicate a better CMC estimation than the R-CMC method (data not shown).

Overfitting One problem that might occur when optimizing spatial filters is overfitting, i.e. the filter optimizes to fluctuations in the data caused by noise/unrelated activity. In the current paper, the spatial filter was optimized on the very same data as it was later applied to. Therefore, precautions were taken to avoid overfitting:

- In order to avoid collinearity of predictors (EEG channels) PCA was employed after visual inspection of the data and prior to regression significantly reducing the number of predictors.
- CMC peak values were verified using permutation tests (Hesterberg et al., 2005) where EMG segments were shuffled destroying the temporal relationship between projected EEG and EMG signals.

Another way to show generalizability of the method would have been e.g. (leave-one-out) cross validation. At the time point of analysis however, this method was too time-consuming and results of permutation tests were comparable.

In addition to the precautions taken, the results of the R-CMC analysis make overfitting for several reasons unlikely:

- CMC peaks values, usually, exceeded the values obtained from random/permutated data by far (and were not just barely above significance level).
- CMC patterns corresponding sLORETA solutions were neurophysiologically meaningful indicating sources in the contralateral sensorimotor areas.

- Generalizability of the filters is demonstrated in the neurofeedback study (paper IV, Chapter 6): spatial filters which were applied during online feedback had been optimized on a preceding training session; subjects were able to use them successfully for neurofeedback.

Increasing the number of EMG channels In the current paper (as well as in the other three papers), the one EMG channel was always selected among the three or more channels which resulted in the largest coherence. This selective choice however means that additional information corresponding to corticomuscular interaction might still be contained in the data which is however weaker and therefore disregarded by the R-CMC method. Therefore, multiple regression could be replaced by canonical correlation allowing to include both all EEG channels and all EMG channels into analysis. Possibly, these may lead to the identification of multiple sources associated with the different positions on the muscle due to different corticomuscular innervation patterns. In addition, with canonical correlation one could also obtain a pattern that corresponds to the muscular activity. Here, the number of EMG channels could be greatly enlarged, e.g. using a high-density surface EMG grid (Steeg et al., 2014).

Amplitude modulation in cortico-spinal interaction 4

The previous chapter was concerned with the detection of coherence as a measure of phase-relationship in corticospinal interaction. The current paper now also considers amplitude modulations of sensorimotor oscillations in their relationship between cortex and spinal cord. Generally, amplitude and phase are two measures of a signal that can change independently of each other (see also Section 2.2.2). Thus, mathematically the presence of phase synchronization between cortex and muscles does not allow conclusions to be drawn regarding amplitude modulations; a relationship between the two measures in corticospinal interaction may arise due to cortical dynamics and can therefore only be addressed empirically.

Amplitude modulations are thought to reflect local synchronization within neuronal groups. Figure 4.2 illustrates how amplitude dynamics reflecting local neuronal synchronization can also correlate between cortex and spinal cord. Such a relationship of amplitude modulation could be detected in the majority of subjects in the current paper using amplitude-envelope correlations of beta oscillations.

4. Amplitude modulation in cortico-spinal interaction

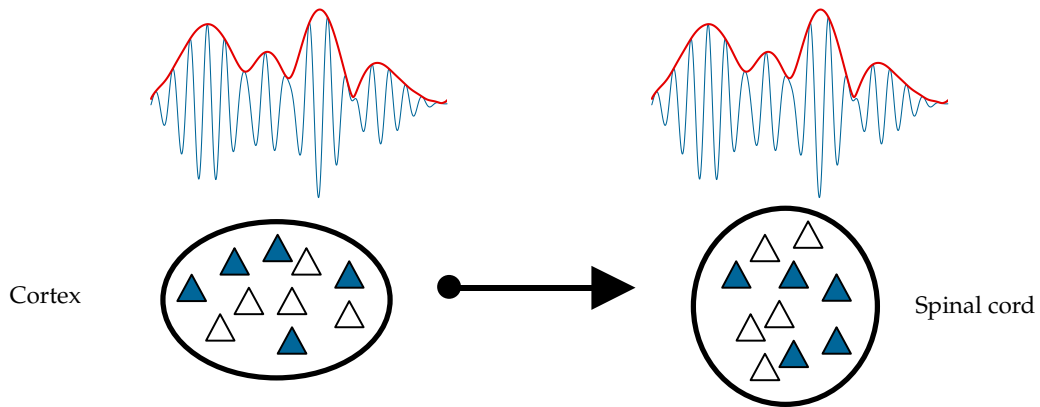


Figure 4.1.: Correlation of local cortical and spinal-cord synchronization: the amplitude envelopes of the signals derived from two neuronal populations show the same modulation.

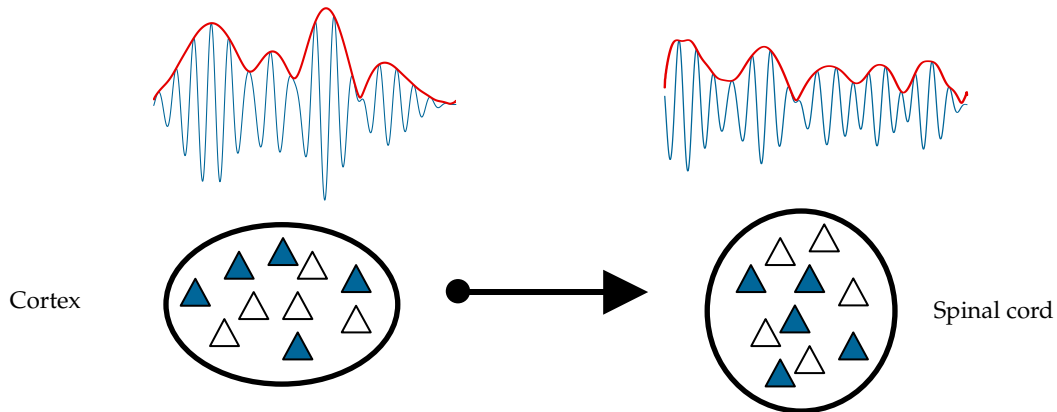


Figure 4.2.: Local cortical and spinal-cord synchronization are uncorrelated: the amplitude envelopes of the signals show a different modulation.



It is not all about phase: Amplitude dynamics in corticomuscular interactions

Zubeyir Bayraktaroglu^{a,b}, Katherina von Carlowitz-Ghori^a, Gabriel Curio^{a,b,c}, Vadim V. Nikulin^{a,b,c,*}

^a Neurophysics Group, Department of Neurology, Charité – Universitätsmedizin, Campus Benjamin Franklin, 12203, Berlin, Germany

^b Center for Stroke Research Berlin, Charité – Universitätsmedizin, Campus Mitte, 10117, Berlin, Germany

^c Bernstein Center for Computational Neuroscience, 10115, Berlin, Germany

ARTICLE INFO

Article history:

Accepted 26 August 2012

Available online 30 August 2012

Keywords:

Amplitude envelope

Phase coupling

Corticomuscular coherence

Synchronization

Beta oscillation

Event-related desynchronization

ABSTRACT

Corticomuscular interactions are studied mostly with EEG/EMG coherence, which, however, does not allow quantification of amplitude dynamics of sensorimotor oscillations. Here, we investigated the amplitude dynamics of sensorimotor EEG beta oscillations during an isometric task and their relation to corticomuscular coherence (CMC). We used amplitude envelopes of beta oscillations, derived from multichannel EEG and EMG recordings, as a measure of local cortical and spinal-cord synchronization. In general, we showed that the amplitude of cortical beta oscillations can influence CMC in two ways. First, we showed that the signal-to-noise ratio of pre-stimulus beta oscillations affects CMC. Second, we demonstrated that the attenuation of beta oscillations upon imperative stimulus correlated with the CMC strength. Attenuation of cortical beta oscillations was previously hypothesized to reflect increased motor cortex excitability. Consequently, this correlation might indicate that high cortical excitability, produced by imperative stimulus, facilitates the recruitment of neuronal networks responsible for establishing reliable corticospinal control manifested in larger CMC. Critically, we demonstrated that the amplitude envelopes of beta oscillations in EEG and EMG are positively correlated on time scales ranging from 50 to 1000 ms. Such correlations indicate that the amplitude of cortical beta oscillations might relate to the rhythmic spiking output of both corticospinal neurons and their spinal targets. Compared to CMC, however, amplitude-envelope correlations were detected in fewer cases, which might relate to a higher susceptibility of these correlations to signal-to-noise ratio. We conclude that EEG beta oscillations, originating from the sensorimotor cortex, can transmit not only their phase but also amplitude dynamics through the spinal motoneurons down to peripheral effectors.

© 2012 Elsevier Inc. All rights reserved.

Introduction

Corticospinal interactions in humans are usually studied with corticomuscular coherence (CMC, Baker, 2007; Jackson et al., 2002; Kilner et al., 2000; Kristeva et al., 2007; Salenius et al., 1997; Schnitzler et al., 2000). While the presence of CMC indicates that the phase of sensorimotor beta oscillations tightly relates to the spiking of muscle motor units, little is known about the relation of beta oscillations' amplitude to the amplitude of muscular oscillations and to CMC in general. Yet, amplitude dynamics are as important for understanding neuronal interactions as frequently used phase synchronization as has been demonstrated in recent modeling experiments (Daffertshofer and van Wijk, 2011). The present study investigated the relation between the amplitude dynamics of cortical and muscle beta oscillations as well as the effect of beta-oscillation amplitude reactivity on CMC.

It has long been assumed that the amplitude of local field potentials (LFP) and EEG signals represents spatially averaged synaptic activity (Mitzdorf, 1985). Recently, it was shown that LFPs reflect fluctuation

in membrane potential due to a common synaptic drive to a given network (Okun et al., 2010; Poulet and Petersen, 2008). In general, stronger synchronization between neurons corresponds to larger amplitude in LFP/EEG signals (Denker et al., 2011; Elul, 1971; Pfurtscheller and Lopes da Silva, 1999). In contrast, EMG reflects primarily motor-unit action potentials and therefore increased amplitude of EMG bursts in a relatively narrow frequency band indicates a larger number of synchronously firing spinal motor units (Christou et al., 2007; Halliday et al., 1995). Therefore, studying amplitude envelopes of neuronal oscillations might clarify whether the dynamics of local synchronization on the cortical level are accompanied by similar changes in the synchronization between motoneurons in the spinal cord. Critically, the presence of CMC per se does not indicate whether the strength of local dynamics (reflected in amplitude) in the spinal cord and cortex are related as well. Fig. 1 illustrates how phase synchronization (measured for instance with coherence) can be present with and without concurrent amplitude-envelope correlations. An important feature of amplitude-envelope correlations (also known as transient coding, Friston, 1997) is that it is not reducible to rate or synchrony coding. It rather shows how intrinsic dynamics of two distinct spatially remote neuronal populations can be similarly modulated.

* Corresponding author at: Charité – Universitätsmedizin, Campus Benjamin Franklin, Neurologie, AG Neurophysik, Hindenburgdamm 30, 12203, Berlin, Germany.
E-mail address: vadim.nikulin@charite.de (V.V. Nikulin).

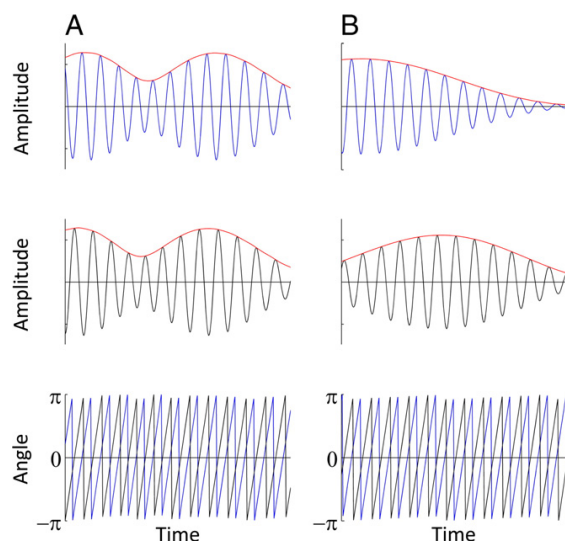


Fig. 1. A scheme for showing a dissociation between phase synchronization and amplitude-envelope correlation. A. A case where amplitude envelopes (red) covary between the two oscillatory processes (blue and black), also there is a constant phase lag (i.e. phase synchronization) between the phases of the processes (lower sub-fig.). B. Phase locking is still present, but amplitude envelopes do not covary. (For interpretation of the references to color in this figure legend, the reader is referred to the web version of this article.)

Therefore, we investigated how the amplitude of beta oscillations can affect CMC. In general, the amplitude of sensorimotor oscillations can influence CMC in two different ways. On the one hand, the signal-to-noise ratio (SNR) of these oscillations may have an effect on the extraction of phase information from the signals (Muthukumaraswamy and Singh, 2011), thus contributing to a better estimation of CMC. For studying the effects of SNR on CMC we used the relative power of beta oscillations in the pre-stimulus interval. On the other hand, amplitude dynamics of neuronal oscillations (due to the task performance) can also neurophysiologically relate to the changes in CMC. To study this dependency we used the correlation of CMC with event related desynchronization (ERD), the latter being a measure of amplitude reactivity (Pfurtscheller and Lopes da Silva, 1999). The relationship between the reactivity of oscillations and CMC might provide a plausible explanation for how specific preceding neuronal states affect upcoming performance requiring precise coordination between phases and amplitudes of cortical and spinal cord neuronal populations.

Materials and methods

Subjects

We studied 11 healthy volunteers (7 males and 4 female), and mean age was 47.7 ± 7.6 (mean \pm SD). Subjects were without any history of neurological or psychiatric disorders. The experimental protocol was approved by the Institutional Review Board of Charité, Berlin, and the subjects gave their written informed consent prior to the experiments. All subjects were right-handed according to the Edinburgh Handedness Inventory (Oldfield, 1971) and had normal or corrected to normal vision.

Paradigm

We used a digit displacement paradigm, which includes a manipulation of a compliant object because CMC was found larger when the

task involved a compliant object compared to a simple isometric condition (Kilner et al., 2000; Riddle and Baker, 2006).

During the experiment the subjects were seated in a comfortable chair, with their arms resting on the chair handles, forearms flexed at 60° , and hands pronated. Subjects were instructed to press a spring-loaded lever with the left or right thumb with a 0.5 newton (N) force, requiring a lever displacement of ~ 3.5 cm. The force was measured with a load sensor (FSG15N1A, Honeywell, USA). Visual feedback of the force level was provided on a computer screen as a horizontal bar of varying lateral extents proportional to the exerted force with fixed vertical lines indicating the target value. A cross in the center of the screen served as an eye-fixation point.

The task was performed with each hand separately and the hand order was counter-balanced between the subjects. In total, one hundred trials were recorded for each hand in four blocks. The subjects were instructed to reach a 0.5 N force level as fast as possible after a single tone and maintain it constant until the presentation of a double tone. In 6 subjects each trial lasted 9 s (5 s pressing and 4 s rest) and in 5 subjects the trial lasted 8 s (4 s pressing and 4 s rest). There were 60 s of rest between the blocks.

Data acquisition

EEG and EMG data were acquired with BrainAmp MR-plus (Brain Products, Germany) amplifiers, filtered in the frequency range of 0.015–250 Hz and sampled at 1000 Hz. The voltage resolution for the EEG and EMG channels was 0.1 μ V and 0.5 μ V, respectively.

EEG

During the acquisition, the EEG was referenced to physically linked earlobes and recorded using an EEG cap (61 Ag/AgCl sintered ring electrodes, EasyCap, Germany) with electrodes having a higher density above the sensorimotor cortices. As verified empirically, physically linked-earlobes did not lead to the distortion of voltage topographies (Gonzalez Andino et al., 1990). Ocular artifacts were recorded with two electrodes placed on the right zygomatic and supraorbital processes.

EMG

We recorded EMG from the abductor pollicis brevis (APB) muscle with three EMG electrodes (Ag/AgCl sintered electrodes 4 mm in diameter) over the thenar side of each hand. The skin surface was abraded with NuPrep (Weaver and Co., USA) before the electrode application. The electrode-skin conductive contact was established with a Ten20 electrode paste (Weaver and Co., USA), and the electrodes were secured to the skin with an adhesive medical tape.

An EMG reference electrode was placed on the styloid process of the ulnar bone and a ground electrode on the inner surface of the wrist at the midline. Ag/AgCl sintered electrodes 12 mm in diameter were used for reference and ground. The following analysis has been performed for all three EMG electrodes located over the thenar side while each of them was referenced to the reference electrode.

Analysis

All data and statistical analyses were performed offline using MATLAB (Mathworks Inc., USA) with custom written functions.

Data preprocessing

The analysis was based on the stable hold period of the task, during which the strongest CMC in the beta band has been shown before (Baker et al., 1997; Kristeva et al., 2007; Riddle and Baker, 2006). For the following statistical analysis we chose the data in the post-stimulus interval between 2 and 4 s after the start tone as a period showing a stable force production. The data were visually inspected for the presence of abrupt force changes in the hold period.

If the force output deviated from the range 0.5 ± 0.1 N, the epoch was discarded. After artifact rejection 322 ± 54 and 311 ± 41 segments (500-ms duration) for the left and right hands, respectively, were utilized for the further analysis.

Signal processing

Corticomuscular coherence. In this study, we used our recently developed technique – Regression CMC (R-CMC) – for the optimal detection of corticomuscular coherence (Bayraktaroglu et al., 2011). In short, R-CMC analysis utilizes a least-squares approach in order to maximize the correlation in a narrow frequency band between a band-pass filtered set of multichannel EEG signals and an EMG signal. The core idea is thus to find a spatial filter for multichannel EEG data which maximally explains EMG activity in a given frequency range. Such optimization is performed in the time domain where a correlation of narrow-band signals is equivalent to the calculation of coherence in the Fourier domain. In the present study we used unrectified band-pass filtered EMG, as previous studies showed that EMG rectification might have disadvantages for CMC estimation (Bayraktaroglu et al., 2011; McClelland et al., 2012; Stegeman et al., 2010).

R-CMC analysis is performed in two steps: (1) To avoid collinearity of predictors (EEG from different channels) and to make the estimation of covariance matrices more robust, a dimension reduction was performed using principal component analysis (PCA). PCA components were selected to account for 99% variability in the data. (2) To account for the conduction delay between the cortex and muscle, least-squares assessments were performed for different delays. The delay was estimated for frequencies between 8 and 44 Hz with 2-Hz steps and 4-Hz band-width. For this estimation EMG was shifted relative to EEG between $-\pi$ and $+\pi$ in $\pi/6$ steps. Separately for each EMG electrode, frequency and delay, a multiple regression was performed and the strongest coherence corresponding to the combination of a specific EMG channel, frequency band and delay was selected for further analysis.

Let \mathbf{y} be the projected EEG data which is maximally synchronous with the EMG data in \mathbf{g} , then the coherence between the projected data (\mathbf{y}) and EMG (\mathbf{g}) across segments is estimated as:

$$\text{Coh}_{g,y} = \frac{|\mathbf{s}_{g,y}|^2}{|\mathbf{s}_g|^2 |\mathbf{s}_y|^2} \quad (1)$$

where \mathbf{s}_g and \mathbf{s}_y are Fourier transforms for EMG and projected EEG data, respectively, and $\mathbf{s}_{g,y}$ is a cross-spectrum. For the calculation of the Fourier transforms, the post-stimulus data (stable post-stimulus period 2–4 s) was divided into 500-ms non-overlapping segments and windowed with a Hanning window.

In order to calculate the spatial pattern corresponding to the EEG vector we utilized an approach proposed by Parra et al. (2002).

During the optimization procedure we excluded components with patterns showing abnormal activity such as mosaic like high-frequency spatial features or strong activity at the temporal or frontal edges of the patterns (a typical indication for the presence of the scalp muscle activity).

We used permutation tests for determining the significance level of the coherence (Hesterberg et al., 2005). For this procedure, we repeated all the steps of R-CMC but using EMG segments that were shuffled with respect to the EEG data. Five-hundred permutations were performed for each set of data, and a specific coherence value was obtained for each permutation. The coherence for un-permuted data was considered significant if it exceeded the 95-percentile value obtained from the coherence distribution derived from the permuted data.

We also calculated time-resolved CMC from -2 to 7 s around the start tone. The coherence was calculated with 500-ms windows which were translated along the whole epoch length with 100 ms

steps. The spatial filter obtained for the stable active period (2–4 s) was used for all time windows.

Phase synchronization index. In addition to coherence, we also calculated the phase synchronization index (SI; Rosenblum et al., 2001).

Let \mathbf{y}_f and \mathbf{g}_f be vectors corresponding to signal \mathbf{y} (EEG component) and \mathbf{g} (EMG) which were band-pass filtered around the frequency f corresponding to the strongest CMC. We use then the Hilbert transform to extract the phases for \mathbf{y}_f and \mathbf{g}_f . Let $\theta(t)$ be the phase difference between \mathbf{y}_f and \mathbf{g}_f at time t and T is a total number of samples, and j is an imaginary unit. SI was then estimated as:

$$SI = \frac{1}{T} \left| \sum_{t=1}^T e^{j\theta(t)} \right|. \quad (2)$$

The phase synchronization index takes values between 0 and 1, where 0 corresponds to absent and 1 to a perfect phase synchrony. We created 500 shuffled data sets and calculated SI. The SI for un-shuffled data was considered significant if it exceeded the 95-percentile value obtained from the SI distribution derived from the shuffled data.

Localization of cortical CMC sources. Patterns corresponding to the optimized EEG components were used for finding neuronal sources with the sLORETA algorithm (Pascual-Marqui, 2002). Consequently, the sources were mapped using the standard MNI305 head (Collins et al., 1994). In order to compensate for inter-individual differences, sLORETA maps for each subject were normalized by dividing the power in each voxel by the mean of power from all voxels.

Amplitude-envelope correlation. Amplitude envelopes of the beta oscillations were calculated as follows. After finding the frequency band corresponding to the strongest CMC, for each band-pass filtered \mathbf{y}_f (EEG) and \mathbf{g}_f (EMG) we obtained vectors \mathbf{a}_y and \mathbf{a}_g , respectively, representing the instantaneous amplitude (envelope) of the signals on the basis of the Hilbert transform. The amplitude of the analytic signal is the length of a vector in a complex plane, while phase is the angle in the same plane. Clearly one can change either length or angle without affecting the other measure. Therefore, measuring phase synchronization or amplitude envelope provides information about different aspects of the underlying processes.

Previous studies showed that amplitude-envelope correlations between neuronal activities at different brain areas depend on the time scale at which they were measured, being usually stronger for larger time scales (Nikouline et al., 2001; Nir et al., 2008). Therefore, in order to estimate the correlation between \mathbf{a}_y and \mathbf{a}_g we introduced a coarse-graining procedure where the data were divided into segments of varying sizes from 50 to 1000 ms with a step of 50 ms, and the mean value was calculated in each segment separately for \mathbf{a}_y and \mathbf{a}_g . Amplitude-envelope correlations were calculated in the time interval of 2–4 s after the presentation of stimulus when the force levels were stabilized. Then the Spearman coefficient of correlation was calculated for coarse-grained \mathbf{a}_y and \mathbf{a}_g for a given window size.

The following procedure was used for the calculation of correlation significance. We created 500 shuffled data sets with permuted position of the windows (with a given size) and calculated the correlation as above, thereby obtaining distributions of correlation coefficients for 500 random sets. The correlation coefficient was considered significant if it exceeded the 95-percentile value obtained from the distribution of rectified correlation coefficients for the shuffled data (Hesterberg et al., 2005).

Reactivity of neuronal oscillations. The \mathbf{a}_y signal, reflecting cortical EEG beta oscillations, was segmented into epochs from -2 to 7 s around

the start tone and the epochs were averaged. The reactivity of the signal in the post-stimulus interval was expressed in % with respect to the amplitude in the preceding pre-stimulus interval (−700 to −200 ms). Below we refer to the attenuation of the amplitude as event related desynchronization (ERD, Pfurtscheller and Lopes da Silva, 1999). ERD measures the strength of the oscillatory response, and it is a dynamic measure since it shows how the neuronal activity changes with respect to some reference interval. Power/amplitude by itself just shows how pronounced the oscillations are. Without knowing what were the preceding values of power it is difficult to say whether the power in a given segment was decreased, increased or stayed the same after the stimulus presentation.

Connectivity analysis. The direction of corticomuscular interactions was estimated with the phase slope index (PSI, Nolte et al., 2008) which allows a reliable estimation of the causal relationships between the two signals. An advantage of the method is that it is not sensitive to volume conduction and provides an estimate of the information flow even if it is difficult to determine a conventional slope in a frequency-phase coordinate system (Halliday et al., 1998; Witham et al., 2010). While the phase slope index (PSI) is superior to conventional measures of directionality detection in EEG, the absolute values of PSI are not indicative of the actual delay. The sign of PSI indicates the direction of interactions. In the statistical analysis we used a binomial test in order to verify whether the majority of cases had a descending or ascending direction of interaction between EEG and EMG. PSI was calculated in the 2–4 s interval, the same time interval used for the calculation of CMC and amplitude-envelope correlations.

Results

Performance

All subjects were able to perform the task and maintained the required force level. When all of the epochs were taken into account, the force level in the 2–4 s interval (the interval used for the calculation of CMC) was 0.49 ± 0.011 N (mean \pm SEM). As mentioned in the Materials and methods section, trials which deviated by more than 0.1 N from the required level were rejected in order to avoid attenuation of CMC due to ongoing movement (Kilner et al., 2000; Riddle and Baker, 2006). After removal of such epochs the mean level of force was 0.49 ± 0.007 N. Fig. 2A shows the grand-average time-course (across subjects and hands) of the applied force.

Corticomuscular coherence

Significant CMC was detected in the beta frequency range (12.5–28.5 Hz) in all subjects, as assessed by the permutation procedure described above. The mean CMC peak frequency was 20.9 ± 1.1 Hz (mean \pm SEM), and the CMC strength was 0.13 ± 0.016 . There were no significant differences in the magnitude of CMC corresponding to the left and right hand performance (Wilcoxon sign rank test, $p = 0.12$). Fig. 2A shows the CMC time-course as an average across subjects where coherence was calculated in individually defined frequency ranges. The coherence did not reach its plateau right after the imperative stimulus, it rather showed a gradual buildup over the first 2 s, i.e., after the target (hold) force level was achieved. Please note that Fig. 2A

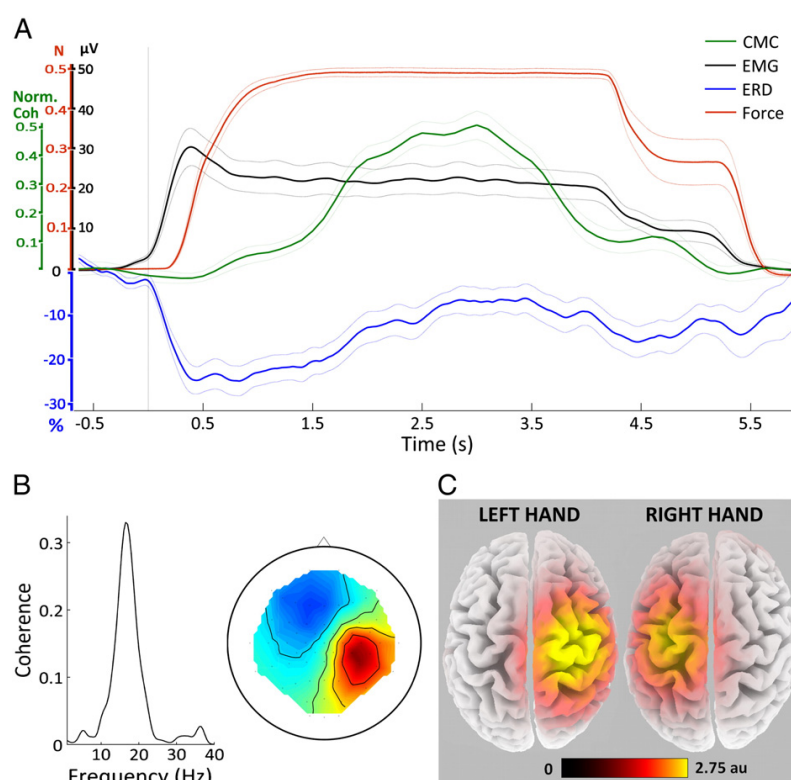


Fig. 2. A. Grand average (mean \pm SEM, dotted) of force, envelope amplitudes of beta-EEG and EMG, and time-resolved CMC (normalized to subject's peak value) during the task. The vertical gray line marks the start signal. The notch appearing on all curves after 4 s relates to the fact that in 5 of the subjects the active period was 4 s. B. The CMC spectrum between EMG and the extracted EEG component along with its spatial topography in a representative subject during the task execution with the left hand. C. Grand averages of sLORETA inverse solutions for the left and right hands, displaying contralateral pericentral activations visualized on the MNI305 average cortical surface, au – arbitrary units.

shows the grand average across all subjects while the inter-measures relationship (e.g., CMC vs ERD) was addressed using Spearman correlation (please see the sections below). The spatial topographies of the CMC components showed a clear lateralization to the hemisphere contralateral to the performing hand, representing either tangential or radial sources. Fig. 2B shows an example for the coherence spectrum between EMG (left hand performance) and EEG components along with its topography. Fig. 2C shows the grand average (across all subjects) for sLORETA solutions separately for the left and right hands. One can observe a clear lateralization of the sources which were located in the sensorimotor cortex with a maximum in the precentral gyrus.

Amplitude-envelope correlation between EEG and EMG

We investigated the EEG/EMG amplitude-envelope correlation on different time scales by introducing a coarse-graining procedure where the mean amplitude was calculated in segments with varying sizes (cf. Materials and methods). The analysis showed significant EEG/EMG envelope correlations in 12 hands of 7 subjects. In these subjects at least 90% of the segment sizes, varying between 50 and 1000 ms, showed a significant correlation (as assessed by the permutation tests) between amplitude envelopes of beta oscillations in EMG and EEG. Fig. 3 shows a single-subject example where the active period (2–4 s) was subdivided into 500-ms segments and the mean amplitude was calculated for each segment in EEG and EMG. The relationship between the EEG and EMG mean amplitudes across all segments of different sizes is shown in the figure. Fig. 4 shows the grand-average of Fisher's Z-transformed correlation values across all subjects and hands where a significant ($p < 0.05$) correlation was observed. Triangles show the strength of the correlation as a function of the segment size for the real data and crosses for the average of shuffled data across all permutations. Both curves show a slight increase of the correlation with the increasing segment size. To a large extent this is due to the fact that smaller degrees of freedom (number of windows with a given size) even for random data might lead to higher correlation values. Note, however, that regardless of this increase, the strength of the correlation corresponding to the

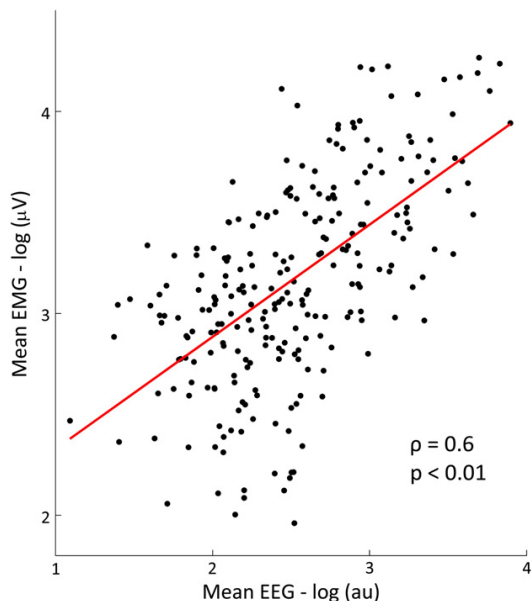


Fig. 3. The correlation of the EEG and EMG envelope amplitudes for the 500-ms integration window in one subject with pronounced amplitude-envelope correlation, au – arbitrary units.

shuffled data was considerably smaller. We then obtained the slope of the regression line from the shuffled data and subtracted it from the real data, thus compensating for the technical change of the correlation due to the smaller number of samples for a longer time segment. Diamond symbols show real data after this subtraction. The corrected figure shows only marginal remaining dependency of the correlation on the segment size (Fig. 4).

We also calculated the correlation between the coefficient of variation of amplitude envelope of cortical beta oscillations and the force during the task. This correlation was not significant in any of the segment sizes (50–1000 ms). For the 500-ms time windows (which we later used for correlation with phase synchronization index) we also compared the strength of amplitude-envelope correlation corresponding to the left and right hand performance and found no significant differences (Wilcoxon sign rank test, $p = 0.17$).

Phase synchronization index

In addition, we studied the dependency between the strength of phase synchronization and envelope correlation (500-ms windows) across subjects. According to the permutation tests, phase synchronization index was significant ($p < 0.05$) for all subjects and hands. Encircled points in Fig. 5 show data where significant amplitude-envelope correlations occurred. Please note that in many instances significant and non-significant values of amplitude-envelope correlations occurred for similar values of phase synchronization index. The correlation between phase synchronization index and envelope correlation was positive and significant: $\rho = 0.56$; $p < 0.01$ (Fig. 5). The correlation between the magnitudes of CMC and synchronization index was also strong and significant ($\rho = 0.59$; $p < 0.005$).

Pre-stimulus power and strength of CMC

In general the strength of any coherence measure depends on how well the phase portrait of the signals is defined (Muthukumaraswamy and Singh, 2011), which in turn also corresponds to how well the spectral peak stands above the noise level (Nikulin et al., 2011). Consequently, for the estimation of the spectral peaks we used the relative spectral power (RSP) of the extracted EEG components (with R-CMC). The values for RSP were calculated as a ratio between the mean power in the 4-Hz wide band (centered around the frequency peak optimized for CMC) and the mean power in the 5–35 Hz frequency range. Fig. 6 shows an example of two spectra from two subjects corresponding to

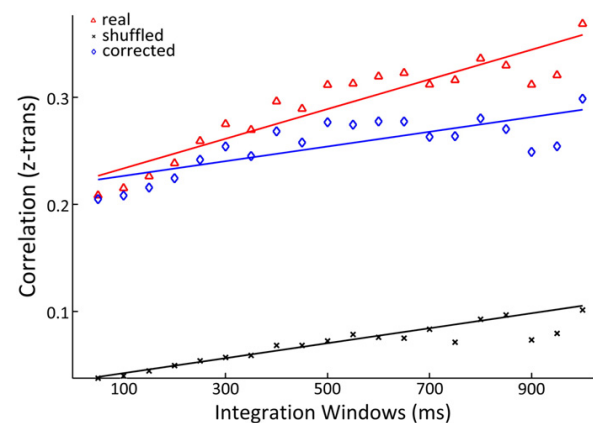


Fig. 4. Average of the EEG–EMG envelope correlations for all subjects with a significant correlation (Z-transformed) for 20 integration windows. The correlation values are given for real EEG–EMG envelopes (triangles) and for shuffled envelopes (crosses). Diamond symbols present the corrected correlation coefficients where the slope of the line from the shuffled data set was taken into account.

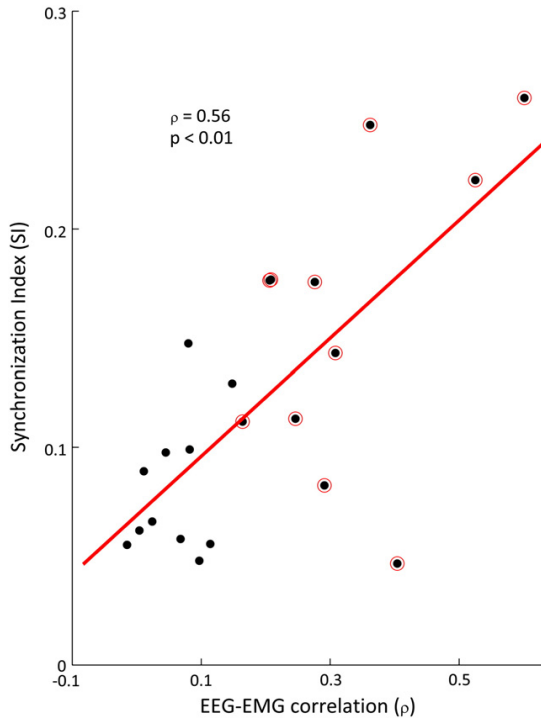


Fig. 5. Synchronization index and EEG–EMG amplitude-envelope correlation.

larger and smaller relative powers of EEG beta oscillations. In order to assess the dependency of the CMC strength on the pre-stimulus RSP, we calculated the Spearman correlation between these two measures

and found it to be positive and significant: $\rho = 0.6$; $p < 0.005$ (Fig. 7A). The Spearman correlation between RSP in the active period (2–4 s) and CMC was also positive and significant ($\rho = 0.65$; $p < 0.002$). In addition, the correlation between RSP and the amplitude-envelope correlation was positive and significant ($\rho = 0.47$; $p < 0.03$).

Reactivity of neuronal oscillations

The amplitude of cortical beta oscillations showed a characteristic attenuation (event-related desynchronization, ERD) upon the presentation of the imperative stimulus and a following return to the baseline (Fig. 2A, showing grand average data across subjects and hands). The peak latency of this attenuation was 0.85 ± 0.45 s after the start of the auditory tone and its peak strength was $-35.3 \pm 14.5\%$ relative to the baseline level. Fig. 7B, shows that the strengths of ERD and CMC (the latter was calculated in the 2–4 s post-stimulus interval) were significantly and negatively correlated ($\rho = -0.73$; $p < 0.001$). In addition, Fig. 7C demonstrates that ERD was also correlated with the relative spectral power (RSP) ($\rho = -0.74$; $p < 0.001$). In contrast to EEG, the amplitude of EMG beta oscillations showed a rapid increase upon the presentation of the imperative stimulus and a relatively stable amplitude level throughout the hold period (Fig. 2A).

Disambiguating the relationship between RSP, CMC and ERD

As mentioned above, our results demonstrated an intriguing correlation between ERD and CMC. Yet, RSP was also correlated with both CMC and ERD. Thus, one possibility was that CMC and ERD might be correlated because of their correlation with RSP. In order to verify that the correlation between ERD and CMC remains even when the correlation with RSP is eliminated, we performed a partial rank correlation analysis. After controlling for the effect of correlation of RSP with CMC and ERD, there was still a significant negative correlation between CMC and ERD albeit slightly attenuated ($\rho = -0.53$ $p < 0.013$).

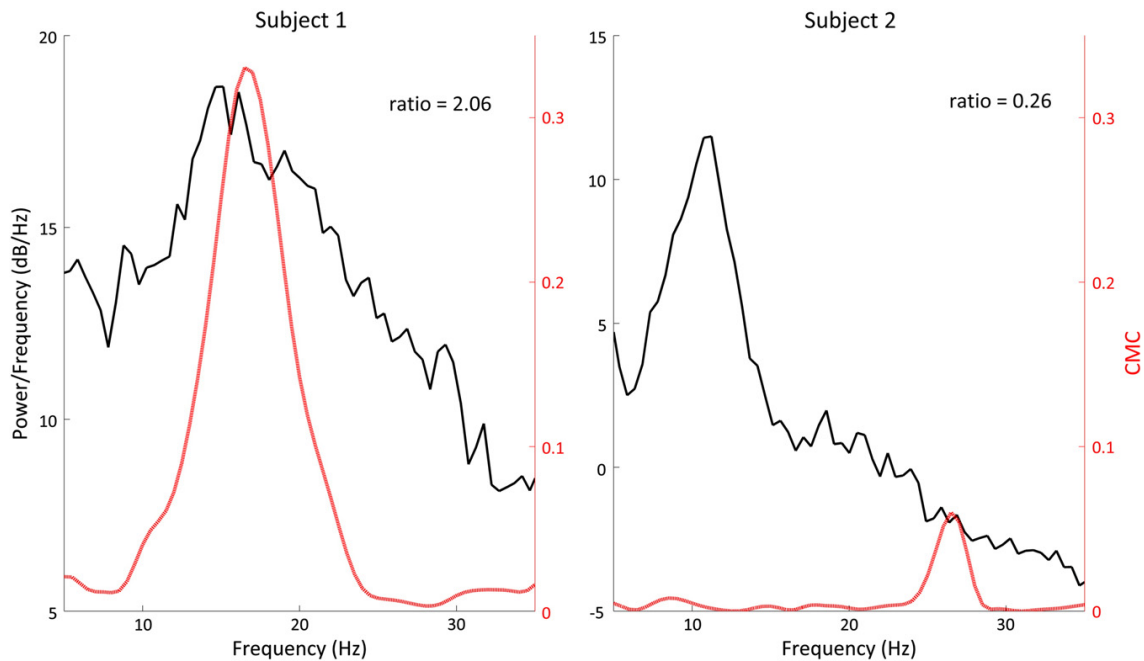


Fig. 6. The power spectra of the EEG components for the pre-stimulus rest period in two subjects. The left (right) panel shows the spectrum of the EEG component with high (low) relative spectral power. In addition, red curves show CMC spectra with peaks for which RSP was calculated. (For interpretation of the references to color in this figure legend, the reader is referred to the web version of this article.)

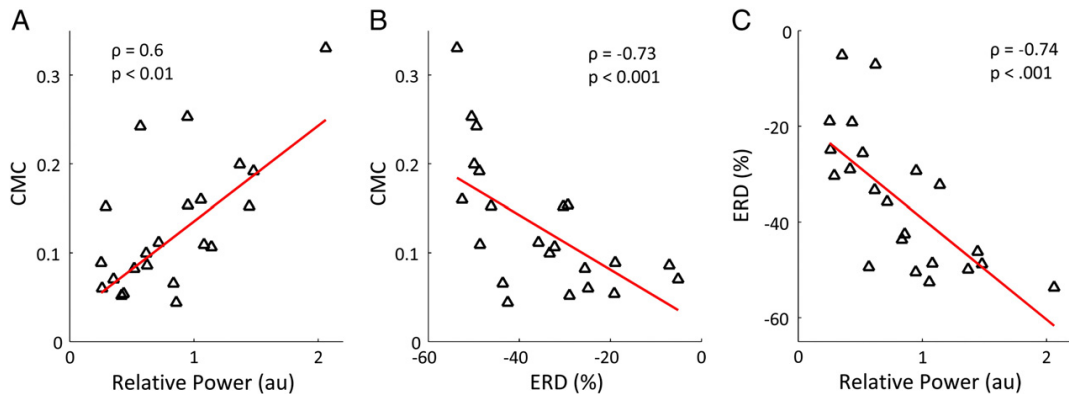


Fig. 7. A. Correlation between CMC and pre-stimulus RSP. B. Correlation between ERD and CMC. C. Correlation between ERD and RSP. au – arbitrary units. Red lines indicate least-squares fits. (For interpretation of the references to color in this figure legend, the reader is referred to the web version of this article.)

Phase slope index

The phase slope index measures the direction of information flow between the two processes. We performed a statistical evaluation of the sign of phase slope index taking into account all cases (11 subjects \times 2 hands = 22 cases) using a binomial test and found a near-significant information flow from cortical to muscle oscillations ($p = 0.052$).

Discussion

The present study showed that corticospinal oscillatory interactions are not only due to the phase coupling but that the amplitude envelopes of beta oscillations in the sensorimotor cortex and muscle are also positively correlated. Moreover, we also demonstrated that the amplitude reactivity of the sensorimotor neuronal oscillations as well as the pre-stimulus spectral relative power relate to the strength of corticomuscular synchronization. Below we elaborate on these new findings.

Corticomuscular coherence

The basic CMC features in the present study are in agreement with the previous results (Kristeva et al., 2007; Mima and Hallett, 1999a; Riddle and Baker, 2006), in particular concerning: (a) both frequency range and CMC magnitude, (b) the spatial maximum of cortical sources coherent with muscle activity in the sensorimotor cortices, and (c) the preferential flow of information from the cortex to the periphery in a directionality analysis. This set of congruent findings secures a reliable anchoring of the present data set in the established CMC knowledge and thereby provides a framework for the novel insight presented here.

Technical details of calculation of coherence

While coherence reflects primarily phase synchronization (Nolte et al., 2004), it also measures amplitude correlation between the two signals. In fact, coherence can be considered as phase synchronization weighted by another term which reflects amplitude co-modulation (Friston et al., 2012; Nolte et al., 2004). In practice, however, phase synchronization (measured through synchronization index) and coherence might give similar results (Mezeiova and Paluš, 2012). Moreover, Nolte et al. (2004) observed that for real and not theoretically constructed signals, it is not clear whether there might be always independence between the amplitude and phase. In addition, they argue that for very

weak signals the noise can destroy the phase and thus coherence (which takes into account amplitude) can give more robust results than the synchronization index.

Correlation of relative spectral power with ERD and CMC

The magnitude of the relative spectral power at the pre-stimulus interval provides a measure for the signal-to-noise ratio (SNR) by indicating how strongly a given spectral peak stands above the background neuronal activity (Nikulin et al., 2011). Different levels of RSP, as we hypothesize and explain below, can in turn affect both ERD and CMC, and produce a spurious relationship between them. If this is the case we should observe RSP of oscillations being correlated with both ERD and CMC. Indeed, we found that the CMC strength can be predicted from the RSP of beta oscillations in the pre-stimulus interval because higher RSP is associated with better SNR of the oscillatory signals and thus with a better defined phase portrait of oscillations (Muthukumaraswamy and Singh, 2011). The latter is a prerequisite for measuring phase synchronization (Rosenblum et al., 2001). The differences in the level of RSP provide a plausible explanation for previously documented but unaccounted variability of the CMC strength across subjects (Mima and Hallett, 1999b; Pohja et al., 2005). Predictability of CMC on the basis of pre-stimulus neuronal activity indicates that the presence of ongoing beta oscillations, which can later undergo phase-locking with the active muscle, might be a prerequisite for observing a pronounced CMC. A correlation of RSP during the active period (2–4 s) with CMC also indicates that the signal-to-noise ratio might affect CMC. Yet, since both CMC and RSP are calculated in this case at the same time interval, no predictions can be made on the necessity of having pre-stimulus ongoing beta oscillations for obtaining stronger CMC.

Accordingly, pre-stimulus RSP is also likely to be the factor contributing to the ERD strength. Small RSP reflects a weak oscillatory process which hardly can demonstrate pronounced attenuation due to a “floor effect”. On the contrary, signals with high RSP can show strong attenuation, i.e., larger ERD values (Lemm et al., 2009). In agreement with this prediction, we observed a negative correlation between ERD and RSP.

The correlation between ERD and CMC might thus be spurious as both are affected by the pre-stimulus RSP. However, when we controlled for the effect of RSP on ERD and CMC, there still remained a significant correlation between ERD and CMC, which would then indicate a functional relationship between the latter two.

The relationship between neuronal reactivity and strength of corticomuscular interactions

We showed that the strength of beta ERD negatively correlated with CMC indicating that stronger attenuation of beta oscillations related to larger CMC. Changes in the amplitude of beta oscillations were hypothesized to reflect cortical excitability (Chen et al., 1998; Mäki and Ilmoniemi, 2010; Pfuertscheller and Lopes da Silva, 1999) and thus our findings show a functional relationship between the stimulus-related level of cortical excitation and CMC strength. The initial attenuation of the cortical CMC beta oscillations, observed in the present study, could indicate a breakdown of local spatial synchronization that in turn might be associated with a more robust recruitment of cortical neurons for the performance of the following steady-state contraction. Mäki and Ilmoniemi (2010) showed that motor evoked potentials, produced by TMS, were larger for smaller beta oscillations, thus implying that higher motor excitability related to smaller beta oscillations. In this sense stronger post-stimulus beta ERD (resulting in a smaller amplitude of oscillations) would be associated with higher motor excitability, which in turn might facilitate the recruitment of neuronal networks responsible for establishing reliable corticospinal control manifested in larger CMC. This is in line with previous findings showing that the strength of CMC correlates with the amount of the preceding desynchronization in the beta frequency range (Omlor et al., 2011): if a steady state contraction was preceded by an unpredictable dynamic force task, then CMC was elevated. At the same time the authors observed a correlation between beta power attenuation and CMC. Here, we extend these findings by showing that not only the power difference between the tasks, but also the instantaneous change in the amplitude of beta oscillations upon the imperative stimulus can shape the strength of the upcoming corticomuscular interactions.

Correlation of beta amplitude envelopes

Fig. 5 shows that although the amplitude-envelope correlation and phase synchronization index correlate, the correlation has only a value of 0.56, thus indicating that the amplitude-envelope correlation is not reducible to the phase synchronization, but can reflect additional features of neuronal interactions, such as the strength of local spatial synchronization.

Changes in the amplitude of oscillations reflect the strength of spatial synchronization as shown in both experimental (Denker et al., 2011; Elul, 1971) and modeling studies (Telenczuk et al., 2010). These amplitude changes are used conventionally as an index of local spatial desynchronization or synchronization between neurons (Pfuertscheller and Lopes da Silva, 1999). Muscle activity in turn reflects discharges of spinal motoneurons where stronger beta-oscillatory EMG bursts reflect a larger number of synchronously firing motoneurons (Conway et al., 1995; Farmer et al., 1993). Thus, the experimental observation of an amplitude co-modulation of beta oscillation in EMG and EEG, as presented here, shows that the strength of local spatial synchronization at the cortical level relates to the strength of synchronization between spinal motoneurons. This in turn indicates that the amplitude of beta oscillations in the sensorimotor cortex might reflect the strength of synchronization among the alpha motor neurons in the spinal cord. Taken together our study provides the first evidence that the changes in the amplitude of cortical beta oscillations might relate to the spiking output of corticospinal neurons.

The results of our study showed that in approximately half of the cases one could observe a significant positive correlation between the amplitude envelopes of beta oscillations in the sensorimotor cortex and muscle activity. The correlation between pre-stimulus RSP and amplitude-envelope correlations was positive and significant, which might attest to the detrimental effect of noise on the extraction of amplitude envelopes. A proper recovery of the EEG beta components

affects the estimation of both phase and amplitude dynamics, which in turn can be the basis of the observed correlation between CMC and amplitude-envelope correlations. A smaller percentage of the cases showing amplitude-envelope correlations can be due to both neurophysiological reasons and to the higher susceptibility of amplitude envelope correlations to SNR because of the additional nonlinearity introduced by calculation of amplitude envelopes. This sensitivity to SNR, however, is difficult to assess since in general rectification introduces complex modifications of the input signals (containing signal and noise) and because of the finite length of the data.

Previous studies showed that amplitude-envelope correlations between narrow-band neuronal signals became stronger with increasing time scale at which the correlations were measured (Nikouline et al., 2001; Nir et al., 2008). A weak dependence of amplitude-envelope correlations on the segment size indicates that the co-fluctuation of amplitudes occurs both at very short and long time scales and that even very fast changes in the amplitude of beta oscillations (i.e., for 50-ms integration windows), are transferred to the oscillatory muscle activity.

Dissociation from CMC and functional interpretation of amplitude-envelope correlation

Moderate strength of amplitude-envelope correlation (~0.2–0.3) indicates that corticospinal interactions only partially define the dynamics of EMG and that other descending tracts, e.g. reticulospinal tract, can also shape the activity of the spinal neurons (Riddle and Baker, 2010; Soteropoulos et al., 2012) and thus be responsible for changes in EMG amplitude. In this case changes in EMG can originate at least partly not from the activity of cortical cells and thus the amplitude envelope of muscle and cortical oscillations would not be tightly related. One can hypothesize that depending on the involvement of different descending tracts into the generation of the movement, different subjects might show some variance in the coupling of cortical and spinal cord dynamics. A previous study on reproducibility of CMC can indeed serve as an evidence for subject-specific manifestation of corticospinal interactions (Pohja et al., 2005).

As mentioned above, the amplitude of cortical oscillations reflects an amount of synchronously firing cortical neurons. Importantly, while corticomuscular phase synchronization relates to a limited subset of somatotopically relevant neuronal activation, the amplitude of oscillations can reflect a far larger number of active neurons not all of them participating in the generation of a given muscular activity. The fact that often values of corticomuscular coherence are less than 0.1 (Kilner et al., 2000; Kristeva et al., 2007; Salenius et al., 1997) indeed indicates that there is only a relatively weak association between cortical and muscular activities. Under such scenario amplitude modulation of cortical beta oscillations can reflect not only the corticospinal descending activity, but also the intrinsic cortical dynamics, which are known to produce a diversity of spatio-temporal clusters leading to amplitude fluctuations on different time scales (Linkenkaer-Hansen et al., 2001; Nikulin and Brismar, 2005). Such intrinsic neuronal dynamics might give rise to changes in amplitude envelopes, which do not relate to corticomuscular control, thus leading to some dissociation between phase synchronization and amplitude dynamics in cortical and muscular activities.

In respect to corticospinal interaction, amplitude dynamics might add to phase synchronization in the following way. Riddle and Baker (2006) showed that the CMC strength is rather correlated with the spatial extent of the preceding movement. The authors observed that beta oscillations were abolished during the movement and were recovered with steady contraction – a result which was also found in the present study. They suggested that CMC can reflect the operation of a testing system which sends probing pulses and evaluates the state of the periphery for the integration in the consecutive motor performance (Baker, 2007; Favorov et al., 1988). Building on this hypothesis, the amplitude-envelope correlation, observed in the

present study, might thus indicate that such probing is a dynamic process, reflecting varying numbers of cortical and spinal cord neurons being synchronous at a given time. This in turn, can reflect a varying spatial extent subserved by the probing pulses.

In conclusion, our study demonstrated that corticomuscular interactions can be transmitted not only by phase synchronization of beta oscillations but also by amplitude dynamics. The latter were expressed in the amplitude-envelope correlations which, however, might be more susceptible to the detrimental effect of noise than CMC. In addition, we found that corticomuscular coherence can be influenced both by the amplitude reactivity of cortical neuronal oscillations (most likely due to the changes in cortical excitability) and by signal-to-noise ratio of the ongoing neuronal oscillations.

Acknowledgments

ZB was supported by the Center for Stroke Research Berlin. VVN and GC were supported by the Berlin Bernstein Center for Computational Neuroscience.

References

- Baker, S.N., 2007. Oscillatory interactions between sensorimotor cortex and the periphery. *Curr. Opin. Neurobiol.* 17, 649–655.
- Baker, S.N., Olivier, E., Lemon, R.N., 1997. Coherent oscillations in monkey motor cortex and hand muscle EMG show task-dependent modulation. *J. Physiol.* 501, 225–241.
- Bayraktaroglu, Z., von Carlowitz-Ghori, K., Losch, F., Nolte, G., Curio, G., Nikulin, V.V., 2011. Optimal imaging of cortico-muscular coherence through a novel regression technique based on multi-channel EEG and un-rectified EMG. *NeuroImage* 57, 1059–1067.
- Chen, R., Yaseen, Z., Cohen, L.G., Hallett, M., 1998. Time course of corticospinal excitability in reaction time and self-paced movements. *Ann. Neurol.* 44, 317–325.
- Christou, E.A., Rudroff, T., Enoka, J.A., Meyer, F., Enoka, R.M., 2007. Discharge rate during low-force isometric contractions influences motor unit coherence below 15 Hz but not motor unit synchronization. *Exp. Brain Res.* 178, 285–295.
- Collins, D.L., Neelin, P., Peters, T.M., Evans, A.C., 1994. Automatic 3D intersubject registration of MR volumetric data in standardized Talairach space. *J. Comput. Assist. Tomogr.* 18, 192–205.
- Conway, B.A., Halliday, D.M., Farmer, S.F., Shahani, U., Maas, P., Weir, A.I., Rosenberg, J.R., 1995. Synchronization between motor cortex and spinal motoneuron pool during the performance of a maintained motor task in man. *J. Physiol.* 489, 917–924.
- Daffertshofer, A., van Wijk, B.C., 2011. On the influence of amplitude on the connectivity between phases. *Front. Neuroinformatics* 5, 6.
- Denker, M., Roux, S., Lindén, H., Diesmann, M., Riehle, A., Grün, S., 2011. The local field potential reflects surplus spike synchrony. *Cereb. Cortex* 21, 2681–2695.
- Elul, R., 1971. The genesis of the EEG. *Int. Rev. Neurobiol.* 15, 227–272.
- Farmer, S.F., Bremner, F.D., Halliday, D.M., Rosenberg, J.R., Stephens, J.A., 1993. The frequency content of common synaptic inputs to motoneurons studied during voluntary isometric contraction in man. *J. Physiol.* 470, 127–155.
- Favorov, O., Sakamoto, T., Asanuma, H., 1988. Functional role of corticoperipheral loop circuits during voluntary movements in the monkey: a preferential bias theory. *J. Neurosci.* 8, 3266–3277.
- Friston, K.J., 1997. Another neural code? *NeuroImage* 5, 213–220.
- Friston, K.J., Bastos, A., Litvak, V., Stephan, K.E., Fries, P., Moran, R.J., 2012. DCM for complex-valued data: cross-spectra, coherence and phase-delays. *NeuroImage* 59, 439–455.
- Gonzalez Andino, S.L., Pascual Marqui, R.D., Valdes Sosa, P.A., Biscay Lirio, R., Machado, C., Diaz, G., Figueredo Rodriguez, P., Castro Torrez, C., 1990. Brain electrical field measurements unaffected by linked earlobes reference. *Electroencephalogr. Clin. Neurophysiol.* 75, 155–160.
- Halliday, D.M., Rosenberg, J.R., Amjad, A.M., Breeze, P., Conway, B.A., Farmer, S.F., 1995. A framework for the analysis of mixed time series/point process data—theory and application to the study of physiological tremor, single motor unit discharges and electromyograms. *Prog. Biophys. Mol. Biol.* 64, 237–278.
- Halliday, D.M., Conway, B.A., Farmer, S.F., Rosenberg, J.R., 1998. Using electroencephalography to study functional coupling between cortical activity and electromyograms during voluntary contractions in humans. *Neurosci. Lett.* 241, 5–8.
- Hesterberg, T., Moore, D.S., Monaghan, S., Clipson, A., Epstein, R., 2005. Bootstrap methods and permutation tests. In: Moore, McCabe (Ed.), *Introduction to the Practice of Statistics*. WH Freeman & Co. ch14.
- Jackson, A., Spinks, R.L., Freeman, T.C.B., Wolpert, D.M., Lemon, R.N., 2002. Rhythm generation in monkey motor cortex explored using pyramidal tract stimulation. *J. Physiol.* 541, 685–699.
- Kilner, J.M., Baker, S.N., Salenius, S., Hari, R., Lemon, R.N., 2000. Human cortical muscle coherence is directly related to specific motor parameters. *J. Neurosci.* 20, 8838–8845.
- Kristeva, R., Patino, L., Omlor, W., 2007. Beta-range cortical motor spectral power and corticomuscular coherence as a mechanism for effective corticospinal interaction during steady-state motor output. *NeuroImage* 36, 785–792.
- Lemm, S., Müller, K.R., Curio, G., 2009. A generalized framework for quantifying the dynamics of EEG event-related desynchronization. *PLoS Comput. Biol.* 5, e1000453.
- Linkenkaer-Hansen, K., Nikouline, V.V., Palva, J.M., Ilmoniemi, R.J., 2001. Long-range temporal correlations and scaling behavior in human brain oscillations. *J. Neurosci.* 21, 1370–1377.
- Mäki, H., Ilmoniemi, R.J., 2010. The relationship between peripheral and early cortical activation induced by transcranial magnetic stimulation. *Neurosci. Lett.* 478, 24–28.
- McClelland, V.M., Cvetkovic, Z., Mills, K.R., 2012. Rectification of the EMG is an unnecessary and inappropriate step in the calculation of corticomuscular coherence. *J. Neurosci. Methods* 205, 190–201.
- Mezeiová, K., Paluš, M., 2012. Comparison of coherence and phase synchronization of the human sleep electroencephalogram. *Clin. Neurophysiol.* 123, 1821–1830.
- Mima, T., Hallett, M., 1999a. Electroencephalographic analysis of cortico-muscular coherence: reference effect, volume conduction and generator mechanism. *Clin. Neurophysiol.* 110, 1892–1899.
- Mima, T., Hallett, M., 1999b. Corticomuscular coherence: a review. *J. Clin. Neurophysiol.* 16, 501–511.
- Mitzdorf, U., 1985. Current source-density method and application in cat cerebral cortex: investigation of evoked potentials and EEG phenomena. *Physiol. Rev.* 65, 37–100.
- Muthukumaraswamy, S.D., Singh, K.D., 2011. A cautionary note on the interpretation of phase-locking estimates with concurrent changes in power. *Clin. Neurophysiol.* 122, 2324–2325.
- Nikouline, V.V., Linkenkaer-Hansen, K., Huttunen, J., Ilmoniemi, R.J., 2001. Interhemispheric phase synchrony and amplitude correlation of spontaneous beta oscillations in human subjects: a magnetoencephalographic study. *Neuroreport* 12, 2487–2491.
- Nikulin, V.V., Brismar, T., 2005. Long-range temporal correlations in electroencephalographic oscillations: relation to topography, frequency band, age and gender. *Neuroscience* 130, 549–558.
- Nikulin, V.V., Nolte, G., Curio, G., 2011. A novel method for reliable and fast extraction of neuronal EEG/MEG oscillations on the basis of spatio-spectral decomposition. *NeuroImage* 55, 1528–1535.
- Nir, Y., Mukamel, R., Dinstein, I., Privman, E., Harel, M., Fisch, L., Gelbard-Sagiv, H., Kipervasser, S., Andelman, F., Neufeld, M.Y., Kramer, U., Arieli, A., Fried, I., Malach, R., 2008. Interhemispheric correlations of slow spontaneous neuronal fluctuations revealed in human sensory cortex. *Nat. Neurosci.* 11, 1100–1108.
- Nolte, G., Bai, O., Wheaton, L., Mari, Z., Vorbach, S., Hallett, M., 2004. Identifying true brain interaction from EEG data using the imaginary part of coherency. *Clin. Neurophysiol.* 115, 2292–2307.
- Nolte, G., Ziehe, A., Nikulin, V.V., Schlögl, A., Krämer, N., Brismar, T., Müller, K.R., 2008. Robustly estimating the flow direction of information in complex physical systems. *Phys. Rev. Lett.* 100, 234101.
- Okun, M., Naim, A., Lampl, I., 2010. The subthreshold relation between cortical local field potential and neuronal firing unveiled by intracellular recordings in awake rats. *J. Neurosci.* 30, 4440–4448.
- Oldfield, R.C., 1971. The assessment and analysis of handedness: the Edinburgh inventory. *Neuropsychologia* 9, 97–113.
- Omlor, W., Patino, L., Mendez-Balbuena, I., Schulte-Mönting, J., Kristeva, R., 2011. Corticospinal beta-range coherence is highly dependent on the pre-stationary motor state. *J. Neurosci.* 31, 8037–8045.
- Parra, L., Alvino, C., Tang, A., Pearlmutter, B., Yeung, N., Osman, A., Sajda, P., 2002. Linear spatial integration for single-trial detection in encephalography. *NeuroImage* 17, 223–230.
- Pascual-Marqui, R.D., 2002. Standardized low-resolution brain electromagnetic tomography (sLORETA): technical details. *Methods Find. Exp. Clin. Pharmacol.* 24D, 5–12.
- Pfurtscheller, G., Lopes da Silva, F.H., 1999. Event-related EEG/MEG synchronization and desynchronization: basic principles. *Clin. Neurophysiol.* 110, 1842–1857.
- Pohja, M., Salenius, S., Hari, R., 2005. Reproducibility of cortex–muscle coherence. *NeuroImage* 26, 764–770.
- Poulet, J.F., Petersen, C.C., 2008. Internal brain state regulates membrane potential synchrony in barrel cortex of behaving mice. *Nature* 454, 881–885.
- Riddle, C.N., Baker, S.N., 2006. Digit displacement, not object compliance, underlies task dependent modulations in human corticomuscular coherence. *NeuroImage* 33, 618–627.
- Riddle, C.N., Baker, S.N., 2010. Convergence of pyramidal and medial brain stem descending pathways onto macaque cervical spinal interneurons. *J. Neurophysiol.* 103, 2821–2832.
- Rosenblum, M.G., Pikovsky, A.S., Kurths, J., Schäfer, C., Tass, P., 2001. Phase synchronization: from theory to data analysis. In: Moss, Gielen (Ed.), *Handbook of Biological Physics*. Elsevier, pp. 279–321.
- Salenius, S., Portin, K., Kajola, M., Salmelin, R., Hari, R., 1997. Cortical control of human motoneuron firing during isometric contraction. *J. Neurophysiol.* 77, 3401–3405.
- Schnitzler, A., Gross, J., Timmermann, L., 2000. Synchronised oscillations of the human sensorimotor cortex. *Acta Neurobiol. Exp.* 60, 271–287.
- Soteropoulos, D.S., Williams, E.R., Baker, S.N., 2012. Cells in the monkey ponto-medullary reticular formation modulate their activity with slow finger movements. *J. Physiol.* 590, 4011–4027.
- Stegeman, D.F., van de Ven, W.J.M., van Elswijk, G.A., Oostenveld, R., Kleine, B.U., 2010. The alpha-motoneuron pool as transmitter of rhythmicities in cortical motor drive. *Clin. Neurophysiol.* 121, 1633–1642.
- Telenczuk, B., Nikulin, V.V., Curio, G., 2010. Role of neuronal synchrony in the generation of evoked EEG/MEG responses. *J. Neurophysiol.* 104, 3557–3567.
- Witham, C.L., Wang, M., Baker, S.N., 2010. Corticomuscular coherence between motor cortex, somatosensory areas and forearm muscles in the monkey. *Front. Syst. Neurosci.* 4, 38.

4.1. Limitations and outlook

The current paper demonstrated amplitude-envelope correlation of beta oscillation in corticospinal interaction and thereby provided evidence that in corticospinal interaction information may not only be transmitted by phase but also by amplitude. Amplitude-envelope correlation did show a correlation with phase synchronization which raises the question whether this measure does provide any information in addition to CMC. This point is extensively addressed within the paper. In conclusion, as the correlation with phase synchronization is rather weak, amplitude-envelope correlation may provide a complementary measure of non-linear relationship in corticospinal interaction.

In addition, the current paper extended on previous findings (Muthukumaraswamy and Singh, 2011) that SNR, which is here measured by pre-stimulus relative spectral power (RSP), can affect the extraction of phase information in corticospinal interaction. As a consequence, the subsequent papers III and IV (Chapter 5 and 6, respectively) could use this knowledge to exclude possible effects of SNR on changes in CMC.

CMC in stroke 5

The previous chapters (Chapters 3 and 4) were concerned with the detection of corticospinal interaction in healthy people. In the current study, the previously acquired knowledge was applied to the detection of CMC in stroke patients. Generally, conducting a study with patients impose higher demands in terms of finding suitable subjects as particularly elderly subjects might suffer from additional disabilities, conducting the experiments (sometimes still in the stroke intensive care unit) and analyzing the data, as often the quality of clinical data is lower than data from healthy people.

However, this study allowed to move from basic neurophysiology closer to a potential clinical application of CMC, namely as a rehabilitation approach in the form of CMC-based neurofeedback. While the next chapter (Chapter 6) will then be concerned with the realization of the neurofeedback, the current paper applied the R-CMC method to clinical data to describe the changes of CMC in the post-stroke period. Based on this 'descriptive' result one can move on to develop methods/strategies which intervene and support the recovery.



Corticomuscular coherence in acute and chronic stroke



Katherina von Carlowitz-Ghori^{a,b,c,1}, Zubeyir Bayraktaroglu^{a,d,1}, Friederike U. Hohlefeld^a, Florian Losch^a, Gabriel Curio^{a,d,e}, Vadim V. Nikulin^{a,d,e,*}

^aNeurophysics Group, Department of Neurology, Charité – University Medicine Berlin, Germany

^bInstitute of Science and Ethics, University of Bonn, Germany

^cDepartment of Software Engineering and Theoretical Computer Science, Berlin Institute of Technology, Berlin, Germany

^dCenter for Stroke Research Berlin, Charité – University Medicine Berlin, Germany

^eBernstein Center for Computational Neuroscience, Berlin, Germany

ARTICLE INFO

Article history:

Accepted 5 November 2013

Available online 16 November 2013

Keywords:

CMC

Reorganization

Motor recovery

EEG

EMG

Synchronization

Oscillations

HIGHLIGHTS

- We studied corticomuscular coherence (CMC) in the acute and chronic stroke following up the course of recovery.
- In acute stroke CMC frequency was decreased on the affected side and CMC amplitude was increased on the unaffected side.
- In the chronic period there was no inter-hemispheric difference in CMC parameters.

ABSTRACT

Objective: Motor recovery after stroke is attributed to neuronal plasticity, however not all post-stroke neuronal changes relate to regaining fine motor control. Corticomuscular coherence (CMC) is a measure allowing to trace neuronal reorganizations which are functionally relevant for motor recovery. Contrary to previous studies which were performed only in chronic stage, we measured CMC in patients with stroke at both acute and chronic stroke stages.

Methods: For the detection of CMC we used multichannel EEG and EMG recordings along with an optimization algorithm for the detection of corticomuscular interactions.

Results: In acute stroke, the CMC amplitude was larger on the unaffected side compared to the affected side and also larger compared to the unaffected side in the chronic period. Additionally, CMC peak frequencies on both sides decreased in the acute compared to the chronic period and to control subjects. In chronic stage, there were no inter-hemispheric or group differences in CMC amplitude or frequency.

Conclusions: The changes in CMC parameters in acute stroke could result from a temporary decrease in inhibition, which normalizes in the course of recovery. As all patients showed very good motor recovery, the modulation of CMC amplitude and frequency over time might thus reflect the process of motor recovery.

Significance: We demonstrate for the first time the dynamical changes of corticomuscular interaction both at acute and chronic stage of stroke.

© 2013 International Federation of Clinical Neurophysiology. Published by Elsevier Ireland Ltd. All rights reserved.

1. Introduction

Motor dysfunction is the most frequent consequence of stroke (Rathore et al., 2002) that dramatically affects the everyday life

of patients. Appropriate treatment and rehabilitation procedures of motor paresis strongly depend on our understanding of the neuronal processes related to recovery of normal motor functioning. It is generally believed that motor recovery after stroke is due to massive neuronal reorganization occurring both locally and remotely to the lesion site (Talelli et al., 2006; Jang, 2007; Nudo, 2007; Grefkes and Fink, 2011). Thus, new areas that were previously not engaged are recruited in a motor activity. Neuroimaging studies reported the involvement of ipsi- and contralesional brain regions in the recovery process (Ward, 2005; Dancause, 2006; Nudo, 2007).

* Corresponding author at: Charité – Universitätsmedizin Berlin, Campus Benjamin Franklin, Department of Neurology, Neurophysics Group, Hindenburgdamm 30, 12203 Berlin, Germany. Tel.: +49 30 8445 4727; fax: +49 30 8445 4264.

E-mail address: vadim.nikulin@charite.de (V.V. Nikulin).

¹ These authors have contributed equally to the work.

However, not every change in brain activation and wiring after stroke can be considered as functionally relevant for re-establishing motor performance. Some alterations in the neuronal dynamics can be unspecific/maladaptive – as a consequence of compensatory movements, ipsilateral involvement and inter-hemispheric competitive interaction (Takeuchi and Izumi, 2012). Maladaptive plasticity interferes with motor recovery and should be differentiated from neuronal processes which are specifically associated with regaining normal motor control. Studies utilizing neuroimaging techniques such as fMRI and PET provide rather an indirect reference with respect to the involvement of activated cortical areas into the recovery processes (Calautti and Baron, 2003; Assaf and Pasternak, 2008).

In the present study we use corticomuscular coherence (CMC) as a tool to identify functionally relevant contributions of reorganized cortical areas to motor recovery. CMC is a well-established neurophysiological measure, which indicates the amount of synchronization between cortical and spinal cord activities during the execution of a movement (Brown et al., 1998; Mima and Hallett, 1999; Salenius and Hari, 2003). CMC appears predominantly during periods of isometric contraction (Kilner et al., 2000; Riddle and Baker, 2006) and reaches its maximum in the beta frequency range (16–32 Hz) over the primary sensorimotor cortices contralateral to the innervated limb (Salenius et al., 1997; Tsujimoto et al., 2009; Witham et al., 2010).

There are only a few stroke-related CMC studies (Mima et al., 2001; Braun et al., 2007; Fang et al., 2009; Meng et al., 2009; Graziadio et al., 2012) and all of them were performed at the chronic stage, mostly at least 1 year after the stroke when many compensatory processes already took place (Rijntjes, 2006). Currently, longitudinal CMC studies following stroke patients from acute to chronic period are missing. Such studies could provide new insight into the temporal evolution of corticomuscular interaction after stroke and add to the understanding of mechanisms underlying motor recovery. The present study demonstrates for the first time the changes in the dynamics of corticomuscular interaction both at acute and early chronic stage of stroke.

2. Materials and methods

The experimental protocol was approved by the Institutional Review Board of the Charité, Berlin, and the subjects gave their written informed consent prior to the experiments. All subjects were right-handed according to the Edinburgh Handedness Inventory (Oldfield, 1971) and had normal or corrected to normal vision.

2.1. Patients

Eleven ischemic stroke patients (5 female, mean age \pm SD: 71.7 ± 11.3 years) with hemiparesis were recruited in 12 months of the study. Only patients with first ever acute ischemic lesions localized in cortical or subcortical regions were included in the study. The lesion location was confirmed with MRI; four patients had left, seven right hemispheric strokes. Exclusion criteria were multiple scattered lesions, previous stroke or lesion, muscle disorders, peripheral neuropathy, hemorrhagic stroke, cognitive impairment and complete plegia. The mean time for the recordings was 3.5 (range: 2–5) days after the stroke. Motor strength of the target muscles (abductor pollicis brevis, APB) was graded according to the Medical Research Council (MRC) scale. To be selected for the study, the patients had to have moderate to severe hemiparesis at the onset of the stroke. On the day of experiment, patients had regained their muscle strength such that it was greater than 3 on the MRC scale except for one patient. The details of the patients are summarized in Table 1.

The same group of patients was contacted 6 months post-stroke and asked to participate in the follow-up study. Seven patients agreed and were recorded 194.6 (range: 174–250) days after the first experiment. In the follow-up period the force level was assessed again and found to be 5 (on the MRC scale) for all patients.

2.2. Controls

Fourteen healthy subjects (4 female, mean age \pm SD: 51.7 ± 10.35 years) without any history of neurological or psychiatric disease served as control.

2.3. Paradigm

We used a digit displacement paradigm, which includes the manipulation of a compliant object because CMC was found to be larger when the task involved a compliant object compared to a simple isometric condition (Kilner et al., 2000; Riddle and Baker, 2006).

During the experiment the patients stayed in the bed, reclined at 60°. Control subjects were seated in a comfortable chair with their arms resting on the chair handles. The subjects were instructed to press a spring-loaded lever with the left or right thumb with 0.5 N force, requiring a lever displacement of ~ 3.5 cm. The force was measured with a load sensor (FSG15N1A, Honeywell, USA). Visual feedback of the force level was provided on a computer screen as a horizontal bar of varying lateral extent proportional to the exerted force with fixed vertical lines indicating the target value. A cross in the center of the screen served as an eye-fixation point.

The task was performed with each hand separately and the hand order was counter-balanced between the subjects. The subjects were instructed to reach the required force level as fast as possible after a single tone and hold it constant until the presentation of a double tone. Subjects performed 4 blocks of 25 trials per hand with 60 s of rest between the blocks. Each trial lasted 9 s consisting of 5 s pressing and 4 s rest.

2.4. Data acquisition

EEG and EMG data were acquired with BrainAmp MR-plus (Brain Products, Germany) amplifiers, filtered in the frequency range of 0.015–250 Hz and sampled at 1000 Hz. The voltage resolution for the EEG and EMG channels was 0.1 μ V and 0.5 μ V, respectively.

2.4.1. EEG

During the acquisition, the EEG was referenced to physically linked earlobes and recorded using an EEG cap (61 Ag/AgCl sintered ring electrodes, EasyCap, Germany) with a denser electrode configuration complying with the 10–5 system (Oostenveland and Praamstra, 2001) above the sensorimotor cortices. Ocular artifacts were recorded with two electrodes placed on the right zygomatic and supraorbital processes.

2.4.2. EMG

EMG was recorded from the abductor pollicis brevis (APB) muscle with three EMG electrodes (Ag/AgCl sintered electrodes 4 mm in diameter) over the thenar side of each hand. The skin surface was abraded with NuPrep (Weaver & Co., USA) before the electrode application. The electrode–skin conductive contact was established with Ten20 electrode paste (Weaver & Co., USA) and the electrodes were secured to the skin with adhesive medical tape.

An EMG reference electrode was placed on the styloid process of the ulnar bone and a ground electrode on the inner surface of

Table 1
Clinical information of patients.^a

Subject	Age	Sex	MRC		Lesion location		Recording day	
			Affected	Unaffected			Acute	Chronic
1	70	F	4	5	Right gyrus pre and post centralis, MCA, M3 occlusion	Cortical	5	181
2	72	F	4	5	Right MCA, subcortical, gyrus frontalis inferior and precentralis, M1 stenosis	Cortical	3	183
3	76	M	4	4	Right gyrus precentralis, subcortical boundary, MCA, M2 stenosis	Cortical	5	–
4	44	M	5	5	Right gyrus precentralis, gyrus frontalis medius, ACA/MCA boundary	Cortical	3	220
5	81	F	5	5	Right gyrus precentralis and parietal cortex, MCA, M4 occlusion	Cortical	4	178
6	90	F	3	5	Left juxtacortical postcentral	Subcortical	3	–
7	74	M	4	5	Right capsulothalamic	Subcortical	3	186
8	71	M	5	5	Left AchA, posterior limb of capsula interna	Subcortical	3	–
9	68	M	5	5	Left centrum semiovale	Subcortical	3	253
10	67	M	5	5	Right centrum semiovale	Subcortical	5	187
11	76	F	4	5	MCA M2, left corona radiata, superior parietal lobul left > right	Subcortical	3	–

^a F, female; M, male; MCA, middle cerebral artery; M1–4, segments of MCA; ACA, anterior cerebral artery; AchA, anterior choroidal artery.

the wrist at the midline. Ag/AgCl sintered electrodes 12 mm in diameter were used for reference and ground.

2.5. Data analysis

2.5.1. Preprocessing

Data analyses were performed offline in MATLAB (Mathworks Inc., USA) environment with custom written functions. The analysis was based on the stable hold period of the task, during which the strongest coherent activity in the beta band has been shown before (Baker et al., 1997; Riddle and Baker, 2006; Kristeva et al., 2007). We chose the post-stimulus interval between 2 and 4 s after the tone onset as a period showing a stable force production (Bayraktaroglu et al., 2011, 2013). The data were visually inspected for the presence of major abrupt force changes in the hold period. If the force output deviated from the range 0.5 ± 0.1 N, the epoch was discarded. Further, epochs containing large-amplitude artifacts in the frequency range of interest (8–44 Hz) were excluded by means of visual inspection. After artifact rejection, the 2-s epochs were divided into segments of 500 ms length yielding 206.5 ± 62.3 and 208.4 ± 62.8 segments for the affected and unaffected hand of the patients, respectively, in the acute period, and 259.4 ± 17.1 and 270.3 ± 18.6 segments for affected and unaffected hand of the patients, respectively, in the chronic period. To take into account that differences in CMC strength may relate to the number of epochs across the subjects, we performed bootstrapping to select an equal number of epochs. The lowest number of artifact-free 2-s epochs among all subjects was 34. Therefore, we selected 30 epochs randomly one-hundred times from all artifact-free epochs and then calculated the CMC spectrum on the resulting 120 segments (30 epochs \times 4 = 120 segments). The CMC peak was finally calculated as the average of one hundred bootstrap sequences.

2.5.2. Corticomuscular coherence

In this study, we used our recently developed technique – Regression CMC (R-CMC) – for the optimal detection of corticomuscular coherence (Bayraktaroglu et al., 2011, 2013). The core idea of R-CMC is to find a spatial filter for multichannel EEG data which maximally explains EMG activity in a given frequency range. Such an optimization is performed in the time domain where the correlation of narrow-band signals is equivalent to the calculation of phase coherence in the Fourier domain. For CMC estimation the EMG signal was not rectified as EMG rectification has been recently shown to have a detrimental effect on CMC estimation in both experimental and theoretical studies (Stegeman et al., 2010; Bayraktaroglu et al., 2011; McClelland et al., 2012; Farina et al., 2013).

R-CMC analysis is performed in two steps: (1) to avoid collinearity of the predictors and to make the estimation of covariance matrices more robust, a dimension reduction was performed using Principal Component Analysis (PCA). PCA components were selected to account for 99% variability of the data. (2) To account for the conduction delay between cortex and muscle, least-squares assessments were performed for different delays. The delay was estimated for frequencies between 8 and 44 Hz with 2 Hz steps and 4 Hz band-width. For this estimation EMG was shifted relative to EEG between $-\pi$ and $+\pi$ in $\pi/6$ steps. Separately for each EMG electrode and delay, multiple regression was performed and the coherence corresponding to the best EMG channel and delay was selected for further analysis.

Let \mathbf{y} be projected EEG data which is maximally synchronous with the EMG data in \mathbf{g} , then the coherence between projected data (\mathbf{y}) and EMG (\mathbf{g}) across segments is estimated as:

$$\text{Coh}_{g,y} = \frac{|\mathbf{s}_{g,y}|^2}{\mathbf{s}_g \times \mathbf{s}_y} \quad (1)$$

where \mathbf{s}_g and \mathbf{s}_y are averaged Fourier powers for EMG and projected EEG data, respectively, and $\mathbf{s}_{g,y}$ is the averaged cross-spectrum. For the calculation of the Fourier transforms, the data was divided into 500-ms non-overlapping segments and windowed with a Hanning window. When presenting results, we refer to CMC amplitude and frequency corresponding to the highest peak in the coherence spectrum.

In order to calculate the spatial pattern of the optimized EEG vector, i.e. the topographical distribution corresponding to the strongest coherent activity, we utilized an approach proposed by Parra et al. (2002). During the optimization procedure we excluded components with patterns showing abnormal activity such as mosaic like high-frequency spatial features or strong activity at the temporal or frontal edges of the patterns (a typical indication for the presence of the scalp muscle activity).

We used permutation tests for determining the significance level of the coherence (Hesterberg et al., 2005). For this procedure, we repeated all the steps of R-CMC but used EMG segments that were shuffled with respect to the EEG data. One-hundred permutations were performed for each set of data, and a specific coherence value was obtained on 30 epochs randomly chosen for each permutation. The coherence was considered significant if the hundred coherence values of unpermuted data (see above) were significantly larger than the coherence values of permuted data (t -test).

Further, we calculated the temporal evolution of CMC from -2 to 7 s around the start tone. The coherence was calculated with 500-ms windows which were translated along the whole epoch length with 100-ms steps. The spatial filter obtained for the stable active period (2–4 s) was used for all time windows.

2.5.3. Localization of cortical CMC sources

Patterns corresponding to the optimized EEG components were used for finding neuronal sources with the sLORETA algorithm (Pascual-Marqui, 2002). For comparing sources of the affected and unaffected side, the data were mapped to correspond to the same hand side of performance. The individual EEG patterns were flipped such that the lesion was always in the right hemisphere corresponding to left hand performance. Accordingly, performance of the unaffected hand was mapped to right hand performance. Consequently, the sources were mapped using the standard MNI305 head (Collins et al., 1994). For comparative purposes, sLORETA maps were normalized by dividing the power in each voxel by the sum of power from all voxels.

2.5.4. Event-related desynchronization (ERD)

The EEG signals were segmented around the starting tone from -2 to 7 s and bandpass-filtered around the peak frequency obtained for the highest CMC value with a bandwidth of ± 2 Hz. Then the spatial filter obtained from CMC estimation was applied. Thereafter, the absolute value of the Hilbert transformed signal was obtained and the epochs were averaged. We refer to the response of the post-stimulus amplitude expressed in percentage with respect to the pre-stimulus (-700 to -200 ms) amplitude as event-related desynchronization (ERD; Pfurtscheller and Lopes da Silva, 1999).

2.5.5. Power and frequency of ongoing oscillations

We determined also two measures of ongoing oscillations in the pre-stimulus interval (-2 to 0 s). For both measures, the analysis of spectral power of ongoing oscillations was based on the projected EEG component, which was optimized for CMC estimation. For the first measure, relative spectral power (RSP) corresponded to the ratio of the mean power in the 4 Hz-wide frequency band around the highest CMC value to the mean power in the broad frequency range of 5–35 Hz. For the second measure, we determined the largest spectral peak (of the R-CMC projected component) in the 8–35 Hz range; this peak was not necessarily corresponding to the peak of the strongest CMC but rather reflecting the largest power in ongoing EEG.

2.5.6. Statistical analysis

Statistical analyses of values for CMC amplitude and frequency were carried out in SPSS (IBM SPSS Inc., USA). For statistical comparison of the CMC parameters within the patient group, a linear mixed model was employed including the repeated variables SIDE (affected and unaffected) and TIME (acute and chronic). The same analysis was performed for force, coefficients of variation of force, ERD amplitude and latency, pre-stimulus RSP, and peak frequency of power. If not indicated otherwise, statistical results are given as mean values \pm standard error of mean (SEM).

3. Results

3.1. Performance

All patients were able to perform the task and maintain the required force level. When all epochs were taken into account, the force level in the 2–4 s interval (which was used for the calculation of CMC) was 0.46 ± 0.03 N and 0.49 ± 0.02 N for the affected and unaffected side of the patients, respectively, in the acute period, and 0.53 ± 0.03 N and 0.50 ± 0.03 N for the affected and unaffected side, respectively, in the chronic period. As mentioned in Section 2, epochs which deviated by more than 0.1 N from the required level were rejected in order to avoid attenuation of CMC due to ongoing movement (Kilner et al., 2000; Riddle and Baker, 2006). After removal of such epochs the mean level of force was 0.50 ± 0.01 N

and 0.52 ± 0.02 N for the affected and unaffected side, respectively, in the acute period, and 0.53 ± 0.03 N and 0.51 ± 0.03 N for the affected and unaffected side, respectively, in the chronic period. Neither before nor after the artifact removal the mean force level differed statistically between side of lesion or time points. Before artifact removal, the coefficients of variation of force levels were 0.36 ± 0.07 and 0.29 ± 0.05 for the affected and unaffected side, respectively, in the acute period, and 0.15 ± 0.02 and 0.15 ± 0.03 in the chronic stage. There was a significant effect of the factor TIME ($p < 0.01$). Pairwise comparison between acute and chronic period was significant for both unaffected ($p < 0.05$) and affected sides ($p < 0.05$). After the removal of artifacts, the coefficients of variation of force levels were 0.13 ± 0.02 and 0.13 ± 0.01 for the affected and unaffected side, respectively, in the acute period, and 0.10 ± 0.01 and 0.10 ± 0.02 for the affected and unaffected side, respectively, in the chronic period. There was still a significant interaction effect of SIDE \times TIME ($p < 0.05$). On the affected side, the difference between acute and chronic period was near significant ($p = 0.05$).

3.2. Corticomuscular coherence

3.2.1. CMC amplitude

In the acute period, CMC amplitude in patients was 0.15 ± 0.02 and 0.20 ± 0.02 for the affected and unaffected side, respectively; and in the chronic period CMC amplitude was 0.16 ± 0.03 and 0.14 ± 0.02 for the affected and unaffected side, respectively. For the 7 patients, that were measured at both time points, the CMC spectra of both sides in acute and chronic stroke are shown in Fig. 1 to illustrate the observed changes in CMC amplitude and frequencies. As an example, the spatial CMC patterns of subject 10 are shown for both sides and both stroke stages in Supplementary Fig. S2. The time course of CMC (averaged across subjects) is displayed in Fig. 2 confirming that the post-stimulus interval 2–4 s was optimal for the calculation of CMC since it corresponded to the strongest coherence. Fig. 3 shows the grand average (across all subjects) for sLORETA solutions separately for the affected and unaffected sides at both acute (A) and chronic (B) stages. For comparative purposes, the single sLORETA solutions were mapped such that the lesion was always in the right hemisphere. For both sides and time points of measurement, CMC sources were localized in the sensorimotor cortices contralateral to the performing hand.

In controls, CMC amplitude was 0.16 ± 0.02 and 0.17 ± 0.02 for left and right hands, respectively. There were no differences in CMC amplitude or frequency between hands. For comparison with the patient group, CMC values corresponding to left and right hands of the controls were therefore averaged to obtain one value for each subject, resulting in a CMC amplitude of 0.16 ± 0.02 .

In patients, statistical comparison showed a significant effect for the factor TIME ($p < 0.05$). The interaction effect of TIME \times SIDE was also near significant ($p = 0.056$). Pairwise comparison showed that in the acute period, the CMC amplitude for the unaffected side of the patients was significantly larger than for the affected side ($p < 0.01$). Additionally, on the unaffected side, the CMC amplitude was significantly larger in the acute period compared to the chronic period ($p < 0.01$). The comparison with the control group, showed no difference of CMC amplitude between controls and affected or unaffected side of patients for acute and chronic stage (t -tests). Fig. 4A illustrates the statistical results for the comparison of CMC amplitudes.

3.2.2. CMC frequency

In the acute period of stroke, CMC was in the range of 8–18 Hz and 8–26 Hz on the affected and unaffected side, respectively, the mean CMC peak frequency being 12.0 ± 0.8 Hz and 14.4 ± 1.5 Hz, respectively. In the chronic period, CMC ranges were 12.5–28 Hz

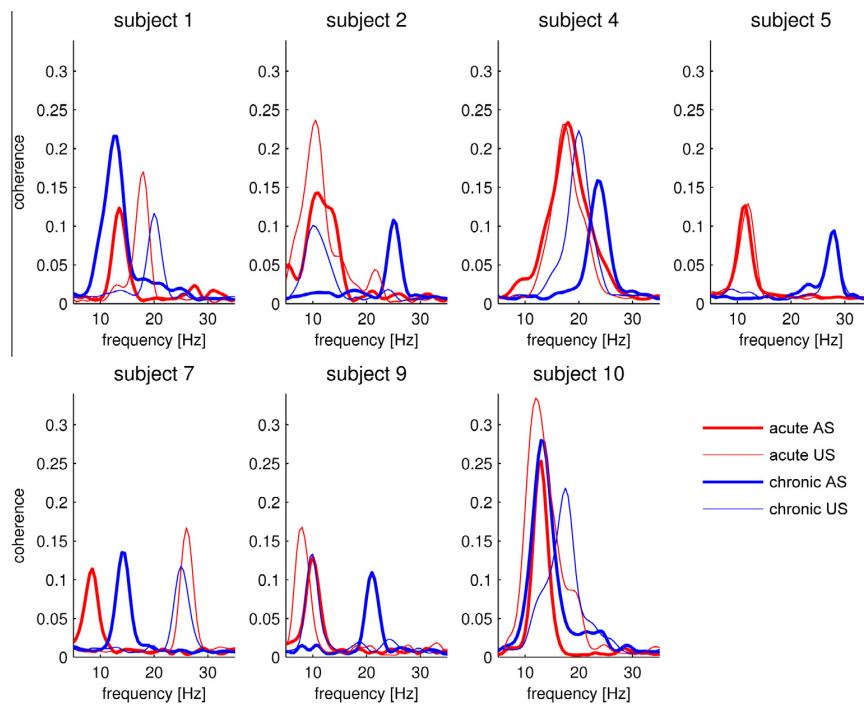


Fig. 1. Individual CMC spectra for both affected and unaffected sides of the 7 subjects who were measured in acute and chronic stroke. Note that curves tend to peak at lower frequencies for the acute period compared to the chronic period. In most cases, the CMC peak amplitude of the unaffected side in the acute period exceeds the three other peaks. AS, affected side; US, unaffected side.

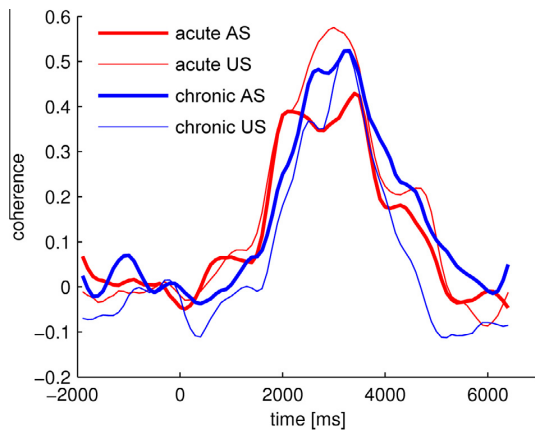


Fig. 2. Grand-average of time-resolved CMC (normalized to the subject's peak value). AS, affected side; US, unaffected side.

and 10–28 Hz with a mean peak frequency of 19.6 ± 2.4 Hz and 18.6 ± 2.6 Hz on the affected and unaffected side, respectively.

CMC peak frequencies in controls were in the frequency range of 9–29 Hz. The mean CMC peak frequency was 18.9 ± 1.5 and 20.1 ± 1.5 Hz for left and right hands, respectively. The average of peak frequencies corresponding to left and right hands resulted in a CMC frequency of 19.5 ± 1.4 Hz.

The statistical comparison of peak frequencies in patients showed a significant effect for the factor TIME ($p < 0.05$). Pairwise comparison of the acute and chronic period revealed a significant

increase of CMC peak frequency on the affected side ($p < 0.05$) in the chronic period. At acute stage, peak frequencies of CMC on both the affected and unaffected side of patients were significantly smaller than in the control group (t -tests, $p < 0.001$ and $p < 0.05$, respectively). The CMC peak frequency was not significantly different between the affected and unaffected sides at acute and chronic stages of stroke. In the chronic period, there was no difference of CMC frequencies between patients and controls. The results of the statistical comparison are displayed in Fig. 4B.

3.2.3. Age effect on CMC

We performed a correlation analysis to see whether there was an age effect on CMC. There was no significant correlation between CMC amplitude and age for the affected and unaffected side of patients ($\rho = -0.42$, $p = 0.09$ and $\rho = -0.44$, $p = 0.07$, respectively) or for controls ($\rho = 0.08$, $p = 0.79$). Further, there was no significant correlation between CMC frequency and age for the affected and unaffected side of patients ($\rho = -0.16$, $p = 0.52$ and $\rho = 0.05$, $p = 0.85$, respectively) or for controls ($\rho = -0.32$, $p = 0.26$).

3.3. ERD

The mean values of ERD peak strength in the post-stimulus interval of 0–2000 ms were $-28.7 \pm 2.1\%$ and $-28.4 \pm 4.1\%$ relative to the baseline value for the affected and unaffected side of patients, respectively, in the acute period, and $-24.1 \pm 8.0\%$ and $-32.4 \pm 4.3\%$ for the affected and unaffected side, respectively, in the chronic period. The peak latencies of the ERD component were 1421 ± 134 ms and 1015 ± 188 ms for the affected and unaffected side, respectively, in the acute period; and 1151 ± 167 ms and 891 ± 180 ms, respectively, in the chronic period. There were no

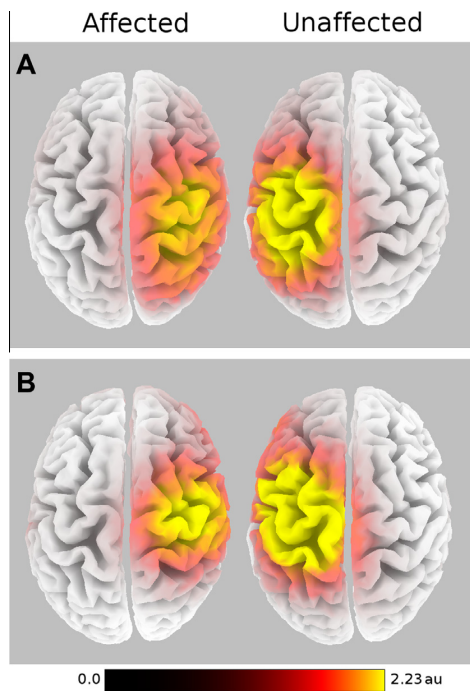


Fig. 3. Grand-averaged (across subjects) sLORETA solutions for the affected and unaffected side in acute (A) and chronic (B) stage. The sLORETA solutions of the patients were mapped such that the lesion was always in the right hemisphere. The sLORETA solutions of both sides and time points showed CMC sources that were localized in the sensorimotor cortices contralateral to the performing hand. au, arbitrary units.

significant statistical main or interaction effects for ERD amplitude. For ERD latency the effect for the factor SIDE was near significant ($p = 0.057$). In the acute period, latencies on the unaffected side tended to be shorter than on the affected side ($p = 0.062$). The time-course of ERD is shown in [Supplementary Fig. S1](#).

3.4. Peak frequencies and power of ongoing oscillations

In the pre-stimulus interval, relative spectral power (RSP) of ongoing oscillations was 1.03 ± 0.18 and 1.16 ± 0.23 for the af-

ected and unaffected side of patients, respectively, in the acute period; and 1.04 ± 0.19 and 1.24 ± 0.25 for the affected and unaffected side, respectively, in the chronic period. There were no significant statistical differences of pre-stimulus RSP between sides and time points of measurement.

Peak frequencies of ongoing oscillations in the pre-stimulus interval were 16.6 ± 2.7 Hz and 17.2 ± 2.9 Hz for the affected and unaffected side, respectively, in the acute period; and 18.8 ± 3.1 Hz and 17.5 ± 3.5 Hz for the affected and unaffected side, respectively, in the chronic period. There were no significant differences for peak frequencies in the pre-stimulus period. The peak frequencies were primarily in the frequency range of beta oscillations (13–35 Hz).

4. Discussion

Our aim was to study corticomuscular coherence in patients with unilateral stroke both in the acute and chronic stage to gain knowledge about the temporal dynamics of corticomuscular interactions in post-stroke recovery. We found a significant slowing of CMC peak frequencies on both sides in the acute period. At the same time, CMC amplitudes were larger on the unaffected side compared to the affected side, and CMC amplitudes on the unaffected side were larger in the acute compared to the chronic period. In the chronic period, CMC peak frequencies had increased and CMC amplitudes did not differ between the affected and unaffected sides. In both acute and chronic stage as well as for both left and right movements, CMC sources of grand-averaged sLORETA solutions were localized primarily in the contralateral sensorimotor cortices.

4.1. The patient group

The patients in the current study were selected for their clinical symptoms. They all suffered from a moderate to severe hemiparesis on the contralesional hand at the onset of stroke. Thus, despite patients having different lesion locations including cortical and subcortical regions, the impaired transmission along the efferent pathway of the corticospinal tract was a common factor in all patients. The recruitment of cortical areas during motor performance ([Ward et al., 2006, 2007](#)) and motor function ([Stinear et al., 2007](#)) have been shown to depend on corticospinal integrity post-stroke. Therefore, functional impairment rather than lesion location seems to be a feasible selection criterion.

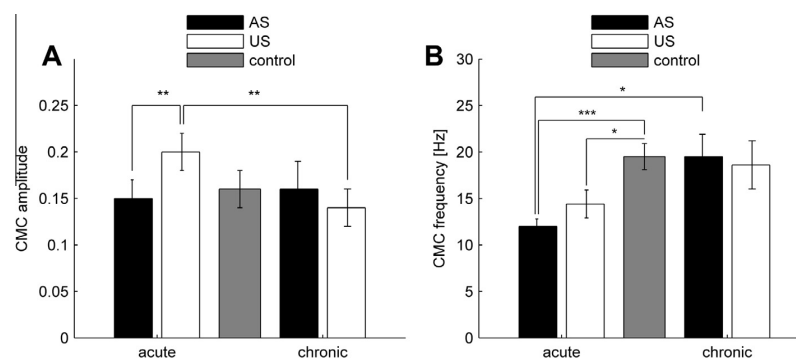


Fig. 4. The results of the statistical comparison of CMC amplitude and frequency. (A) Pairwise comparison of CMC amplitude showing that on the unaffected side in acute stage, CMC amplitudes were significantly increased compared to the affected side in acute stage ($p < 0.01$) and the unaffected side in chronic stage ($p < 0.01$) and (B) pairwise comparison of CMC peak frequencies revealed a significant increase of peak frequencies on the affected side in chronic stage compared to acute stage ($p < 0.05$). In acute stage, CMC peak frequencies on both the affected and unaffected side of patients were significantly smaller than in the control group ($p < 0.001$ and $p < 0.05$, respectively). AS, affected side; US, unaffected side.

Note that on the day of the first recording, patients had already regained enough muscle strength (assessed by MRC scores) to perform the experiment. Thus, we were able to detect changes in CMC between acute and chronic stage while MRC scores were not sensitive enough for this differentiation.

4.2. CMC in acute stroke

To our knowledge, this study is the first to measure CMC in the acute stage of stroke. We found lower CMC frequencies on both sides compared to the chronic period and the control subjects.

It is unlikely that the shift to lower frequencies is caused by an artifact such as scalp muscle activity. We addressed the problem of interfering strong sources already in our previous study (Bayraktaroglu et al., 2011) where we performed simulations using realistic head modeling. In these simulations we had one cortical dipole interacting with muscle activity and an interfering, uncorrelated dipole which was up to 20 times stronger. For background neuronal noise, we added 500 dipoles producing 1/f noise. Our results showed that R-CMC reliably extracted the cortical sources showing CMC, avoiding the extraction of the interfering source.

Interestingly, Mima et al. (2001, Fig. 1B) showed the example of a chronic stroke patient with CMC frequency at lower frequency (11 Hz) which they however did not elaborate on. Slowing of CMC frequencies can be interpreted in two different ways. Firstly, the CMC peak in the low frequency range might reflect an underlying process different from the CMC peak in the higher frequency range. In this case, the relation between these two processes would have changed in the post-stroke period: while in the acute period the process at low frequency was more dominant than the process at the higher frequency, in the chronic period the relation was reversed. Secondly, the CMC peak might have progressively shifted from lower to higher frequencies in the course of post-stroke recovery. As the current study involved only two measurements, both possibilities could apply. Thus, by referring to *slowing of CMC frequencies* we imply both interpretations. Slowing of CMC frequencies and increased CMC amplitudes have been related to healthy aging (Graziadio et al., 2010; Kamp et al., 2011). The authors argue that M1 power increase and the shift towards lower frequencies might represent a neurophysiological marker of healthy aging which is possibly compensated by an increased CMC amplitude. The underlying functional alterations causing these changes in CMC in aging could be the same as for stroke. This would affirm that in the current study the CMC amplitude is increased on the unaffected side in the acute period rather than CMC amplitudes being decreased on the other side/time point of measurement. An increase in CMC amplitude on the unaffected side is also supported by the comparison with the control group in the current study (Fig. 4A). Graziadio et al. (2010) related a broader spread of frequencies including coherence in the alpha range in elderly (>55 years) to a breakdown of recurrent inhibition. They found that a greater deviation from 23 Hz corresponded to poorer performance. We hypothesize that slowing of CMC frequency in the acute stage of stroke might result from a temporary decrease of inhibition. A potential role of inhibition leading to the changes in CMC will be addressed in further detail below.

4.3. CMC in chronic stroke

Previous CMC studies were performed at the chronic stage of stroke and included patients with various degrees of recovery (Mima et al., 2001; Braun et al., 2007; Fang et al., 2009; Meng et al., 2009; Graziadio et al., 2012). They consistently indicated a functional involvement of the lesioned hemisphere; the results about the CMC amplitude and peak frequency were however less consistent. Mima et al. (2001) and Meng et al. (2009) reported sig-

nificantly lower CMC amplitudes for affected hand movements, including spatial shifts without any changes in CMC peak frequency. Braun et al. (2007) showed that CMC amplitudes did not differ between recovered patients and controls, but in patients CMC was larger in amplitude and distributed over a broader frequency interval on the affected side compared to the unaffected side. In a dynamic reaching task, Fang et al. (2009) compared CMC between cortical regions and upper limb muscles in poorly recovered stroke patients and controls. They found that while motor coordination deficits abolished gamma band CMC in stroke patients, there were only small differences in beta-band CMC between the two groups. Graziadio et al. (2012), who included patients with various degrees of recovery, found no difference between stroke patients and controls in CMC amplitudes or frequencies but hemispheric symmetry of CMC correlated with recovery. Only Fang et al. (2009), who found no hemispheric differences in CMC amplitude, included poorly recovered patients but at the same time also used a different experimental task. The others (Mima et al., 2001; Braun et al., 2007; Meng et al., 2009) found differences in CMC amplitude despite good recovery. Therefore, the degree of recovery does not seem to be the only explanation for the differences in CMC amplitude. It is more likely that a mixture of several parameters including the recovery of the patients, the time elapsed after the stroke occurrence and specific motor paradigms utilized by different researchers led to the diverse outcomes in CMC amplitude in these studies, making a comparison of the results difficult.

Although the results of CMC amplitude in stroke vary, a common finding – consistent with the results of the present study – is that there are no inter-hemispheric differences in CMC peak frequency in chronic stroke among the studies that report on CMC peak frequencies (Mima et al., 2001; Meng et al., 2009; Graziadio et al., 2012).

Our measurements at chronic stage were performed on average 194.6 days after the stroke, this time interval being the earliest among the time intervals used in the previous studies on CMC in stroke. Importantly, our results showed that already after this comparatively short time interval there were no inter-hemispheric differences in the amplitude of CMC or its peak frequencies.

4.4. Factors potentially contributing to the modulation of CMC

Although we found the stated significant differences in the parameters of CMC between sides and between stroke stages, one could also observe a certain variability across subjects in amplitude and frequency of CMC. The inhomogeneity among the patients can most likely be attributed to the general inter-individual variability of CMC which also occurs in healthy people including the occurrence of CMC in alpha range in some cases (Mima and Hallett, 1999; Ushiyama et al., 2011).

In the following we elaborate on factors that were shown to be related to differences in CMC and which might be of relevance for the current study.

4.4.1. Age

Previous studies have shown an age effect on CMC (Graziadio et al., 2010; Kamp et al., 2011). Kamp et al. (2011) found CMC frequency to be negatively and CMC amplitude to be positively correlated with age. For the age groups above 40 years there was however no difference in CMC frequency. Yet, there was a trend of CMC amplitude to be higher in elderly (58–77 years) compared to middle-aged people (41–55 years). Graziadio et al. (2010) did not find a difference in CMC amplitude when comparing elderly (>55 years) with young adults (20–35 years). In the current study the control group was younger than the patients group; however, there was no correlation of CMC amplitude or frequency with

age. A possible explanation would be that the youngest subject in the control group was 39 years old. Thus, both patient and control group corresponded to those studies' middle-aged and elderly groups where no significant differences were found. Taken together, the CMC changes found in the current study cannot be related to age. Changes in CMC amplitude occurred for the within-subject comparison and related only to the unaffected side. Moreover, while at acute stage peak frequencies were significantly lower, they aligned with the peak frequencies of controls at chronic stage. The increase in the chronic period thus argues against an effect of age.

4.4.2. Motor performance

CMC changes depend on the exerted force (Brown et al., 1998; Mima et al., 1999), however CMC amplitude is not affected by weak to moderate forces (Mima et al., 1999). To ensure further that our findings were not due to different motor performance of the paretic and non-paretic hands, we excluded trials deviating more than 0.1 N from the required force level such that there were no significant differences between the mean force levels either between affected/unaffected hand or between time points of measurement (acute vs. chronic stages). Coefficients of variation of force had a tendency to be larger on the affected side in acute compared to chronic stage. CMC amplitude changes, however, occurred on the unaffected side and can therefore not be attributed to variations in force levels.

We controlled for equal force levels by choosing a fixed force level of 0.5 N rather than, as often used, a percentage of maximum voluntary contraction (MVC). A certain percentage, i.e. 5%, of MVC could have led to very small force levels for some of the patients, especially at acute stage, making performance difficult. Further, while the motor system in the stroke patients was affected, the majority of patients did not show any tactile impairment. Taking MVC as a reference for the target force level would have increased the tactile stimulation (due to recovered motor strength) in the second measurement. As feedback afferent pathways potentially play a role in CMC generation (Riddle and Baker, 2005; Baker, 2007), thus equal force levels in the current study ensured that somatosensory feedback did not induce the differences in the measured CMC.

4.4.3. ERD and power of beta oscillations

Findings on movement-related ERD in paretic stroke subjects vary (Platz et al., 2000; Gerloff et al., 2006; Stępień et al., 2011). Here, we did not find any significant differences in the magnitudes or latencies of ERD comparing sides and time point of measurement. Thus, ERD, which is considered to be an electrophysiological correlate of activated neuronal networks (Pfurtscheller and Lopes da Silva, 1999), is unlikely to explain the differences in the CMC parameters.

Engel and Fries (2010) suggested that beta oscillations relate to the maintenance of the current sensorimotor set, while in contrast, an abnormal enhancement of beta activity would be likely to result in a persistence of the current sensorimotor set and a deterioration of flexible behavioral and cognitive control. Previously, the recovery of stroke patients was shown to be positively correlated with the hemispheric symmetry of beta-band power (Graziadio et al., 2012). In acute stroke patients, Tecchio et al. (2005) found smaller relative beta-band power at rest in the affected compared to the unaffected hemisphere. This inter-hemispheric difference in relative but not in absolute beta-band power was also observed in chronic patients (Tecchio et al., 2006). Here, we compared relative spectral power (RSP) of beta oscillations before movement onset and found it to be not different between sides and time points of measurement (acute vs. chronic stage). We therefore can exclude that changes in CMC are caused by changes in the amplitude of

neuronal oscillations, which in turn relate to the signal-to-noise ratio (Nikulin et al., 2011) and thus can effect the estimation of CMC (Bayraktaroglu et al., 2013).

4.5. Dissociation of CMC and beta oscillations

Our finding is in line with the earlier studies suggesting a functional dissociation between different components of beta oscillations (Pfurtscheller et al., 1997; Hall et al., 2011) as well as between the power of beta oscillations and CMC (Baker and Baker, 2003; Riddle et al., 2004). Diazepam, a GABA_A receptor agonist, slightly reduced beta CMC amplitude while EEG beta power doubled (Baker and Baker, 2003). On the contrary, Riddle et al. (2004) showed the opposite reaction when administering the anti-convulsive drug Carbamazepine: CMC amplitude increased whereas beta power and also CMC frequency remained unchanged.

In the present study not only the magnitude of beta power, but also the peak frequencies of ongoing pre-stimulus beta oscillations during rest remained unchanged between the sides and time points of measurement. In comparison, CMC frequencies were lower on both sides in acute stage thus further reinforcing the assumption of a dissociation between beta oscillation and CMC.

4.6. Potential role of GABA-mediated inhibition

We hypothesize that the changes in CMC, observed in the present study, might relate to the time-course of changes in cortical inhibition following stroke. The modulation of GABA availability is thought to be important for the cortical reorganization in the acute period of functional recovery after a lesion (Levy et al., 2002). This is supported by Clarkson et al. (2010) who showed that reducing excessive GABA-mediated tonic (extrasynaptic) inhibition promotes the recovery after stroke in mice. Such a reduced tonic inhibition might lead to slowing frequency of beta oscillations as shown by Jensen et al. (2005). They demonstrated in a simulation that inhibitory current to inhibitory interneurons led to an increase in beta power, widening of the spectral peak and slowing of frequency. Consistent with this finding, in another simulation study lacking recurrent inhibition was shown to result in an enlarged CMC peak at 10 Hz (Williams and Baker, 2009). Here we argue that in successful motor recovery the general slowing of CMC frequency and the increase of coherence amplitude on the unaffected side might reflect a reduction of tonic inhibition by GABA_A receptors. Inhibition was shown to be decreased in either only ipsilesional (Swayne et al., 2008) or both contra- and ipsilesional motor cortices (Bütefisch et al., 2008; Huynh et al., 2013) in acute and subacute stroke patients and became correlated with functional recovery 3 months post-stroke (Swayne et al., 2008). An imbalance of transcallosal inhibition (Bütefisch et al., 2008) could explain the hemispheric asymmetry of CMC amplitudes in the acute period shown in the current study. These CMC changes in amplitude and frequency potentially might be a sign of cortical reorganization in the acute period after stroke and beneficial for motor recovery as, on the contrary, the GABA-agonist Diazepam slightly reduces CMC (Baker and Baker, 2003) and has a negative effect on stroke recovery (Goldstein, 1998). The changes of CMC at acute stage are then followed by the return to higher CMC peak frequencies and inter-hemispherically symmetric amplitudes in the chronic phase of stroke. The modulation of CMC amplitude and frequency over time might thus reflect the course of motor recovery.

Acknowledgements

Z.B. was supported by the Center for Stroke Research Berlin. V.V.N. and G.C. were supported by the Berlin Bernstein Center for Computational Neuroscience.

Appendix A. Supplementary data

Supplementary data associated with this article can be found, in the online version, at <http://dx.doi.org/10.1016/j.clinph.2013.11.006>.

References

- Assaf Y, Pasternak O. Diffusion tensor imaging (DTI)-based white matter mapping in brain research: a review. *J Mol Neurosci* 2008;34:51–61.
- Baker SN. Oscillatory interactions between sensorimotor cortex and the periphery. *Curr Opin Neurobiol* 2007;17:649–55.
- Baker MR, Baker SN. The effect of diazepam on motor cortical oscillations and corticomuscular coherence studied in man. *J Physiol* 2003;546:931–42.
- Baker SN, Olivier E, Lemon RN. Coherent oscillations in monkey motor cortex and hand muscle EMG show task-dependent modulation. *J Physiol* 1997;501:225–41.
- Bayraktaroglu Z, von Carlowitz-Ghori K, Losch F, Nolte G, Curio G, Nikulin VV. Optimal imaging of cortico-muscular coherence through a novel regression technique based on multi-channel EEG and un-rectified EMG. *NeuroImage* 2011;57:1059–67.
- Bayraktaroglu Z, von Carlowitz-Ghori K, Curio G, Nikulin VV. It is not all about phase: amplitude dynamics in corticomuscular interactions. *NeuroImage* 2013;64:496–504.
- Braun C, Staudt M, Schmitt C, Preissl H, Birbaumer N, Gerloff C. Crossed cortico-spinal motor control after capsular stroke. *Eur J Neurosci* 2007;25:2935–45.
- Brown P, Salenius S, Rothwell JC, Hari R. Cortical correlate of the piper rhythm in humans. *J Neurophysiol* 1998;80:2911–7.
- Bütefisch CM, Weßling M, Netz J, Seitz RJ, Hömberg V. Relationship between interhemispheric inhibition and motor cortex excitability in subacute stroke patients. *Neurorehabil Neural Repair* 2008;22:4–21.
- Calautti C, Baron J-C. Functional neuroimaging studies of motor recovery after stroke in adults a review. *Stroke* 2003;34:1553–66.
- Clarkson AN, Huang BS, MacIsaac SE, Mody I, Carmichael ST. Reducing excessive GABA-mediated tonic inhibition promotes functional recovery after stroke. *Nature* 2010;468:305–9.
- Collins DL, Neelin P, Peters TM, Evans AC. Automatic 3D intersubject registration of MR volumetric data in standardized Talairach space. *J Comput Assist Tomogr* 1994;18:192–205.
- Dancuse N. Vicarious function of remote cortex following stroke: recent evidence from human and animal studies. *Neuroscientist* 2006;12:489–99.
- Engel AK, Fries P. Beta-band oscillations – signalling the status quo? *Curr Opin Neurobiol* 2010;20:156–65.
- Fang Y, Daly JJ, Sun J, Hovorac K, Fredrickson E, Pundik S, et al. Functional corticomuscular connection during reaching is weakened following stroke. *Clin Neurophysiol* 2009;120:994–1002.
- Farina D, Negro F, Jiang N. Identification of common synaptic inputs to motor neurons from the rectified electromyogram. *J Physiol (London)* 2013;591:2403–18.
- Gerloff C, Bushara K, Sailer A, Wassermann EM, Chen R, Matsuoka T, et al. Multimodal imaging of brain reorganization in motor areas of the contralesional hemisphere of well recovered patients after capsular stroke. *Brain* 2006;129:791–808.
- Goldstein LB. Potential effects of common drugs on stroke recovery. *Arch Neurol* 1998;55:454–6.
- Graziadio S, Basu A, Tomasevic L, Zappasodi F, Tecchio F, Eyre JA. Developmental tuning and decay in senescence of oscillations linking the corticospinal system. *J Neurosci* 2010;30:3663–74.
- Graziadio S, Tomasevic L, Assenza G, Tecchio F, Eyre JA. The myth of the “unaffected” side after unilateral stroke: is reorganisation of the non-infarcted corticospinal system to re-establish balance the price for recovery? *Exp Neurol* 2012;238:168–75.
- Grefkes C, Fink GR. Reorganization of cerebral networks after stroke: new insights from neuroimaging with connectivity approaches. *Brain* 2011;134:1264–76.
- Hall SD, Stanford IM, Yamawaki N, McAllister CJ, Rönnqvist KC, Woodhall GL, et al. The role of GABAergic modulation in motor function related neuronal network activity. *NeuroImage* 2011;56:1506–10.
- Hesterberg T, Moore DS, Monaghan S, Clipson A, Epstein R. Bootstrap methods and permutation tests. In: Moore DS, McCabe GP, editors. *Introduction to the Practice of Statistics*. 5th ed. New York: W. H. Freeman; 2005. p. 1–70.
- Huynh W, Vucic S, Krishnan AV, Lin CS-Y, Hornberger M, Kiernan MC. Longitudinal plasticity across the neural axis in acute stroke. *Neurorehabil Neural Repair* 2013;27:219–29.
- Jang SH. A review of motor recovery mechanisms in patients with stroke. *NeuroRehabilitation* 2007;22:253–9.
- Jensen O, Goel P, Kopell N, Pohja M, Hari R, Ermentrout B. On the human sensorimotor-cortex beta rhythm: sources and modeling. *NeuroImage* 2005;26:347–55.
- Kamp D, Krause V, Butz M, Schnitzler A, Pollok B. Changes of cortico-muscular coherence: an early marker of healthy aging? *AGE* 2011;35:49–58.
- Kilner JM, Baker SN, Salenius S, Hari R, Lemon RN. Human cortical muscle coherence is directly related to specific motor parameters. *J Neurosci* 2000;20:8838–45.
- Kristeva R, Patino L, Omlor W. Beta-range cortical motor spectral power and corticomuscular coherence as a mechanism for effective corticospinal interaction during steady-state motor output. *NeuroImage* 2007;36:785–92.
- Levy LM, Ziemann U, Chen R, Cohen LG. Rapid modulation of GABA in sensorimotor cortex induced by acute deafferentation. *Ann Neurol* 2002;52:755–61.
- McClelland VM, Cvetkovic Z, Mills KR. Rectification of the EMG is an unnecessary and inappropriate step in the calculation of corticomuscular coherence. *J Neurosci Methods* 2012;205:190–201.
- Meng F, Tong K-Y, Chan S-T, Wong W-W, Lui K-H, Tang K-W, et al. Cerebral plasticity after subcortical stroke as revealed by cortico-muscular coherence. *IEEE Trans Neural Syst Rehabil Eng* 2009;17:234–43.
- Mima T, Hallett M. Corticomuscular coherence: a review. *J Clin Neurophysiol* 1999;16:501–11.
- Mima T, Simpkins N, Oluwatimilehin T, Hallett M. Force level modulates human cortical oscillatory activities. *Neurosci Lett* 1999;275:77–80.
- Mima T, Toma K, Koshy B, Hallett M. Coherence between cortical and muscular activities after subcortical stroke. *Stroke* 2001;32:2597–601.
- Nikulin VV, Nolte G, Curio G. A novel method for reliable and fast extraction of neuronal EEG/MEG oscillations on the basis of spatio-spectral decomposition. *NeuroImage* 2011;55:1528–35.
- Nudo RJ. Postinfarct cortical plasticity and behavioral recovery. *Stroke* 2007;38:840–5.
- Oldfield RC. The assessment and analysis of handedness: the Edinburgh inventory. *Neuropsychologia* 1971;9:97–113.
- Oostenveld R, Praamstra P. The five percent electrode system for high-resolution EEG and ERP measurements. *Clin Neurophysiol* 2001;112:713–9.
- Parra L, Alvino C, Tang A, Pearlmutter B, Yeung N, Osman A, et al. Linear spatial integration for single-trial detection in encephalography. *NeuroImage* 2002;17:223–30.
- Pascual-Marqui RD. Standardized low-resolution brain electromagnetic tomography (sLORETA): technical details. *Methods Find Exp Clin Pharmacol* 2002;24(Suppl D):5–12.
- Pfurtscheller G, Lopes da Silva FH. Event-related EEG/MEG synchronization and desynchronization: basic principles. *Clin Neurophysiol* 1999;110:1842–57.
- Pfurtscheller G, Stancák Jr A, Edlinger G. On the existence of different types of central beta rhythms below 30 Hz. *Electroenceph Clin Neurophysiol* 1997;102:316–25.
- Platz T, Kim IH, Pintschovius H, Winter T, Kieselbach A, Villringer K, et al. Multimodal EEG analysis in man suggests impairment-specific changes in movement-related electric brain activity after stroke. *Brain* 2000;123:2475–90.
- Rathore SS, Hinn AR, Cooper LS, Tyroler HA, Rosamond WD. Characterization of incident stroke signs and symptoms: findings from the atherosclerosis risk in communities study. *Stroke* 2002;33:2718–21.
- Riddle CN, Baker SN. Manipulation of peripheral neural feedback loops alters human corticomuscular coherence. *J Physiol* 2005;566:625–39.
- Riddle CN, Baker SN. Digit displacement, not object compliance, underlies task dependent modulations in human corticomuscular coherence. *NeuroImage* 2006;33:618–27.
- Riddle CN, Baker MR, Baker SN. The effect of carbamazepine on human corticomuscular coherence. *NeuroImage* 2004;22:333–40.
- Rijntjes M. Mechanisms of recovery in stroke patients with hemiparesis or aphasia: new insights, old questions and the meaning of therapies. *Curr Opin Neurol* 2006;19:76–83.
- Salenius S, Hari R. Synchronous cortical oscillatory activity during motor action. *Curr Opin Neurobiol* 2003;13:678–84.
- Salenius S, Portin K, Kajola M, Salmelin R, Hari R. Cortical control of human motoneuron firing during isometric contraction. *J Neurophysiol* 1997;77:3401–5.
- Stegeman DF, van de Ven WJM, van Elswijk GA, Oostenveld R, Kleine BU. The alpha-motoneuron pool as transmitter of rhythmicities in cortical motor drive. *Clin Neurophysiol* 2010;121:1633–42.
- Stepien M, Conradi J, Waterstraat G, Hohlefeld FU, Curio G, Nikulin VV. Event-related desynchronization of sensorimotor EEG rhythms in hemiparetic patients with acute stroke. *Neurosci Lett* 2011;488:17–21.
- Stinear CM, Barber PA, Smale PR, Coxon JP, Fleming MK, Byblow WD. Functional potential in chronic stroke patients depends on corticospinal tract integrity. *Brain* 2007;130:170–80.
- Swayne OBC, Rothwell JC, Ward NS, Greenwood RJ. Stages of motor output reorganization after hemispheric stroke suggested by longitudinal studies of cortical physiology. *Cereb Cortex* 2008;18:1909–22.
- Takeuchi N, Izumi S-I. Maladaptive plasticity for motor recovery after stroke: mechanisms and approaches. *Neural Plast* 2012;2012:1–9.
- Talenti P, Greenwood RJ, Rothwell JC. Arm function after stroke: neurophysiological correlates and recovery mechanisms assessed by transcranial magnetic stimulation. *Clin Neurophysiol* 2006;117:1641–59.
- Tecchio F, Zappasodi F, Pasqualetti P, Tombini M, Salustri C, Oliviero A, et al. Rhythmic brain activity at rest from rolandic areas in acute mono-hemispheric stroke: a magnetoencephalographic study. *NeuroImage* 2005;28:72–83.
- Tecchio F, Zappasodi F, Pasqualetti P, Tombini M, Caulo M, Ercolani M, et al. Long-term effects of stroke on neuronal rest activity in rolandic cortical areas. *J Neurosci Res* 2006;83:1077–87.
- Tsujimoto T, Mima T, Shimazu H, Isomura Y. Directional organization of sensorimotor oscillatory activity related to the electromyogram in the monkey. *Clin Neurophysiol* 2009;120:1168–73.
- Ushiyama J, Suzuki T, Masakado Y, Hase K, Kimura A, Liu M, et al. Between-subject variance in the magnitude of corticomuscular coherence during tonic isometric

- contraction of the tibialis anterior muscle in healthy young adults. *J Neurophysiol* 2011;106:1379–88.
- Ward NS. Neural plasticity and recovery of function. In: Laureys S, editor. *Progress in brain research. The boundaries of consciousness: neurobiology and neuropathology*. Elsevier; 2005. p. 527–35.
- Ward NS, Newton JM, Swayne OBC, Lee L, Thompson AJ, Greenwood RJ, et al. Motor system activation after subcortical stroke depends on corticospinal system integrity. *Brain* 2006;129:809–19.
- Ward NS, Newton JM, Swayne OBC, Lee L, Frackowiak RSJ, Thompson AJ, et al. The relationship between brain activity and peak grip force is modulated by corticospinal system integrity after subcortical stroke. *Eur J Neurosci* 2007;25:1865–73.
- Williams ER, Baker SN. Renshaw cell recurrent inhibition improves physiological tremor by reducing corticomuscular coupling at 10 Hz. *J Neurosci* 2009;29:6616–24.
- Witham CL, Wang M, Baker SN. Corticomuscular coherence between motor cortex, somatosensory areas and forearm muscles in the monkey. *Front Syst Neurosci* 2010;4:1–14.

5.1. Limitations and outlook

The current study demonstrated changes of CMC amplitude and frequency in the course of post-stroke recovery. I want to discuss some points that were not or only briefly mentioned within the paper.

Severity of stroke Due to the measurement in the acute phase of stroke, we included patients who had already regained enough muscle strength such that they were able to perform the motor task. All of the patients showed very good recovery in the later measurement. Thus, this study demonstrates CMC behavior in mostly successful motor recovery. This however means that the current study does provide little information about patients who are more severely affected and possibly do not recover well. Therefore, we do not know whether and how CMC behaves differently in these cases. At the same time, patients with residual deficits may benefit more by a new rehabilitation approach than patients with good recovery. CMC however requires muscle contraction to be measured which makes it hard to realize such a study in severely affected patients. So the question remains as to how to take corrective action and whether CMC-based neurofeedback could offer a possibility to intervene in order to aid a better recovery.

Link to behavioral measures Moreover, the current study could not link CMC changes to behavioral changes, i.e. motor recovery, as e.g. Graziadio et al. (2012) found a correlation between CMC symmetry and recovery. First, this also relates to the circumstance that the measurements at acute stage required the patients to be able to perform movement. Therefore, patients were also likely to have a good recovery later on which led to little gradation within the group. Second, the MRC scale used in the study was probably not sensitive enough to account for residual deficits which possibly remained. At the same time, changes in CMC were present. Here, a more sensitive behavioral measure is necessary which detects also slight difficulties in fine motor skills rather than considering only motor strength. A link to a behavioral measure will be necessary to judge the success of a rehabilitation approach.

Temporal pattern of CMC changes As already mentioned, the changes in CMC from the acute to chronic phase of stroke could occur in two ways: Either CMC gradually

shifts in frequency or in acute stroke one process dominates, while in the chronic phase another process does. Having only two measurements we can not know which of the two explanations is more likely. Therefore, as a next step, a more detailed temporal pattern of CMC changes post-stroke might be obtained. Such a temporal pattern of CMC would also be interesting in another respect: the second measurement of the current study was already earlier than the measurements in other studies and already no more differences in patients compared to normal subjects were present. More measurements between these two time points could show when no more post-stroke changes in CMC occur.

Heterogeneity of CMC changes The current paper mentioned the heterogeneity of CMC changes among subjects meaning overall higher/lower peak frequencies, small or large changes in peak frequencies or amplitudes between sides/time point of measurement, etc. Such heterogeneity was explained by individual differences (Ushiyama et al., 2011b). Additionally, there is a within-subject variability (Pohja et al., 2005) which was also apparent in the study of the next chapter (von Carlowitz-Ghori et al., 2015). Such variability can however only obscure effects; the main effect in this study may therefore be despite the heterogeneity but not a consequence of it. Finding similarities among subgroups (e.g. cortical vs. subcortical lesion location) could possibly explain some of the inhomogeneity among CMC results. Nevertheless, comparisons between groups are difficult, even if age-matched, because not all confounding variables might be identified and controlled for. Particularly, with increasing age also other diseases become more frequent again increasing the number of potentially confounding variables. This is however a general limitation, not only of this study.

Being the first CMC study in acute stroke, we provided new insights into post-stroke changes of CMC. At the same time this study also gave rise to a number of new questions. Further studies are required before the realization of CMC-based neurofeedback as rehabilitation approach in stroke patients can be addressed.

Neurofeedback on the basis of CMC 6

So far, the R-CMC method had been applied in offline data analysis. For this chapter the method was adapted for the online detection of CMC in a neurofeedback approach. Online detection of CMC means that coherence has to be estimated on short time segments. Here true phase interactions are masked by spurious/random interactions.

This fact may be illustrated by the following analogy:

Imagine pedestrians walking on a busy street. Over a short distance, there will be many people walking at the same speed in the same direction. However, most of these people will just happen to walk the same way without knowing each other; thus their synchronous walking is purely accidental. Would one watch them for longer, their ways would disperse. Only people walking at the same speed in the same direction for a longer distance are likely to indeed be walking synchronously, i.e. they know each other and walk together adjusting their speed and direction to each other. Over a short distance, this truly synchronously walking people are, of course, also included, only they will be concealed among all the people randomly walking synchronously.

Transferred to the online estimation of CMC, coherence values are higher being composed of both true and random interactions. In the current study, subjects were presented with this online-estimated CMC value and asked to modulate it by a mental strategy. Due to the random interactions, the presented value is also partially changing randomly. This imposes difficulties both for the subjects and the analysis: subjects have to identify their own contribution to changes; the analysis may not show an effect due to masking of these spurious phase interactions.

Nevertheless, even for the short time segments an effect could be found, which was confirmed by the analysis of the concatenated data. The results indicate that subjects indeed gained voluntary control over CMC.

VOLUNTARY CONTROL OF CORTICOMUSCULAR COHERENCE THROUGH NEUROFEEDBACK: A PROOF-OF-PRINCIPLE STUDY IN HEALTHY SUBJECTS

K. VON CARLOWITZ-GHORI,^{a,b} Z. BAYRAKTAROGLU,^{a,c}
G. WATERSTRAAT,^a G. CURIO^{a,d} AND V. V. NIKULIN^{a,d*}

^a Neurophysics Group, Department of Neurology, Charité – University Medicine Berlin, Germany

^b Department of Software Engineering and Theoretical Computer Science, Berlin Institute of Technology, Berlin, Germany

^c Istanbul University, Istanbul Faculty of Medicine, Department of Physiology, Turkey

^d Bernstein Center for Computational Neuroscience, Berlin, Germany

Abstract—Corticomuscular coherence (CMC) relates to synchronization between activity in the motor cortex and the muscle activity. The strength of CMC can be affected by motor behavior. In a proof-of-principle study, we examined whether independent of motor output parameters, healthy subjects are able to voluntarily modulate CMC in a neurofeedback paradigm. Subjects received visual online feedback of their instantaneous CMC strength, which was calculated between an optimized spatial projection of multichannel electroencephalography (EEG) and electromyography (EMG) in an individually defined target frequency range. The neurofeedback training consisted of either increasing or decreasing CMC strength using a self-chosen mental strategy while performing a simple motor task. Evaluation of instantaneous coherence showed that CMC strength was significantly larger when subjects had to increase than when to decrease CMC; this difference between the two task conditions did not depend on motor performance. The exclusion of confounding factors such as motor performance, attention and task complexity in study design provides evidence that subjects were able to voluntarily modify CMC independent of motor output parameters. Additional analysis further strengthened the assumption that the subjects' response was specifically shaped by the neurofeedback. In perspective, we suggest that CMC-based neurofeedback could provide a therapeutic approach in clinical conditions, such as motor stroke, where CMC is altered. © 2015 IBRO. Published by Elsevier Ltd. All rights reserved.

Key words: cortex, EEG, neurofeedback, oscillations, synchronization.

*Correspondence to: V. V. Nikulin, Charité – Universitätsmedizin CBF, Neurologie, AG Neurophysik, Hindenburgdamm 30, 12203 Berlin, Germany. Tel: +49-30-8445-4727; fax: +49-30-8445-4264. E-mail address: vadim.nikulin@charite.de (V. V. Nikulin).
Abbreviations: CMC, corticomuscular coherence; CV, coefficient of variation; EEG, electroencephalography; EMG, Electromyography; MVC, maximum voluntary contraction; PCA, principal component analysis; RSP, relative spectral power.

<http://dx.doi.org/10.1016/j.neuroscience.2015.01.013>

0306-4522/© 2015 IBRO. Published by Elsevier Ltd. All rights reserved.

INTRODUCTION

By means of electroencephalography (EEG), magnetoencephalography (MEG) or real-time functional magnetic resonance imaging (fMRI), neurofeedback provides access to brain activity that usually is not perceptible and thus cannot be modulated intentionally. Given the access, however, subjects can learn to voluntarily control brain activity associated with a specific region or function. EEG-mediated neurofeedback experiments are commonly based on brain rhythms such as slow cortical potentials (SCP), sensorimotor rhythms (SMR), theta/beta or alpha/theta ratios (e.g., Gruzelier et al., 2006; Arns et al., 2014). Coherence, however, has, to our knowledge, only been applied in one recent neurofeedback study: Sacchet et al. (2012) demonstrated that two healthy participants could modify their interhemispheric coherence during a motor task by choosing an appropriate movement and thereby control a cursor on the screen. Prior to the experiment, two motor behaviors had been identified that were associated with the largest difference in coherence, i.e., left finger tapping vs. bimanual alternative tapping or rest, respectively. However, it is not known whether coherence can be voluntarily modified using mental strategies without changing motor output parameters.

In the current study, we provided subjects with their instantaneous corticomuscular coherence (CMC) in a neurofeedback paradigm. CMC relates to the amount of synchronization between motor-cortical activity and the activity in a contracting muscle (Conway et al., 1995; Baker, 2007). For sustained isometric muscle contraction with low to moderate force, synchronization occurs in the beta-frequency range (13–30 Hz). CMC is thought to be important for fine motor control (Schnitzler et al., 2000; Jackson et al., 2002; Baker, 2007; Lattari et al., 2010). Movement-dependent modulation, such as type, strength and steadiness of motor contraction, was shown to affect CMC strength and frequency (Conway et al., 1995; Baker et al., 1997; Brown et al., 1998; Mima et al., 1999; Witte et al., 2007). Further, CMC increased after (short-term) motor learning/adaptation and CMC even became visible due to motor learning in subjects who previously did not present CMC (Perez et al., 2006; Mendez-Balbuena et al., 2012). Besides movement-dependent modulation, CMC strength was shown to be affected by motor-unrelated, cognitive processes, including cognitive effort, attention and anticipation. Safri et al. (2006, 2007) demonstrated that when cognitive effort was required to

ignore a visual distractor, CMC strength increased. In contrast, divided attention because of a secondary task led to decreased CMC strength (Kristeva-Feige et al., 2002; Safri et al., 2007). Moreover, during isometric contraction, gamma-band CMC was shown to be selectively modulated by cognitive demands, i.e., by the subjects' expectation of performing a movement (Schoffelen et al., 2005, 2011). This provides an evidence that CMC could be modulated by a cognitive control.

The current knowledge about CMC led us to hypothesize that CMC could be voluntarily modified in a neurofeedback-based paradigm. At the same time, great care has to be taken to ensure that CMC is indeed modified per se and not merely changed by motor output parameters, training or cognitive load of the neurofeedback itself. The current study aimed at providing a proof-of-principle that subjects are able to modify their CMC when provided as neurofeedback.

EXPERIMENTAL PROCEDURES

Subjects

Eleven healthy individuals participated in the study (eight female/three male, mean age \pm SD: 37.8 \pm 17.1 years). Nine subjects were right-handed and two left-handed according to the Edinburgh Handedness Inventory (Oldfield, 1971). The procedures were approved by the local ethics committee and all subjects gave informed consent. The selection of subjects was either based on a recording of an earlier CMC study ($N = 5$; von Carlowitz-Ghori et al., 2014) or a test recording (comparable to the *force-feedback* condition described below but using only few electrodes; $N = 6$) showing well detectable CMC.

Paradigm

Subjects were seated in a comfortable chair with their forearms placed on the armrests. The experiment consisted of two main parts. The first part, which we refer to as *force-feedback condition* was required to calculate an optimized spatial filter which then was used for the projection of EEG signals in the second part. Subjects were instructed to perform a simple motor task which required them to move a lever with their right thumb against a load and then hold. This required a lever displacement of approximately 3.5 cm. The subjects were instructed to reach the target force level as fast as possible after a single tone (2000 Hz, duration 100 ms) and hold it constant until the presentation of a double tone (2000 Hz/1000 Hz, duration 100 ms). Previous studies reported that CMC was larger when the task involved a compliant object compared to a simple isometric condition (Kilner et al., 2000; Riddle and Baker, 2006). The force was measured with a load sensor (FSG15N1A, Honeywell, Golden Valley, Minnesota, USA). Visual feedback of the force was given on a computer screen (synchronized to the monitor's refresh rate) as a centered horizontal bar which varied in length depending on the exerted force. There was a fixation cross in the middle and two fixed vertical

bars indicated the target force which was set to 15% of the maximum voluntary contraction (MVC). The distance between the two vertical bars was approximately 8.5 cm. MVC was determined prior to the recording by performing the motor task with maximum force.

The second part, referred to as *neurofeedback condition*, involved the same motor task as in the *force-feedback* condition but this time subjects were provided with the visual feedback of their instantaneous CMC strength. The instantaneous CMC strength was displayed as a horizontally varying bar and updated continuously. The resolution of the coherence values was 0.01 which corresponded to approximately 0.85 mm on the screen. The delay of CMC presentation on the screen due to the data buffer refresh rate and CMC estimation was in a few milliseconds range and thus negligibly small. Fixed vertical bars indicated perfect coherence of 1; the fixation cross corresponded to a coherence of 0. Subjects were prompted to either increase or decrease the instantaneous CMC strength using a self-chosen mental strategy without changing motor output parameters. Subjects were informed about the measure of interest, CMC, and its basic principle. In order to avoid influencing the subject's choice of strategy, there were, however, no examples of mental strategies given. Prior to each trial, an upward or downward facing triangle indicated whether the task was to increase (*NF_increase*) or decrease (*NF_decrease*) CMC. These two task conditions were chosen because they are per se equal in cognitive load and task complexity: for both conditions the task instructions were identical except for prompting to either increase or decrease CMC. *NF_increase* and *NF_decrease* trials occurred in random order. If the force exceeded $\pm 30\%$ of the target force, an error message prompted to increase/decrease the force. After completion of each block, subjects rated their concentration and how good they judged their control over the bar. Further they were questioned on the mental strategies used.

Each experimental session comprised one block of the *force-feedback* condition and four blocks of the *neurofeedback* condition. Each block had 50 trials of 14-s length which consisted of 10 s of pressing and 4 s of rest. The measurements were repeated on three separate days over a period of on average 7.1 \pm 2.8 days (range: 3–14 days).

Data acquisition

EEG and electromyography (EMG) data were acquired with BrainAmp EEG amplifiers (Brain Products, Gilching, Germany), hardware-filtered in the frequency range of 0.015–250 Hz and sampled at 1000 Hz. The voltage resolution for the EEG and EMG channels was 0.1 μ V and 0.5 μ V, respectively. For EEG data acquisition, an EEG cap with 61 Ag/AgCl-sintered ring electrodes (EasyCap, Herrsching, Germany) was used; the electrode configuration was denser over sensorimotor cortices. The reference electrode for the EEG was placed on the nose. In addition, electrooculograms were recorded by positioning two electrodes on the right zygomatic and supraorbital processes. EMG was

recorded from the abductor pollicis brevis (APB) muscle on the right hand with three EMG electrodes (Ag/AgCl-sintered, 4-mm diameter). Reference and ground electrode (Ag/AgCl sintered, 12-mm diameter) for the EMG were placed on the ulnar styloid process and the inside surface of the wrist, respectively, and were fixed with medical tape.

CMC estimation

For coherence estimation we used the R-CMC method (Bayraktaroglu et al., 2011) which finds the spatial filter for multi-channel EEG data that maximally explains EMG activity in a given frequency range. The method is applied on narrowly bandpass-filtered data and consists of two steps. First, principal component analysis (PCA) is applied for dimension reduction of EEG data. PCA components are selected that account for 99% of the variance in data. In the second step, multiple regression is performed where the PCA components serve as predictors for the EMG signal. Coherence is estimated using the regression coefficients as spatial filter for EEG signals.

If x corresponds to the projected EEG signals which are maximally synchronous with the EMG signal y , then coherence is estimated as:

$$\text{coh}_{x,y} = |s_{x,y}|^2 / (s_{xx}s_{yy})$$

where s_{xx} and s_{yy} are the power spectral densities of the projected EEG signals and the EMG signal, respectively, and $s_{x,y}$ the cross-spectrum of x and y . For the calculation of the cross- and autospectra, the data were divided into 500-ms segments and windowed with a Hanning window. The segments had a 50% overlap in instantaneous coherence estimation and no overlap in overall coherence estimation.

Instantaneous coherence estimation in the neurofeedback condition

After recording of the force-feedback condition, data were visually inspected for major artifacts and performance errors. Further, noisy channels were excluded from instantaneous coherence estimation. The individual peak frequency f_{target} had been determined on the basis of earlier recordings and was reconfirmed by calculating the coherence between Laplacian-filtered EEG data and EMG signals. As the R-CMC optimization procedure as described below in the section 'Overall coherence estimation' was too time-consuming during the experiment, for the calculation of the target frequency we applied Laplacian filtering which provides a good approximation for a local source. Furthermore, the EMG channel yielding the largest coherence values in the specified frequency range was selected. The R-CMC spatial filter was calculated on the force-feedback data which had been bandpass-filtered with a 4th-order Butterworth filter in the range $f_{\text{target}} \pm 2$ Hz.

During neurofeedback, CMC was continuously estimated in a moving window of 1500-ms length between EEG signals projected with the R-CMC spatial filter and the signal of the selected EMG channel. The value represented by the bar was the mean CMC

strength in the frequency range $f_{\text{target}} \pm 2$ Hz in the coherence spectrum.

For all three recording sessions f_{target} and the selected EMG channel were kept the same; the R-CMC spatial filter was always calculated on the preceding force-feedback condition.

Offline data analysis

Data analysis was performed in MATLAB (Mathworks Inc., Natick, Massachusetts, USA) with custom-written functions. The main focus of the analysis was the comparison between the conditions *NF_increase* and *NF_decrease*. Factors such as cognitive load, number of epochs, motor performance differed between the force-feedback and neurofeedback conditions and thus did not allow for a direct comparison.

Preprocessing. The analysis was focused on the stable hold period of the task in which the strongest coherent activity in beta band had been shown (Baker et al., 1997; Riddle and Baker, 2006). This period corresponded to the post-stimulus interval of 2–10 s after the start tone (Fig. 1B). Data of all four blocks for each session were concatenated and visually inspected for performance errors and artifacts in the frequency range of interest. Furthermore, motor performance was assessed using the mean force level and the coefficient of variation (CV) of force as measures. To ensure equal motor performance between *NF_increase* and *NF_decrease*, a stratification method was applied (Roelfsema et al., 1998; Schoffelen et al., 2011). Artifact-free epochs were binned according to their mean force level. The eight bins were equally spaced with the outer edges corresponding to the overall smallest or largest mean force value, respectively, in that session/subject. From each bin, the same number of epochs for both *NF_increase* and *NF_decrease* was selected: for the condition with the lower number of epochs in a given bin, all epochs were included; for the other condition, the same number of epochs was randomly drawn from the epochs in that bin. The procedure is illustrated in Fig. 1A. As coherence strength is affected by the length of data, this procedure has the additional advantageous effect that data lengths for the two conditions are equalized.

Muscle activity. Before and after the stratification procedure, muscle output during the stable hold period was analyzed for the EMG channel used for online-coherence estimation. Two measures of the EMG activity were taken. For the first, the EMG signal was highpass-filtered at 10 Hz with a 4th-order Butterworth filter and rectified. For the second, the EMG signal was bandpass-filtered in the range $f_{\text{target}} \pm 2$ Hz. In both cases, the trials were then averaged and the mean value in the post-stimulus interval of 2–10 s was selected for further analysis.

Instantaneous coherence estimation. A flowchart of the following coherence analysis is given in Fig. 2.

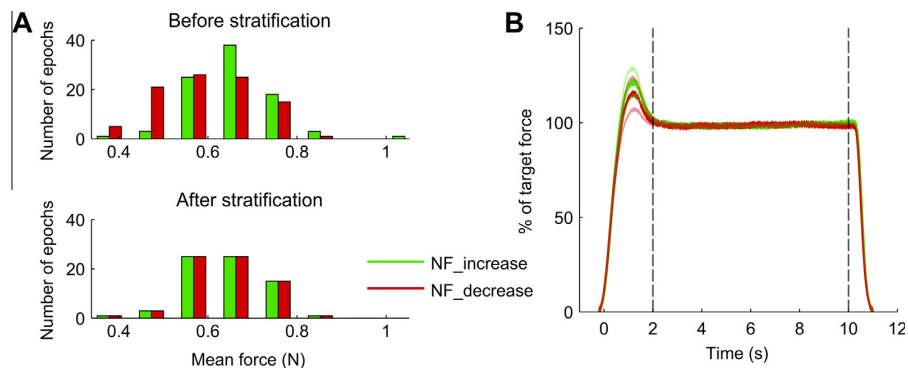


Fig. 1. (A) Stratification method for equalization of mean force level distributions between the conditions *NF_increase* and *NF_decrease*. The procedure included the removal of epochs with extreme force levels. The upper panel shows the number of epochs of the two task conditions in the eight bins before stratification using the first session of subject 1 as an example. For lower mean force levels more epochs belong to the *NF_decrease* condition whereas for higher mean force levels there are more epochs in the *NF_increase* condition. After stratification, shown in the lower panel, the number of epochs is the same in all bins for both conditions. (B) Grand-averaged force (across subjects/sessions, thin lines represent \pm SEM) over the course of the trial after stratification. Coherence was analyzed during the steady-hold phase which corresponded to the post-stimulus interval of 2–10 s and is indicated by the two vertical dashed lines.

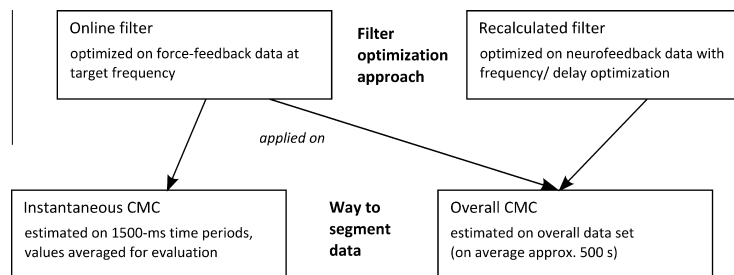


Fig. 2. Flowchart illustrating the different methods for coherence analysis. The upper boxes show the two approaches to optimize spatial filters: The online and the recalculated filter. The two filters were applied on data which are either segmented into 1500-ms time windows or combined in one data set per session (lower boxes). Arrows indicate the three types of analyses that were performed.

Instantaneous coherence estimation was evaluated after stratification on non-overlapping 1500-ms data periods in the post-stimulus interval 2–10 s. The data segments were projected with the R-CMC spatial filter used during online presentation, which we refer to as *online filter*. CMC strength corresponded to the mean in the frequency range $f_{\text{target}} \pm 2$ Hz in the coherence spectrum. For each condition the instantaneous CMC strength values were averaged.

Overall coherence estimation. For offline analysis of overall CMC, all epochs of a condition were concatenated after the stratification procedure, and CMC was calculated over the entire length of the two obtained datasets in the following two ways: (1) EEG data were projected using the spatial filter which had been applied online (*online filter*) and coherence was estimated between the projected EEG data and the selected EMG channel. As *CMC strength*, here we report the maximum coherence in the frequency range $f_{\text{target}} \pm 2$ Hz. (2) R-CMC spatial filters were

re-calculated for each condition on the neurofeedback data itself. For each 2-Hz step between 8 and 35 Hz, the EMG signal was shifted relative to EEG data between $-\pi$ and $+\pi$ in $\pi/6$ steps. Coherence was estimated by calculating R-CMC spatial filters for each frequency step, delay and EMG channel. We refer to the spatial filter, yielding the largest overall coherence peak, as *recalculated filter* and to *CMC strength* and *frequency* corresponding to the highest peak in the resulting coherence spectrum. The recalculated filter was optimized for every condition/session in order to compare the obtained pattern and spectra to those obtained by the online filter. Note that only information provided through *instantaneous coherence estimation* on the basis of the online filter was available for subjects. While instantaneous and overall coherence was estimated on same data, the crucial difference was in the length of the data used for calculation of CMC. In case of instantaneous coherence estimation, CMC was performed in each 1500-ms period. Thus, random, transient phase consistency had a tendency to produce

a positive bias, which however, was the same for the *NF_increase* and *NF_decrease* conditions. On the contrary, the estimation of overall CMC was based on the entire duration of the neurofeedback session (similar to most CMC experiments in the literature) and thus phase consistency was required for a much longer time interval.

Topographical CMC patterns. The topographical distribution corresponding to the strongest coherent activity was obtained using an approach proposed by Parra et al. (2002) which is based on the coupling of CMC component activity with the sensor-space data. To ensure that all artifact-afflicted epochs or noisy channels, which would lead to unfavorable effects, were excluded, patterns were examined for abnormal activity such as mosaic-like high-frequency spatial features or strong activity at the temporal or frontal edges of the patterns (typically indicating scalp muscle activity). In case of the recalculated filter, EEG components with such patterns were disregarded.

Significance testing. The significance of the overall CMC strength values was determined by permutation tests (Hesterberg et al., 2005). For this procedure, we repeated all steps of coherence estimation but EMG segments were shuffled with respect to EEG data, thereby destroying the temporal relationship between the two signals. In the case of coherence values obtained by the online filter, the online filter was used to project EEG data in the permutation test and the permutation values corresponded to the largest value in the frequency range $f_{\text{target}} \pm 2$ Hz. The permutation test for coherence values from recalculated filters included the delay optimization procedure in the peak frequency range. For each coherence value to be tested, five-hundred permutations were performed. The coherence value was considered significant if less than 2.5% of permutation values exceeded it. Subjects were excluded from further analysis if there was no significant coherence in at least one condition.

Relative spectral power (RSP) of beta oscillations. We determined the RSP of ongoing beta oscillations in the pre-stimulus interval (–2500 to –450 ms) and during task performance (2–10 s). The analysis was based on the projected EEG component, which was optimized for CMC estimation online filter. RSP corresponded to the ratio of the mean power in the 4-Hz-wide frequency band centered at f_{target} to the mean power in the broad frequency range of 5–35 Hz.

Statistical analysis. For statistical analysis, which was carried out in SPSS (IBM SPSS Inc., Armonk, New York, USA), a repeated-measures ANOVA was employed with the main factors CONDITION (*NF_increase*, *NF_decrease*) and SESSION (1, 2, 3). Post-hoc pairwise comparisons were Bonferroni-corrected. To test for correlation of measures, they were averaged across sessions and non-parametric Spearman's rank correlation coefficient was calculated in MATLAB.

RESULTS

Behavioral measures

As subjects could freely choose their mental strategy, there was a wide range of strategies ranging from a focus on the visual feedback or motor performance to very abstract images or emotions. The focus on visual feedback, i.e., imagining extending/shortening the horizontal bar which displayed the instantaneous CMC strength, was the strategy chosen most often. No mental strategy/category of strategies could be identified as being more effective than others. The neurofeedback condition was generally considered more demanding but also more engaging than the force-feedback condition.

Motor performance was assessed using mean force levels and the CV of force as measures; the values for all the behavioral measures are summarized in Table 1. Before the stratification procedure, there was a significant effect for CONDITION ($p = 0.014$), mean force levels in *NF_increase* were larger than in *NF_decrease* in all three sessions ($p = 0.017$, $p = 0.043$, $p = 0.008$). Further, the CV of force demonstrated a significant effect of CONDITION ($p = 0.041$), in session 1, the CV of force was smaller in the *NF_increase* condition than in the *NF_decrease* condition. Moreover, there was a significant main effect of CONDITION for the number of epochs ($p < 0.001$); due to artifact correction, there were less epochs in the condition *NF_increase* than in *NF_decrease* in all three sessions ($p = 0.043$, $p = 0.001$, $p = 0.004$).

The statistical analysis of EMG activity in the broad frequency range showed a significant effect of CONDITION ($p = 0.005$). For all three sessions values were larger in the *NF_increase* than in the *NF_decrease* condition ($p = 0.006$, $p = 0.35$, $p = 0.008$). For EMG activity at f_{target} there was a significant effect of CONDITION ($p = 0.035$) with values being larger for the *NF_increase* than for the *NF_decrease* condition but no posthoc effects.

After the stratification procedure, there were no longer any significant differences between conditions or sessions for mean force levels and CV of force. The number of epochs was identical for both conditions. The grand-average (across subjects and conditions) of the mean force levels are displayed in Fig. 1B as percentage of the target force; the force levels of the conditions *NF_increase* and *NF_decrease* do not show a difference within the analysis window. EMG activity in the broad frequency range still showed a significant effect of CONDITION ($p = 0.004$) with values for the condition *NF_increase* being larger than for *NF_decrease* in sessions 1 and 2 ($p = 0.014$, $p = 0.027$). EMG activity at f_{target} did not show any main or interaction effects. The difference in broad-band EMG levels, however, was not associated with the changes in CMC as we show below.

Table 1 summarizes mean force levels, CV of force, EMG activity and number of epochs before and after stratification for the *NF_increase* and *NF_decrease* conditions and all sessions.

Table 1. Mean force levels, CV of force, EMG activity and number of epochs before and after stratification for all conditions and sessions. Data are presented as mean \pm SEM

	Session	Condition		
		Force-feedback	NF_increase	NF_decrease
<i>Before stratification</i>				
Mean force [N]	1	0.830 \pm 0.100	0.844 \pm 0.107	0.776 \pm 0.092
	2	0.831 \pm 0.101	0.832 \pm 0.103	0.773 \pm 0.093
	3	0.826 \pm 0.095	0.840 \pm 0.106 ^a	0.772 \pm 0.099 ^a
CV of force	1	0.050 \pm 0.004	0.168 \pm 0.014	0.187 \pm 0.016
	2	0.046 \pm 0.005	0.179 \pm 0.027	0.182 \pm 0.021
	3	0.046 \pm 0.004	0.186 \pm 0.029 ^a	0.192 \pm 0.029 ^a
EMG activity [μ V]	1	105.1 \pm 14.4	113.9 \pm 14.8	104.8 \pm 13.1
	2	120.7 \pm 12.1	129.5 \pm 21.6	117.2 \pm 17.3
	3	107.0 \pm 11.9	117.0 \pm 16.3 ^a	106.9 \pm 14.2 ^a
EMG activity f_{target} [μ V]	1	18.7 \pm 3.2	20.8 \pm 3.4	19.1 \pm 3.3
	2	21.0 \pm 3.3	21.5 \pm 4.2	20.2 \pm 3.6
	3	19.7 \pm 2.8	21.2 \pm 3.6 ^a	19.8 \pm 3.1 ^a
Number of epochs	1	46.3 \pm 0.8	86.1 \pm 2.7	90.8 \pm 1.8
	2	43.7 \pm 1.0	84.4 \pm 2.9	93.0 \pm 2.8
	3	45.4 \pm 0.6	86.1 \pm 2.2 ^a	91.4 \pm 2.4 ^a
<i>After stratification</i>				
Mean force	1		0.816 \pm 0.102	0.816 \pm 0.102
	2		0.804 \pm 0.097	0.801 \pm 0.097
	3		0.802 \pm 0.102	0.801 \pm 0.102
CV of force	1		0.166 \pm 0.014	0.167 \pm 0.016
	2		0.177 \pm 0.025	0.178 \pm 0.022
	3		0.176 \pm 0.024	0.182 \pm 0.031
EMG activity [μ V]	1		112.4 \pm 14.3	106.8 \pm 13.4
	2		128.4 \pm 20.9	118.6 \pm 17.8
	3		113.2 \pm 15.4 ^a	109.2 \pm 14.8 ^a
EMG activity f_{target} [μ V]	1		20.7 \pm 3.3	19.2 \pm 3.1
	2		21.6 \pm 4.2	20.4 \pm 3.6
	3		20.5 \pm 3.3	20.4 \pm 3.3
Number of epochs	1		63.6 \pm 3.9	
	2		62.2 \pm 6.0	
	3		62.9 \pm 5.5	

^a Significant main effect of CONDITION comparing NF_increase and NF_decrease ($p < 0.05$).

Note that the reported results are for nine subjects only, as two subjects were excluded from analysis because of lacking coherence in some conditions.

CMC

Instantaneous coherence estimation. The instantaneous CMC strength values (mean \pm SEM) are displayed in Table 2. There was a significant main effect of CONDITION ($p = 0.012$), with corresponding mean values for NF_increase being larger than for NF_decrease, and an interaction effect of CONDITION*SESSION ($p = 0.047$). Post-hoc comparisons revealed that in session 2, CMC strength in NF_increase was significantly larger than in NF_decrease ($p < 0.001$); and in session 1, CMC strength in NF_increase tended to be larger than in NF_decrease being close to significance ($p = 0.063$).

Overall coherence estimation. The CMC strength and frequencies (mean \pm SEM) for the different conditions and sessions using both online and recalculated filters are summarized in Table 2. Fig. 3 shows CMC spectra and patterns obtained with the online and recalculated filter in subject 1. For the online filter, CMC strength values of all subjects are displayed in Fig. 4A. Note that though tables and figures also include the force-feedback condition, we did not directly compare it to the neurofeedback condition for several reasons. The online filter was optimized on the force-feedback data. Further cognitive load, CV of force and number of epochs differed. These factors may give a bias toward larger CMC strength values in the force-feedback condition but are unrelated to voluntary modulation of CMC.

The statistical comparison of CMC strength values obtained with the online filter showed a significant main effect for CONDITION ($p = 0.044$). In session 2, CMC strength was significantly larger for NF_increase than for NF_decrease ($p = 0.022$). The statistical results are illustrated in Fig. 4B. In the force-feedback condition,

Table 2. The CMC strength and frequencies for the different conditions and sessions using both online and recalculated filters. Data are presented as mean \pm SEM

	Session	Condition		
		Force-feedback	NF_increase	NF_decrease
<i>Online filter</i>				
CMC strength (instantaneous)	1		0.245 \pm 0.008	0.237 \pm 0.007
	2		0.252 \pm 0.011	0.236 \pm 0.010
	3		0.251 \pm 0.008 ^a	0.247 \pm 0.008 ^a
CMC strength (overall)	1	0.066 \pm 0.010	0.062 \pm 0.018	0.045 \pm 0.011
	2	0.071 \pm 0.015	0.078 \pm 0.025	0.057 \pm 0.021
	3	0.085 \pm 0.014	0.064 \pm 0.013 ^a	0.053 \pm 0.010 ^a
CMC frequency (f_{target})	1–3	20.3 \pm 1.4	20.3 \pm 1.4	20.3 \pm 1.4
<i>Recalculated filter</i>				
CMC strength	1	0.088 \pm 0.015	0.101 \pm 0.022	0.085 \pm 0.016
	2	0.099 \pm 0.017	0.111 \pm 0.029	0.101 \pm 0.029
	3	0.127 \pm 0.015	0.124 \pm 0.027	0.113 \pm 0.021
CMC frequency [Hz]	1	20.1 \pm 1.6	19.9 \pm 1.7	21.3 \pm 1.7
	2	19.7 \pm 2.0	19.4 \pm 1.9	19.2 \pm 1.8
	3	18.4 \pm 1.7 ^b	18.2 \pm 2.1	18.7 \pm 2.0

^a Significant main effect of CONDITION comparing NF_increase and NF_decrease ($p < 0.05$).

^b Significant main effect of SESSION ($p < 0.05$).

there was no significant difference between sessions in CMC strength.

$\Delta\text{CMConline}$ did not depend on the CMC strength of force-feedback or neurofeedback conditions, respectively, where $\Delta\text{CMConline}$ denotes the difference in CMC strength between NF_increase and NF_decrease averaged across sessions using the online filter. In Fig. 5 the subjects' sorted $\Delta\text{CMConline}$ values are depicted, showing that the CMC strength in NF_increase was larger than in NF_decrease in most of the subjects. First, there were no significant correlations of $\Delta\text{CMConline}$ with the mean force or CV of force before stratification. Further, no correlation was present between $\Delta\text{CMConline}$ and EMG activity either in the broad or target frequency range. Before stratification there was a negative correlation of $\Delta\text{CMConline}$ and Δepos ($\rho = -0.77$, $p = 0.019$), where Δepos corresponds to the difference in the number of epochs between the NF_increase and NF_decrease conditions. This effect was eliminated by the stratification procedure.

For CMC strengths and CMC frequencies, obtained with the recalculated filter in the neurofeedback condition, there were no significant differences for conditions or sessions. The statistical results of the CMC strength comparison are illustrated in Fig. 6B while the individual values are depicted in Fig. 6A. In the force-feedback condition, there was a main effect for SESSION in CMC strength ($p = 0.044$); pairwise comparison showed a significant increase in CMC strength from the first to third session ($p = 0.039$); there was no significant difference in CMC peak frequency.

Further, Spearman's correlation between $\Delta\text{CMConline}$ and $\Delta\text{CMCreCalc}$ was calculated, where $\Delta\text{CMCreCalc}$ denotes – analogous to $\Delta\text{CMConline}$ – the average pairwise difference in CMC strength between NF_increase and NF_decrease using the recalculated filter. There was no significant correlation between $\Delta\text{CMConline}$ and $\Delta\text{CMCreCalc}$.

RSP of beta oscillations

For the pre-stimulus period, the statistical analysis of beta RSP showed that for the main factor CONDITION ($p = 0.077$) values tended to be larger for NF_increase than for NF_decrease. During task performance, beta RSP did not show any significant main or interaction effects. There was no significant correlation of $\Delta\text{CMConline}$ with beta RSP before or during task performance.

DISCUSSION

In the current study we provided a proof-of-principle that healthy subjects were able to voluntarily modify CMC in a neurofeedback-based paradigm independent of motor output parameters. CMC strength in the target frequency range was significantly larger when subjects were prompted to increase than when to decrease CMC. While cortico-cortical coherence as a measure of functional connection has previously been employed in a neurofeedback paradigm (Sacchet et al., 2012), the current study demonstrates intentional modulation of CMC independent of motor output parameters. From neurofeedback and brain-computer-interface studies it is known that about 15–30% of participants are unable to learn volitional control of brain activity (Kober et al., 2013). Despite intra- and inter-individual performance differences being present also in the current study, we were able to show significant modulation of CMC on a group level. This effect may not be considerably pronounced but nonetheless reached statistical significance.

This difference between the two neurofeedback conditions was present for both instantaneous and overall CMC using the online filter. However, instantaneous CMC was calculated on relatively short time windows (1500 ms), where detection of spurious

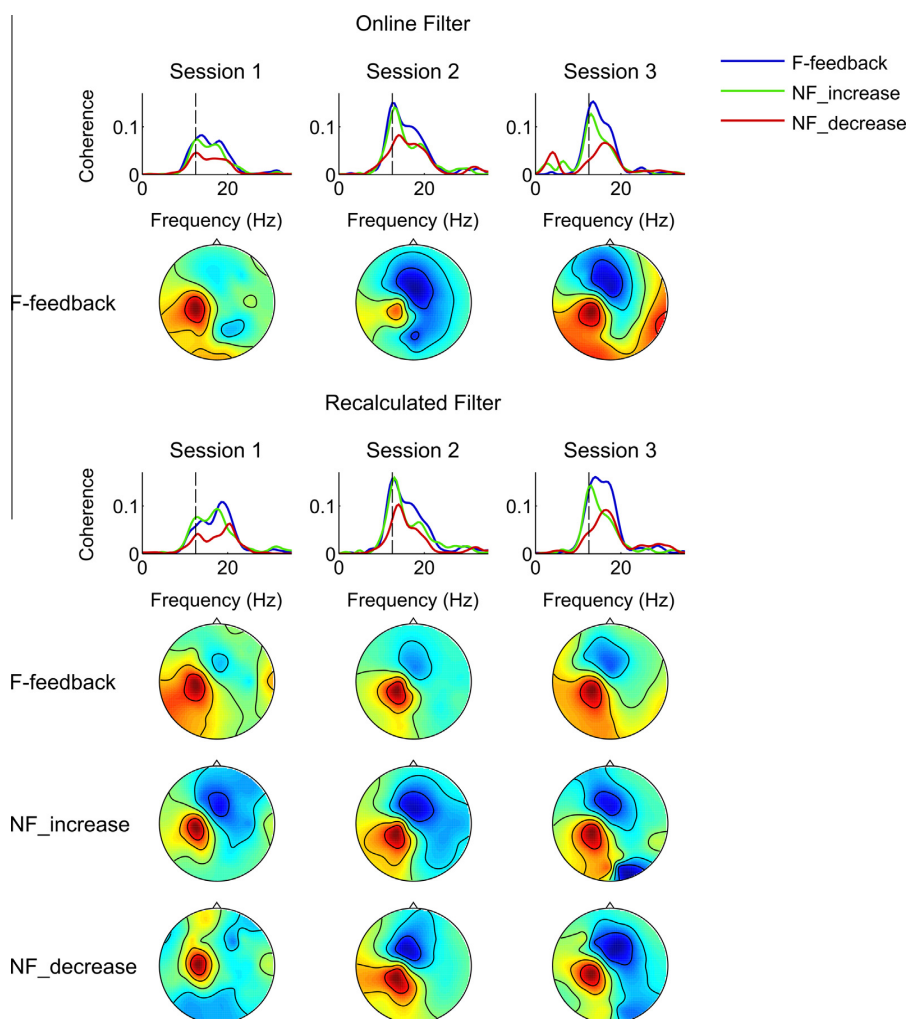


Fig. 3. CMC spectra and spatial patterns of subject 1 for the online filter (top) and the recalculated filter (bottom). The vertical dashed lines in the CMC spectra correspond to the target frequency. Note, that for recalculated filters patterns correspond to CMC at peak frequency.

synchrony is more likely than for longer time intervals. Therefore, functional phase relationships in instantaneous CMC might to a varying degree be masked by random interactions. Yet, despite this masking effect, instantaneous CMC showed stronger values in the *NF_increase* compared to the *NF_decrease* condition. Overall CMC estimation, on the other hand, reflects phase dynamics over a long time interval (the entire neurofeedback session) where only functionally consistent phase interactions survive the averaging procedure. Since spurious/stochastic phase interactions average out, the overall CMC values also became smaller, as visible from Table 2. Nevertheless, we yet again observed stronger CMC values for the *NF_increase* compared to the *NF_decrease* condition. The agreement of the results for instantaneous and overall CMC excludes that a positive synchrony bias (due to the short length of the segments) caused the

difference between the two conditions and therefore argues against the results being due to spurious phase interactions.

Addressing confounding factors

Potentially confounding factors were addressed by the study design and preprocessing of the data to allow the conclusion that the effect of CMC modulation can be attributed to voluntary modification. The study was designed such that subjects were prompted in random order to either increase or decrease CMC (*NF_increase*/*NF_decrease*). This allowed to directly compare the two task conditions ensuring that differences in CMC strength were not due to the neurofeedback condition per se: the neurofeedback condition required more cognitive effort than the force-feedback condition and attention had to be divided between the CMC feedback

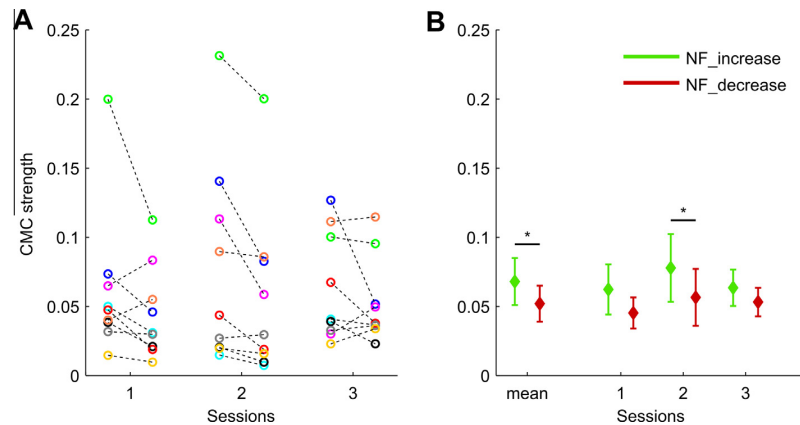


Fig. 4. (A) Individual overall CMC strength values using the online filter. For each session, the values on the left hand side correspond to the *NF_increase* condition and on the right hand side to the *NF_decrease* condition; each color represents one subject. (B) Statistical comparison of CMC strength values. There was a significant main effect of CONDITION with CMC strength being larger for *NF_increase* than for *NF_decrease* ($p = 0.044$). Post-hoc comparison showed that in session 2, CMC strength was significantly larger for *NF_increase* than for *NF_decrease* ($p = 0.022$). (For interpretation of the references to color in this figure legend, the reader is referred to the web version of this article.)

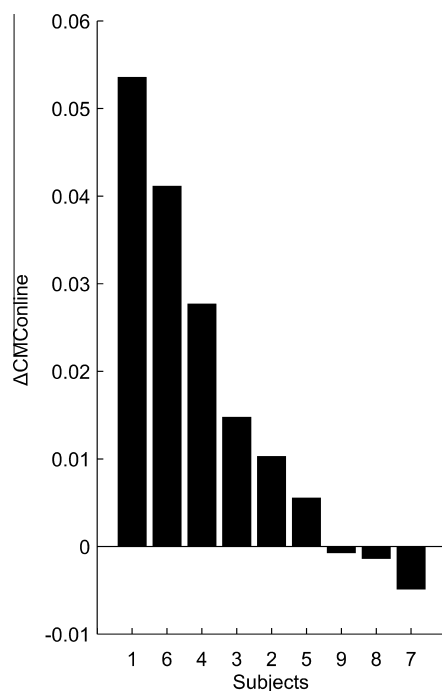


Fig. 5. Subjects' sorted $\Delta CMConline$ values. $\Delta CMConline$ denotes the difference in overall CMC strength between the *NF_increase* and *NF_decrease* conditions averaged across sessions using the online filter. In most of the subjects, CMC strength in the *NF_increase* condition was larger than in the *NF_decrease* condition.

and keeping the target force level – factors which were shown to modulate CMC strength (Kristeva-Feige et al., 2002; Safri et al., 2006, 2007). Besides the self-report of subjects, also a higher CV of force could be an indication that the neurofeedback condition was more demanding. Therefore, we did not compare the neurofeedback to

the force-feedback condition directly. Furthermore, motor adaptation (Perez et al., 2006; Mendez-Balbuena et al., 2012) or muscle fatigue (Yang et al., 2009; Ushiyama et al., 2011a) cannot be accounted for the difference between the two neurofeedback-task conditions as the order of conditions was randomized.

Besides EEG/EMG signals, the topographical CMC patterns (as displayed in Fig. 3) were examined for artifacts, e.g., due to scalp muscle activity, which could have (unintentionally) been used to control the feedback signal (Sherlin et al., 2011). There was no evidence that CMC estimation was confounded by artifacts.

Further, we neither found changes in beta RSP between conditions nor a correlation of beta RSP with the difference in CMC strength values $\Delta CMConline$ (*NF_increase* – *NF_decrease*) obtained with the online filter. We therefore can exclude that CMC modulation is confounded by amplitude changes of neuronal oscillations which were shown to affect the estimation of CMC (Bayraktaroglu et al., 2013) as they relate to the signal-to-noise ratio (Nikulin et al., 2011).

We found mean force levels to be larger in the *NF_increase* than in the *NF_decrease* condition while for the CV of force the relationship was reversed. For low to moderate forces CMC strength was shown not to be affected by force strength (Brown et al., 1998) but rather by the precision of the exerted force (Witte et al., 2007). In the current study, $\Delta CMConline$ was neither correlated with the difference in mean force level nor CV of force, the latter being used as a measure of force stability. To equalize both motor performance and number of epochs for the conditions *NF_increase* and *NF_decrease*, a stratification method was applied (Roelfsema et al., 1998; Schoffelen et al., 2011). Though this meant discarding some data, it ensured that CMC was not modulated as such by the force parameters. Assessed motor output parameters also included muscle activity measured with EMG. Although quite small, we found differences between

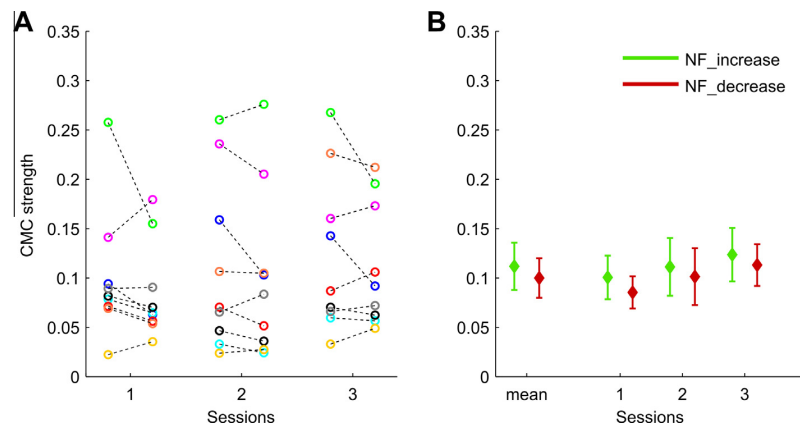


Fig. 6. (A) Individual overall CMC strength values using the recalculated filter. For each session, the values on the left hand side correspond to the *NF_increase* condition and on the right hand side to the *NF_decrease* condition; each color represents one subject. (B) Statistical comparison of CMC strength values showed no significant main or interaction effects. (For interpretation of the references to color in this figure legend, the reader is referred to the web version of this article.)

the two neurofeedback conditions for EMG activity in the broad frequency. As there was no difference in EMG activity at the target frequency, the activity modulation in the broad frequency might be a concomitant factor, i.e., subjects associated CMC with force (as force was provided as feedback in the force-feedback condition) and therefore had unintentionally a higher level of muscle activity during the *NF_increase* condition compared to the *NF_decrease* condition. Yet, these differences in EMG levels were unlikely to cause difference in CMC as neither of the two measures of EMG activity correlated with CMC modulation (ΔCMC_{Online}) thus advocating against a confounding effect of EMG activity.

Coherence strength

Subjects were only included into the study when they presented CMC above a significance level. There is a large between- and within-subject variability of CMC strength (Pohja et al., 2005; Ushiyama et al., 2011b). Two subjects were excluded from the analysis because they did not present significant CMC in all of the conditions/sessions. The rationale behind this selection criterion is that spatial filters cannot be considered meaningful when no coherence is present.

In the neurofeedback condition, there was no significant change of CMC strength between sessions. Against expectations, the difference between *NF_increase* and *NF_decrease* was smallest in the third session. The current study set priority on addressing concomitant factors which might have contributed to CMC modulation. Our study is the first to demonstrate that neurofeedback on the basis of CMC is possible in principle. On this basis, further research will address how to optimize parameters which might increase ΔCMC_{Online} and lead to an increasing effect over time. Such parameters include varying the duration, frequency or total number of sessions or the use of a block design instead of a random order of condition. Contrary to the neurofeedback condition, we found an

increase of CMC strength in the force-feedback condition from the first to third session using the recalculated filter. This could potentially be an effect of the neurofeedback training or of motor adaptation as previously reported (Perez et al., 2006; Mendez-Balbuena et al., 2012). These authors, however, showed motor adaptation only within a one-day session but did not examine longer time periods. In the current study, CMC strength increased over a time period of about a week. Nevertheless, ΔCMC_{Online} did not depend on the coherence strength of force-feedback or neurofeedback condition as such. Thus, a large CMC does not seem to be a prerequisite for successfully manipulating it.

Significant difference for the online filter but not the recalculated filter

We found a significant difference in both instantaneous and overall CMC strength between *NF_increase* and *NF_decrease* using the online filter; there was, however, no significant difference using the recalculated filter. Let us consider a possible effect of motor output on CMC estimation. If the motor output had affected CMC estimation, differences in CMC between the conditions should also occur when the recalculated filter is applied as the motor output for the two ways of analysis (online and recalculated filter) was identical. One could even expect a larger effect for the recalculated filter as it was optimized on the neurofeedback data itself. Indeed, recalculated filters resulted in a consistently larger overall CMC peak strength than online filters and the target frequency did not always match with the peak frequency. Yet, there were no task-related differences in CMC for the recalculated filter which led to the conclusion that any remaining differences in motor output, as the residual EMG difference between the *NF_increase* and *NF_decrease* conditions, were not the reason for changes in CMC. CMC changes are more likely to be due to modulating the strength of the corticomuscular coupling which was suggested to

contribute to effective interaction (Fries, 2005; Schoffelen et al., 2005). Here, online and recalculated filters spatially shape the EEG signals in a slightly different way. The difference in CMC between the two task conditions was only significant when applying the spatial filter that was actually used online during task performance. This online filter shaped the feedback which subjects were provided with and subjects could only modify the signal they had access to. Those neural oscillations which were relevant for the significant difference between conditions using the online filter could have been suppressed by the recalculated filter which was optimized to yield the largest possible coherence and which disregarded effects of the neurofeedback. This finding provides further evidence that subjects voluntarily modified their CMC.

Neurophysiological mechanisms underlying neurofeedback

The effective volitional control of neural activity has been demonstrated in numerous studies in both animals and humans (Fetz, 2007) with neurofeedback being based on different levels of neuronal activity (Orsborn and Carmena, 2013). However, mechanisms underlying the acquisition of self-regulatory capacity of brain activity remain unclear.

In the current study, subjects increased/decreased CMC, thus changing the functional coupling between the cortex and the spinal cord. We found the CMC modulation to be independent of motor performance, which implies that subjects acquired self-regulation of CMC strength using mental processes. From the reported mental strategies it is not possible to infer underlying strategies leading to the observed CMC modulation. Such strategies may, however, include the same neurophysiological structures as e.g., in motor imagery (Jeannerod, 1995; Jeannerod and Frak, 1999; Solodkin et al., 2004) or motor attention (Rushworth et al., 2001, 2003). In addition, as a sensory/afferent contribution to CMC is suggested (Baker, 2007), CMC modulation might also share mechanisms with somatosensory attention (van Ede and Maris, 2013). The self-regulatory capacity in neurofeedback is thought to be irrespective of the neurophysiological measure being manipulated. Kober et al. (2013) associated neurofeedback performance with implicit learning mechanisms. In their study, successful subjects reported using no specific mental strategy anymore which suggests the development of automatic regulation skills. Effective strategies were found to vary among individuals (Nan et al., 2012) which is congruent with the results of our study showing variability in mental strategies.

Clinical potential

Neurofeedback has been examined for its therapeutic potential in a variety of disorders where it could provide a non-invasive and well-tolerated alternative form of treatment. Particularly in attention-deficit hyperactivity disorder (ADHD), neurofeedback training seems to be a promising alternative to pharmacological intervention including evidence of long-term effects (for reviews see

Moriyama et al., 2012; Arns et al., 2014). In the current study, we demonstrated that healthy people are able to voluntarily modulate their CMC based on neurofeedback. Building on the present results, CMC neurofeedback could provide a therapeutic approach in conditions where CMC was shown to be altered, such as in stroke (Mima et al., 2001; Braun et al., 2007; Fang et al., 2009; Meng et al., 2009; Graziadio et al., 2012; Rossiter et al., 2013; von Carlowitz-Ghori et al., 2014). CMC allows directly accessing functionally relevant contribution of cortical areas that undergo massive reorganization in stroke recovery. We conjecture that through neurofeedback patients might be enabled to modulate CMC involving functionally competent and relevant cortical areas participating in plastic changes following a stroke. Being presented with instantaneous CMC feedback, patients could learn an association of specific motor commands with the strength of CMC, which is to be calculated between neuronal oscillations of unaffected cortical areas and muscle activity. These in turn would allow for a facilitation of recovery processes where cortical areas, previously not active in the execution of a given movement, would start to be engaged in the generation of motor control of the paretic body part.

Acknowledgments—V.V.N. and G.C. were supported by the Berlin Bernstein Center for Computational Neuroscience project B1 (BCCN 01GQ 1001C).

REFERENCES

- Arns M, Heinrich H, Strehl U (2014) Evaluation of neurofeedback in ADHD: the long and winding road. *Biol Psychol* 95:108–115.
- Baker SN (2007) Oscillatory interactions between sensorimotor cortex and the periphery. *Curr Opin Neurobiol* 17:649–655.
- Baker SN, Olivier E, Lemon RN (1997) Coherent oscillations in monkey motor cortex and hand muscle EMG show task-dependent modulation. *J Physiol* 501:225–241.
- Bayraktaroglu Z, von Carlowitz-Ghori K, Curio G, Nikulin VV (2013) It is not all about phase: amplitude dynamics in corticomuscular interactions. *NeuroImage* 64:496–504.
- Bayraktaroglu Z, von Carlowitz-Ghori K, Losch F, Nolte G, Curio G, Nikulin VV (2011) Optimal imaging of cortico-muscular coherence through a novel regression technique based on multi-channel EEG and un-rectified EMG. *NeuroImage* 57:1059–1067.
- Braun C, Staudt M, Schmitt C, Preissl H, Birbaumer N, Gerloff C (2007) Crossed cortico-spinal motor control after capsular stroke. *Eur J Neurosci* 25:2935–2945.
- Brown P, Salenius S, Rothwell JC, Hari R (1998) Cortical correlate of the piper rhythm in humans. *J Neurophysiol* 80:2911–2917.
- Conway BA, Halliday DM, Farmer SF, Shahani U, Maas P, Weir AJ, Rosenberg JR (1995) Synchronization between motor cortex and spinal motoneuronal pool during the performance of a maintained motor task in man. *J Physiol* 489:917–924.
- Fang Y, Daly JJ, Sun J, Hovorac K, Fredrickson E, Pundik S, Sahgal V, Yue GH (2009) Functional corticomuscular connection during reaching is weakened following stroke. *Clin Neurophysiol* 120:994–1002.
- Fetz EE (2007) Volitional control of neural activity: implications for brain–computer interfaces. *J Physiol* 579:571–579.
- Fries P (2005) A mechanism for cognitive dynamics: neuronal communication through neuronal coherence. *Trends Cogn Sci* 9:474–480.
- Graziadio S, Tomasevic L, Assenza G, Tecchio F, Eyre JA (2012) The myth of the “unaffected” side after unilateral stroke: is

- reorganisation of the non-infarcted corticospinal system to re-establish balance the price for recovery? *Exp Neurol* 238: 168–175.
- Gruzelier J, Egner T, Vernon D (2006) Validating the efficacy of neurofeedback for optimising performance. In: *Progress in Brain Research* (Christa Neuper and Wolfgang Klimesch, eds), pp 421–431 *Event-Related Dynamics of Brain Oscillations*. Elsevier. Available at: <http://www.sciencedirect.com/science/article/pii/S0079612306590272> [Accessed April 1, 2014].
- Hesterberg T, Moore DS, Monaghan S, Clipson A, Epstein R (2005) Bootstrap methods and permutation tests. In: *Introduction to the practice of statistics*, vol. 5, pp 1–70.
- Jackson A, Spinks RL, Freeman TCB, Wolpert DM, Lemon RN (2002) Rhythm generation in monkey motor cortex explored using pyramidal tract stimulation. *J Physiol* 541:685–699.
- Jeannerod M (1995) Mental imagery in the motor context. *Neuropsychologia* 33:1419–1432.
- Jeannerod M, Frak V (1999) Mental imaging of motor activity in humans. *Curr Opin Neurobiol* 9:735–739.
- Kilner JM, Baker SN, Salenius S, Hari R, Lemon RN (2000) Human cortical muscle coherence is directly related to specific motor parameters. *J Neurosci* 20:8838–8845.
- Kober SE, Witte M, Ninaus M, Neuper C, Wood G (2013) Learning to modulate one's own brain activity: the effect of spontaneous mental strategies. *Front Hum Neurosci* 7:695.
- Kristeva-Feige R, Fritsch C, Timmer J, Lücking C-H (2002) Effects of attention and precision of exerted force on beta range EEG–EMG synchronization during a maintained motor contraction task. *Clin Neurophysiol* 113:124–131.
- Lattari E, Velasques B, Paes F, Cunha M, Budde H, Basile L, Cagy M, Piedade R, Machado S, Ribeiro P (2010) Corticomuscular coherence behavior in fine motor control of force: a critical review. *Rev Neurol* 51:610–623.
- Mendez-Balbuena I, Huethe F, Schulte-Mönting J, Leonhart R, Manjarrez E, Kristeva R (2012) Corticomuscular coherence reflects interindividual differences in the state of the corticomuscular network during low-level static and dynamic forces. *Cereb Cortex* 22:628–638.
- Meng F, Tong K-Y, Chan S-T, Wong W-W, Lui K-H, Tang K-W, Gao X, Gao S (2009) Cerebral plasticity after subcortical stroke as revealed by cortico-muscular coherence. *IEEE Trans Neural Syst Rehabil Eng* 17:234–243.
- Mima T, Simpkins N, Oluwatimilehin T, Hallett M (1999) Force level modulates human cortical oscillatory activities. *Neurosci Lett* 275:77–80.
- Mima T, Toma K, Koshy B, Hallett M (2001) Coherence between cortical and muscular activities after subcortical stroke. *Stroke* 32:2597–2601.
- Moriyama TS, Polanczyk G, Caye A, Banaschewski T, Brandeis D, Rohde LA (2012) Evidence-based information on the clinical use of neurofeedback for ADHD. *Neurotherapeutics* 9:588–598.
- Nan W, Rodrigues JP, Ma J, Qu X, Wan F, Mak P-I, Mak PU, Vai MI, Rosa A (2012) Individual alpha neurofeedback training effect on short term memory. *Int J Psychophysiol* 86:83–87.
- Nikulin VV, Nolte G, Curio G (2011) A novel method for reliable and fast extraction of neuronal EEG/MEG oscillations on the basis of spatio-spectral decomposition. *NeuroImage* 55:1528–1535.
- Oldfield RC (1971) The assessment and analysis of handedness: the Edinburgh inventory. *Neuropsychologia* 9:97–113.
- Orsborn A, Carmena JM (2013) Creating new functional circuits for action via brain-machine interfaces. *Front Comput Neurosci* 7:157.
- Parra L, Alvino C, Tang A, Pearlmutter B, Yeung N, Osman A, Sajda P (2002) Linear spatial integration for single-trial detection in encephalography. *NeuroImage* 17:223–230.
- Perez MA, Lundbye-Jensen J, Nielsen JB (2006) Changes in corticospinal drive to spinal motoneurons following visuo-motor skill learning in humans. *J Physiol* 573:843–855.
- Pohja M, Salenius S, Hari R (2005) Reproducibility of cortex–muscle coherence. *NeuroImage* 26:764–770.
- Riddle CN, Baker SN (2006) Digit displacement, not object compliance, underlies task dependent modulations in human corticomuscular coherence. *NeuroImage* 33:618–627.
- Roelfsema PR, Lamme VAF, Spekreijse H (1998) Object-based attention in the primary visual cortex of the macaque monkey. *Nature* 395:376–381.
- Rossiter HE, Eaves C, Davis E, Boudrias M-H, Park C, Farmer S, Barnes G, Litvak V, Ward NS (2013) Changes in the location of cortico-muscular coherence following stroke. *NeuroImage* 2:50–55.
- Rushworth MFS, Johansen-Berg H, Göbel SM, Devlin JT (2003) The left parietal and premotor cortices: motor attention and selection. *NeuroImage* 20(Suppl. 1):S89–S100.
- Rushworth MFS, Krams M, Passingham RE (2001) The attentional role of the left parietal cortex: the distinct lateralization and localization of motor attention in the human brain. *J Cognitive Neurosci* 13:698–710.
- Sacchet MD, Sitaram R, Braun C, Birbaumer N, Fetz E (2012) Volitional control of neuromagnetic coherence. *Front Neurosci* 6:189.
- Safri NM, Murayama N, Hayashida Y, Igasaki T (2007) Effects of concurrent visual tasks on cortico-muscular synchronization in humans. *Brain Res* 1155:81–92.
- Safri NM, Murayama N, Igasaki T, Hayashida Y (2006) Effects of visual stimulation on cortico-spinal coherence during isometric hand contraction in humans. *Int J Psychophysiol* 61:288–293.
- Schnitzler A, Gross J, Timmermann L (2000) Synchronised oscillations of the human sensorimotor cortex. *Acta Neurobiol Exp (Wars)* 60:271–287.
- Schoffelen J-M, Oostenveld R, Fries P (2005) Neuronal coherence as a mechanism of effective corticospinal interaction. *Science* 308:111–113.
- Schoffelen J-M, Poort J, Oostenveld R, Fries P (2011) Selective movement preparation is subserved by selective increases in corticomuscular gamma-band coherence. *J Neurosci* 31:6750–6758.
- Sherlin LH, Arns M, Lubar J, Heinrich H, Kerson C, Strehl U, Serman MB (2011) Neurofeedback and basic learning theory: implications for research and practice. *J Neurotherapy* 15:292–304.
- Solodkin A, Hlustik P, Chen EE, Small SL (2004) Fine modulation in network activation during motor execution and motor imagery. *Cereb Cortex* 14:1246–1255.
- Ushiyama J, Katsu M, Masakado Y, Kimura A, Liu M, Ushiba J (2011a) Muscle fatigue-induced enhancement of corticomuscular coherence following sustained submaximal isometric contraction of the tibialis anterior muscle. *J Appl Physiol* 110:1233–1240.
- Ushiyama J, Suzuki T, Masakado Y, Hase K, Kimura A, Liu M, Ushiba J (2011b) Between-subject variance in the magnitude of corticomuscular coherence during tonic isometric contraction of the tibialis anterior muscle in healthy young adults. *J Neurophysiol* 106:1379–1388.
- van Ede F, Maris E (2013) Somatosensory demands modulate muscular beta oscillations, independent of motor demands. *J Neurosci* 33:10849–10857.
- Von Carlowitz-Ghori K, Bayraktaroglu Z, Hohlefeld FU, Losch F, Curio G, Nikulin VV (2014) Corticomuscular coherence in acute and chronic stroke. *Clin Neurophysiol* 125:1182–1191.
- Witte M, Patino L, Andrykiewicz A, Hepp-Reymond M-C, Kristeva R (2007) Modulation of human corticomuscular beta-range coherence with low-level static forces. *Eur J Neurosci* 26:3564–3570.
- Yang Q, Fang Y, Sun C-K, Siemionow V, Ranganathan VK, Khoshkhabi D, Davis MP, Walsh D, Sahgal V, Yue GH (2009) Weakening of functional corticomuscular coupling during muscle fatigue. *Brain Res* 1250:101–112.

6.1. Limitations and outlook

The study was the first to apply CMC in a neurofeedback paradigm. The results indicate an effect of voluntary control on CMC which was not influenced by motor output parameters.

Optimizing design parameters As this was the first study of this kind aiming at demonstrating the feasibility of CMC-based neurofeedback, the paradigm was not yet optimized for yielding the largest possible effect. The design parameters such as length, number and frequency of sessions, trial length and design of presentation (block design vs. random order of conditions) were set following experiences from previous CMC measurements and other neurofeedback studies. As already mentioned in the paper, the priority of the study was to ensure that concomitant factors did not contribute to the effect. Therefore, the choice of design parameters might have been suboptimal. Optimizing these parameters could give a larger effect, which was, though significant in the current study, not particularly pronounced. A motivational incentive/reward may also improve the effect of neurofeedback (Sherlin et al., 2011). Possibly, a online success rate as implemented in the BCI-type paradigm by Sacchet et al. (2012) could serve this purpose. Additionally, such a paradigm would have the advantage to provide individual learning curves.

Between-subject variability The current study showed a group effect of manipulating CMC strength; there was however a certain between-subject variability of CMC control. Figure 5 of the paper demonstrates these individual differences in voluntary control. This variability in control may be attributed to the so-called BCI-illiteracy phenomenon (Kober et al., 2013; Blankertz et al., 2010): some subjects are not able to learn voluntary control of brain signals; they could have diminished the group effect. Their existence does not argue against CMC-based neurofeedback, however it might be worthwhile to investigate individual success in learning the control of CMC. The current study included two conditions asking the subjects in random order to increase and decrease CMC strength. Changing between these two conditions does certainly increase task difficulty which may inhibit learning voluntary control of CMC in some subjects. An alternative design could include a sham-control group where feedback is unrelated to the neurophysiological parameter.

Lack of time effect Moreover, contrary to expectations, there was no effect of time, i.e. the difference between the two conditions did not increase in the course of the three sessions. Such an increased difference over time would be indicative of a learning effect and strengthen the evidence for a voluntary control of CMC. The lack of a time effect may be due to the choice of design which could have inhibited learning, e.g. a too large time interval between sessions or reduced motivation after the first session. Optimizing the design parameters may therefore not only lead to a larger effect but also to an increase over time. Further, there was also a large within-subject variability of CMC strength which may have obscured a small effect of time. Here, increasing the number of sessions could be a possibility to address this problem. In the current study, the number of sessions was a compromise due to the preparation time which may be reduced by using less electrodes (see below). Though there is no effect of time in the course of the three sessions, there still may be an effect of time within a session. Analysis of smaller data segments however did not confirm this assumption (data not shown). This may again be attributed to the large within-subject variability. In contrast to the neurofeedback task, there was an increase in CMC amplitude in the force-feedback task from the first to third session. This may be due to neurofeedback or motor adaptation, why, however an effect of time occurred only in the force-feedback task remains unclear.

Electrode setting A drawback of EEG experiments is that preparation is generally quite time-consuming. The study included three sessions per subjects; for each session more than sixty electrodes had to be prepared. Here, future studies could aim at reducing the number of electrodes without impairing CMC estimation significantly. Channel reduction could be adapted from approaches as already applied in BCI classification experiments (e.g. Sannelli et al., 2010; Arvaneh et al., 2011). Optimization based on multiple regression, as implemented in the R-CMC method, generally yields better results using more explanatory variables (here: number of EEG signals). Yet, the method still could be applied without significant loss to smaller but optimized electrode settings. Less electrodes (and therefore less preparation time), would also allow for more training sessions which instead could be shorter.

Computer-aided learning In the current study, the spatial filter used for online CMC estimation was obtained individually from the preceding offline training session. In neurofeedback the measure is neurophysiologically meaningful aiming at changes in the brain and behavioral correlates (in contrast to BCI classification aiming at controlling a device). Therefore, the computer system is not meant to closely adapt to the subject since the training of signal control has to remain on the subject's side to provoke changes in brain activity. This is particularly relevant e.g. in respect to stroke patients where one would like to achieve/enhance the involvement of specific cortical regions in establishing CMC. Nonetheless, adaptive online learning techniques (e.g. Vidaurre et al., 2010; Shenoy et al., 2006) could aid the subjects' learning, e.g. by updating spatial filters online to adjust for changes in the activity pattern associated with a higher CMC.

The objective to demonstrate voluntary control of CMC was achieved by the current study. In future, tuning the parameters of the design and CMC estimation may yield better effects.

Summary and Conclusion

7

The four papers constituting the work of my thesis were centered around phenomenon of CMC: paper I (Chapter 3) introduced the new detection method R-CMC, paper II (Chapter 4) investigated the relation of CMC to amplitude modulation of beta oscillations, paper III and IV (Chapters 5 and 6) were concerned with the more demanding detection of CMC in clinical data and in real-time application, respectively.

One main objective of this thesis was to optimally detect CMC in offline analysis as well during real-time CMC-neurofeedback. Paper I (Bayraktaroglu et al., 2011) introduced the newly developed procedure R-CMC for the extraction of spatial filters which allows to obtain the maximized coherence between cortical and muscle activity. R-CMC uses multiple regression where narrowly filtered EEG signals serve as predictors for EMG activity. This procedure includes the optimization for frequency and delay to find the highest coherence. The obtained regression coefficients were applied as spatial filters to data either offline (Papers I-IV) or online in neurofeedback on short-time intervals (Paper IV). In the latter case, spatial filters were trained on a measurement recorded prior to the neurofeedback. Another important aspect of paper I was related to the issue of EMG rectification: the EMG signal is commonly rectified prior to coherence analysis. However until recently its justification was neither thoroughly tested experimentally nor theoretically. In paper I, we also examined the effect of EMG rectification on CMC estimation with experimental data comparing different approaches including the R-CMC method mentioned above. In all approaches, rectification led to similar or significantly reduced CMC values arguing against the use of EMG rectification. The detrimental effect of EMG rectification for CMC estimation is in line with other recent theoretical and experimental studies (Farina et al., 2013; McClelland et al., 2012; Stegeman et al., 2010).

In addition to phase-locking between cortical and muscle activity as measured by CMC, in paper II (Bayraktaroglu et al., 2013) of this thesis we investigated how local neuronal

interaction in the motor cortex can be reflected in the local activity at the spinal cord (as indirectly measured on the basis of muscle activity). Generally, it is assumed that distant neuronal populations may interact with each other by synchronization of oscillatory activity (Schoffelen et al., 2005; Womelsdorf et al., 2007). Coherence between the two neuronal groups might reflect a mechanism of effective interaction. However, also synchronization within a local neuronal group might have consequences for neuronal interactions. The signal amplitude is modulated by the number of neurons in synchrony. We found a correlation of amplitude modulations between beta oscillations in the sensorimotor cortex and the hand muscle. These amplitude dynamics might convey additional information for corticomuscular interactions.

All of the few stroke-related CMC studies (Braun et al., 2007; Fang et al., 2009; Meng et al., 2009; Mima et al., 2001) were performed at the chronic stage, mostly at least one year after the stroke when many compensatory processes already took place (Rijntjes, 2006). Longitudinal CMC studies following stroke patients from acute to chronic period could provide new insight into the temporal evolution of corticomuscular interaction after stroke and add to the understanding of mechanisms underlying motor recovery. In paper III (von Carlowitz-Ghori et al., 2014) we demonstrated for the first time the changes in the dynamics of corticomuscular interaction both at acute and early chronic stage of stroke. In acute stroke, the CMC amplitude was larger on the unaffected side compared to the affected side and also larger compared to the unaffected side in the chronic period. Additionally, CMC peak frequencies on both sides were decreased in the acute period. The changes in CMC parameters in acute stroke could result from a temporary decrease in inhibition, which normalizes in the course of recovery. As all patients showed very good motor recovery, the modulation of CMC amplitude and frequency over time might thus reflect the process of motor recovery.

On the basis of the experiments for offline CMC detection, we developed a paradigm for online CMC monitoring which could be used as a visual neurofeedback in a novel rehabilitation approach for motor recovery: By means of EEG or fMRI, neurofeedback provides feedback of a subject's brain activity that is usually outside voluntary control because it cannot be consciously accessed. Given this access, subjects can learn to voluntarily control brain activity associated with a specific region/function. Sacchet et al. (2012) demonstrated that subjects could increase or decrease CMC by choosing between different motor behaviors associated with low or high coherence. However, it is not known whether (without changing motor behavior) CMC can be voluntarily modified by intrinsically learning to associate the CMC strength with a certain activation pattern using mental imagery. In paper IV (von Carlowitz-Ghori et al., 2015), we

showed that healthy people are able to voluntarily modify their CMC strength using neurofeedback independent of motor output parameters: the instantaneous CMC of a subject's motor action is visualized on a screen in form an increasing/decreasing bar, allowing to develop mental strategies and over the course of several days learning to influence the CMC strength. In perspective, these measurements could provide a basis for a novel motor rehabilitation approach in stroke patients: using CMC neurofeedback could allow associating CMC strength with certain motor commands, and thereby facilitating the process of motor recovery.

Although the four papers covered different aspects of corticospinal interaction, they complement each other. Several findings contributed to the subsequent publications directly or indirectly (and partially also vice versa) as illustrated in Figure 7.1:

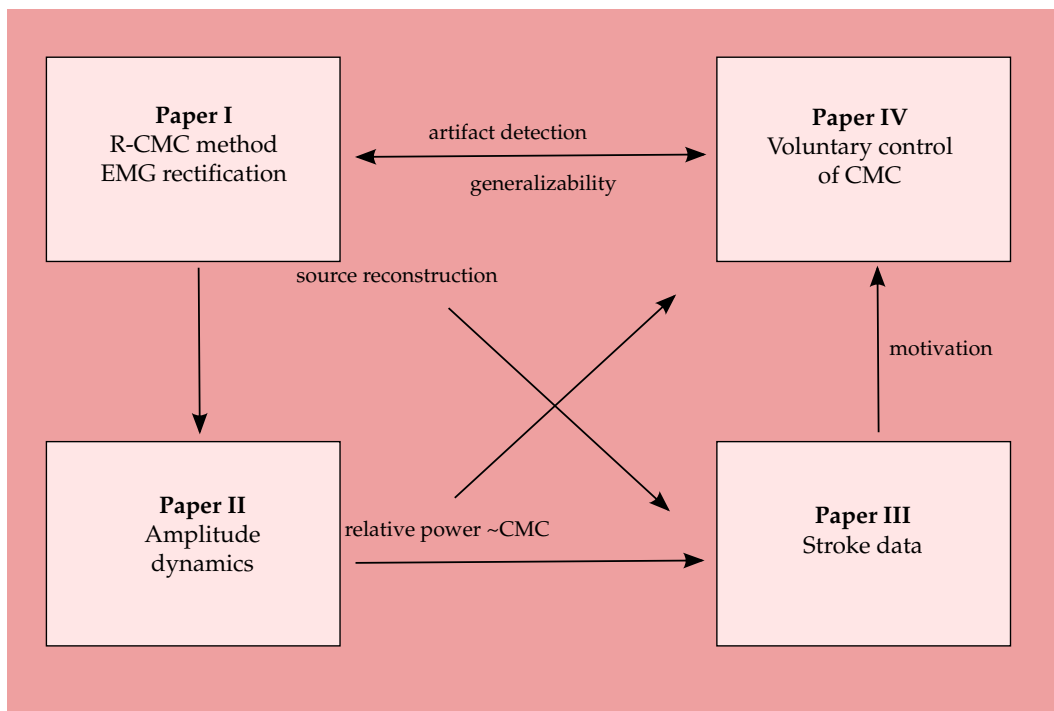


Figure 7.1.: Relation of the papers to each other

- First of all, the R-CMC method which was applied in all of studies after its advantages were apparent. This refers primarily to the better performance, i.e. larger CMC peak amplitudes, in comparison with other commonly used methods. One further advantage of the method is the possibility to use CMC topographies for source reconstruction which was of particular relevance in stroke data (paper

III) where sources contributing to corticospinal interactions might have been re-localized.

In addition, spatial patterns of CMC allowed to detect artifact-contamination due to volume conduction (e.g. from scalp or neck muscle activation) which applies especially to paper IV as muscle activity could have been used unintentionally to control the signal in neurofeedback.

- In return, paper IV confirmed the generalizability of the R-CMC method: spatial filters optimized on the previously recorded training data were applied for online feedback of CMC.
- The unfavorable effects of EMG rectification as demonstrated in paper I could be avoided by using the unrectified EMG signal in all subsequent analyses.
- After the relation between pre-stimulus relative spectral power (RSP) and CMC had been recognized in paper II, this knowledge could also support the findings in the papers III and IV by excluding a potentially confounding effect of the SNR on CMC estimation.
- The feasibility study of CMC-based neurofeedback in healthy subjects (paper IV) was motivated by its potential application in stroke patients (paper III) to facilitate motor recovery.
- Further mutual influences relate to parameter settings in the experimental design and analyses.

In conclusion, this thesis introduced the new method R-CMC for the optimized detection of CMC which could be applied in offline analysis for both normal subjects and stroke patients. Moreover, it demonstrates the voluntary manipulation of CMC through online feedback independent of motor output parameters.

Bibliography 8

- Amaral, D. G. (2012). Functional Organization of Perception and Movement. In Kandel, E. R., Schwartz, J. H., Jessell, T. M., Siegelbaum, S. A., and Hudspeth, A. J., editors, *Principles of Neural Science*. McGraw-Hill Publ.Comp., New York, 5th edition.
- Andrykiewicz, A., Patino, L., Naranjo, J. R., Witte, M., Hepp-Reymond, M.-C., and Kristeva, R. (2007). Corticomuscular synchronization with small and large dynamic force output. *BMC Neuroscience*, 8(1):101.
- Arvaneh, M., Guan, C., Ang, K. K., and Quek, C. (2011). Optimizing the Channel Selection and Classification Accuracy in EEG-Based BCI. *IEEE Transactions on Biomedical Engineering*, 58(6):1865–1873.
- Baker, M. R. and Baker, S. N. (2003). The effect of diazepam on motor cortical oscillations and corticomuscular coherence studied in man. *The Journal of Physiology*, 546(3):931–942.
- Baker, S. N. (2007). Oscillatory interactions between sensorimotor cortex and the periphery. *Current Opinion in Neurobiology*, 17(6):649–655.
- Baker, S. N., Kilner, J. M., Pinches, E. M., and Lemon, R. N. (1999). The role of synchrony and oscillations in the motor output. *Experimental Brain Research*, 128(1-2):109–117.
- Baker, S. N., Olivier, E., and Lemon, R. N. (1997). Coherent oscillations in monkey motor cortex and hand muscle EMG show task-dependent modulation. *The Journal of Physiology*, 501(1):225–241.
- Bayraktaroglu, Z., von Carlowitz-Ghori, K., Curio, G., and Nikulin, V. V. (2013). It is not all about phase: Amplitude dynamics in corticomuscular interactions. *NeuroImage*, 64:496–504.

8. Bibliography

- Bayraktaroglu, Z., von Carlowitz-Ghori, K., Losch, F., Nolte, G., Curio, G., and Nikulin, V. V. (2011). Optimal imaging of cortico-muscular coherence through a novel regression technique based on multi-channel EEG and un-rectified EMG. *NeuroImage*, 57(3):1059–1067.
- Blankertz, B., Sannelli, C., Halder, S., Hammer, E. M., Kübler, A., Müller, K.-R., Curio, G., and Dickhaus, T. (2010). Neurophysiological predictor of SMR-based BCI performance. *NeuroImage*, 51(4):1303–1309.
- Blankertz, B., Tomioka, R., Lemm, S., Kawanabe, M., and Müller, K.-R. (2008). Optimizing Spatial filters for Robust EEG Single-Trial Analysis. *IEEE Signal Processing Magazine*, 25(1):41–56.
- Boashash, B. (1992). Estimating and interpreting the instantaneous frequency of a signal. I. Fundamentals. *Proceedings of the IEEE*, 80(4):520–538.
- Boonstra, T. W. (2010). The nature of periodic input to the muscles. *Journal of Neurophysiology*, 104(1):576–576.
- Boonstra, T. W. and Breakspear, M. (2012). Neural mechanisms of intermuscular coherence: Implications for the rectification of surface electromyography. *Journal of Neurophysiology*, 107(3):796–807.
- Braun, C., Staudt, M., Schmitt, C., Preissl, H., Birbaumer, N., and Gerloff, C. (2007). Crossed cortico-spinal motor control after capsular stroke. *European Journal of Neuroscience*, 25(9):2935–2945.
- Brown, P., Salenius, S., Rothwell, J. C., and Hari, R. (1998). Cortical correlate of the piper rhythm in humans. *Journal of Neurophysiology*, 80(6):2911–2917.
- Burke, R. E. (1975). Motor unit properties and selective involvement in movement. *Exercise and Sport Sciences Reviews*, 3:31–81.
- Campfens, S. F., Kooij, H. v. d., and Schouten, A. C. (2013). Face to phase: pitfalls in time delay estimation from coherency phase. *Journal of Computational Neuroscience*, 37(1):1–8.
- Caviness, J. N., Adler, C. H., Sabbagh, M. N., Connor, D. J., Hernandez, J. L., and Lagerlund, T. D. (2003). Abnormal corticomuscular coherence is associated with the small amplitude cortical myoclonus in Parkinson’s disease. *Movement Disorders*, 18(10):1157–1162.

8. Bibliography

- Caviness, J. N., Shill, H. A., Sabbagh, M. N., Evidente, V. G., Hernandez, J. L., and Adler, C. H. (2006). Corticomuscular coherence is increased in the small postural tremor of parkinson's disease. *Movement Disorders*, 21(4):492–499.
- Chakarov, V., Naranjo, J. R., Schulte-Mönting, J., Omlor, W., Huethe, F., and Kristeva, R. (2009). Beta-range EEG-EMG coherence with isometric compensation for increasing modulated low-level forces. *Journal of Neurophysiology*, 102(2):1115–1120.
- Christou, E. A. and Neto, O. P. (2010). Reply to boonstra: The nature of periodic input to the muscle. *Journal of Neurophysiology*, 104(1):577–577.
- Conway, B. A., Halliday, D. M., Farmer, S. F., Shahani, U., Maas, P., Weir, A. I., and Rosenberg, J. R. (1995). Synchronization between motor cortex and spinal motoneuronal pool during the performance of a maintained motor task in man. *The Journal of Physiology*, 489(Pt 3):917–924.
- Dähne, S., Meinecke, F. C., Haufe, S., Höhne, J., Tangermann, M., Müller, K.-R., and Nikulin, V. V. (2014). SPoC: A novel framework for relating the amplitude of neuronal oscillations to behaviorally relevant parameters. *NeuroImage*, 86:111–122.
- Dakin, C. J., Dalton, B. H., Luu, B. L., and Blouin, J.-S. (2014). Rectification is required to extract oscillatory envelope modulation from surface electromyographic signals. *Journal of Neurophysiology*, 112(7):1685–1691.
- De Lange, F. P., Jensen, O., Bauer, M., Toni, I., Lange, F. P. d., Jensen, O., Bauer, M., and Toni, I. (2008). Interactions between posterior gamma and frontal alpha/beta oscillations during imagined actions. *Frontiers in Human Neuroscience*, 2:7.
- Dum, R. P. and Strick, P. L. (2002). Motor areas in the frontal lobe of the primate. *Physiology & Behavior*, 77(4-5):677–682.
- Engel, A. K. and Fries, P. (2010). Beta-band oscillations – signalling the status quo? *Current Opinion in Neurobiology*, 20(2):156–165.
- Enoka, R. M. and Pearson, K. G. (2012). The Motor Unit and Muscle Action. In Kandel, E. R., Schwartz, J. H., Jessell, T. M., Siegelbaum, S. A., and Hudspeth, A. J., editors, *Principles of Neural Science*. McGraw-Hill Publ.Comp., New York, 5th edition.
- Fang, Y., Daly, J. J., Sun, J., Hovorac, K., Fredrickson, E., Pundik, S., Sahgal, V., and Yue, G. H. (2009). Functional corticomuscular connection during reaching is weakened following stroke. *Clinical Neurophysiology*, 120(5):994–1002.

8. Bibliography

- Farina, D., Negro, F., and Jiang, N. (2013). Identification of common synaptic inputs to motor neurons from the rectified electromyogram. *The Journal of Physiology*, 591(Pt 10):2403–2418.
- Farmer, S. F. and Halliday, D. M. (2014). Reply to McClelland et al.: EMG rectification and coherence analysis. *Journal of Neurophysiology*, 111(5):1151–1152.
- Fisher, R. J., Galea, M. P., Brown, P., and Lemon, R. N. (2002). Digital nerve anaesthesia decreases EMG-EMG coherence in a human precision grip task. *Experimental Brain Research*, 145(2):207–214.
- Freund, H. J. (1983). Motor unit and muscle activity in voluntary motor control. *Physiological Reviews*, 63(2):387–436.
- Gerloff, C., Braun, C., Staudt, M., Hegner, Y. L., Dichgans, J., and Krägeloh-Mann, I. (2006). Coherent corticomuscular oscillations originate from primary motor cortex: Evidence from patients with early brain lesions. *Human Brain Mapping*, 27(10):789–798.
- Gray, C. M., König, P., Engel, A. K., and Singer, W. (1989). Oscillatory responses in cat visual cortex exhibit inter-columnar synchronization which reflects global stimulus properties. *Nature*, 338(6213):334–337.
- Graziadio, S., Basu, A., Tomasevic, L., Zappasodi, F., Tecchio, F., and Eyre, J. A. (2010). Developmental tuning and decay in senescence of oscillations linking the corticospinal system. *The Journal of Neuroscience*, 30(10):3663–3674.
- Graziadio, S., Tomasevic, L., Assenza, G., Tecchio, F., and Eyre, J. (2012). The myth of the ‘unaffected’ side after unilateral stroke: Is reorganisation of the non-infarcted corticospinal system to re-establish balance the price for recovery? *Experimental Neurology*, 238(2):168–175.
- Grosse, P. and Brown, P. (2005). Corticomuscular and Intermuscular Frequency Analysis: Physiological Principles and Applications in Disorders of the Motor System. In Niedermeyer, E. and Silva, F. H. L. d., editors, *Electroencephalography: Basic Principles, Clinical Applications, and Related Fields*. Lippincott Williams & Wilkins.
- Grosse, P., Guerrini, R., Parmeggiani, L., Bonanni, P., Pogosyan, A., and Brown, P. (2003). Abnormal corticomuscular and intermuscular coupling in high-frequency rhythmic myoclonus. *Brain*, 126(2):326–342.

8. Bibliography

- Halliday, D. M., Conway, B. A., Farmer, S. F., and Rosenberg, J. R. (1998). Using electroencephalography to study functional coupling between cortical activity and electromyograms during voluntary contractions in humans. *Neuroscience Letters*, 241(1):5–8.
- Halliday, D. M. and Farmer, S. F. (2010). On the need for rectification of surface EMG. *Journal of Neurophysiology*, 103(6):3547–3547.
- Haufe, S., Meinecke, F., Görgen, K., Dähne, S., Haynes, J.-D., Blankertz, B., and Bießmann, F. (2014). On the interpretation of weight vectors of linear models in multivariate neuroimaging. *NeuroImage*, 87:96–110.
- Hesterberg, T., Moore, D. S., Monaghan, S., Clipson, A., and Epstein, R. (2005). Bootstrap methods and permutation tests. *Introduction to the Practice of Statistics*, 5:1–70.
- Hjorth, B. (1975). An on-line transformation of EEG scalp potentials into orthogonal source derivations. *Electroencephalography and Clinical Neurophysiology*, 39(5):526–530.
- Hoerl, A. E. and Kennard, R. W. (1970). Ridge Regression: Biased Estimation for Nonorthogonal Problems. *Technometrics*, 12(1):55–67.
- James, L. M., Halliday, D. M., Stephens, J. A., and Farmer, S. F. (2008). On the development of human corticospinal oscillations: age-related changes in EEG-EMG coherence and cumulant. *European Journal of Neuroscience*, 27(12):3369–3379.
- Jolliffe, I. T. (2002). *Principal Component Analysis*. Springer Series in Statistics, New York, 2nd edition.
- Kalaska, J. F. and Rizzolatti, G. (2012). Voluntary Movement: The Primary Motor Cortex. In Kandel, E. R., Schwartz, J. H., Jessell, T. M., Siegelbaum, S. A., and Hudspeth, A. J., editors, *Principles of Neural Science*. Mcgraw-Hill Publ.Comp., New York, 5th edition.
- Kamp, D., Krause, V., Butz, M., Schnitzler, A., and Pollok, B. (2011). Changes of corticomuscular coherence: an early marker of healthy aging? *AGE*, 35(1):49–58.
- Kanazawa, H., Kawai, M., Kinai, T., Iwanaga, K., Mima, T., and Heike, T. (2014). Cortical muscle control of spontaneous movements in human neonates. *European Journal of Neuroscience*, 40(3):2548–2553.

8. Bibliography

- Kilner, J. M., Baker, S. N., Salenius, S., Hari, R., and Lemon, R. N. (2000). Human cortical muscle coherence is directly related to specific motor parameters. *The Journal of Neuroscience*, 20(23):8838–8845.
- Kilner, J. M., Baker, S. N., Salenius, S., Jousmäki, V., Hari, R., and Lemon, R. N. (1999). Task-dependent modulation of 15-30 hz coherence between rectified EMGs from human hand and forearm muscles. *The Journal of Physiology*, 516(2):559–570.
- Kilner, J. M., Fisher, R. J., and Lemon, R. N. (2004). Coupling of oscillatory activity between muscles is strikingly reduced in a deafferented subject compared with normal controls. *Journal of Neurophysiology*, 92(2):790–796.
- Kober, S. E., Witte, M., Ninaus, M., Neuper, C., and Wood, G. (2013). Learning to modulate one's own brain activity: the effect of spontaneous mental strategies. *Frontiers in Human Neuroscience*, 7:695.
- Koles, Z. J. (1991). The quantitative extraction and topographic mapping of the abnormal components in the clinical EEG. *Electroencephalography and clinical Neurophysiology*, 79(6):440–447.
- Kopell, N., Ermentrout, G. B., Whittington, M. A., and Traub, R. D. (2000). Gamma rhythms and beta rhythms have different synchronization properties. *Proceedings of the National Academy of Sciences*, 97(4):1867–1872.
- Kristeva-Feige, R., Fritsch, C., Timmer, J., and Lücking, C.-H. (2002). Effects of attention and precision of exerted force on beta range EEG-EMG synchronization during a maintained motor contraction task. *Clinical Neurophysiology*, 113(1):124–131.
- Lattari, E., Velasques, B., Paes, F., Cunha, M., Budde, H., Basile, L., Cagy, M., Piedade, R., Machado, S., and Ribeiro, P. (2010). Corticomuscular coherence behavior in fine motor control of force: a critical review. *Revista de neurologia*, 51(10):610–623.
- Lemon, R. N. (2008). Descending Pathways in Motor Control. *Annual Review of Neuroscience*, 31(1):195–218.
- MacKay, W. A. (1997). Synchronized neuronal oscillations and their role in motor processes. *Trends in Cognitive Sciences*, 1(5):176–183.
- McClelland, V. M., Cvetkovic, Z., and Mills, K. R. (2012). Rectification of the EMG is an unnecessary and inappropriate step in the calculation of corticomuscular coherence. *Journal of Neuroscience Methods*, 205(1):190–201.

8. Bibliography

- McClelland, V. M., Cvetkovic, Z., and Mills, K. R. (2014). Inconsistent effects of EMG rectification on coherence analysis. *The Journal of Physiology*, 592(1):249–250.
- Mendez-Balbuena, I., Huethe, F., Schulte-Mönting, J., Leonhart, R., Manjarrez, E., and Kristeva, R. (2012). Corticomuscular coherence reflects interindividual differences in the state of the corticomuscular network during low-level static and dynamic forces. *Cerebral Cortex*, 22(3):628–638.
- Meng, F., Tong, K.-Y., Chan, S.-T., Wong, W.-W., Lui, K.-H., Tang, K.-W., Gao, X., and Gao, S. (2009). Cerebral plasticity after subcortical stroke as revealed by corticomuscular coherence. *IEEE Transactions on Neural Systems and Rehabilitation Engineering*, 17(3):234–243.
- Mezeiová, K. and Paluš, M. (2012). Comparison of coherence and phase synchronization of the human sleep electroencephalogram. *Clinical Neurophysiology*, 123(9):1821–1830.
- Mima, T. and Hallett, M. (1999a). Corticomuscular coherence: A review. *Journal of Clinical Neurophysiology November 1999*, 16(6):501–511.
- Mima, T. and Hallett, M. (1999b). Electroencephalographic analysis of cortico-muscular coherence: reference effect, volume conduction and generator mechanism. *Clinical Neurophysiology*, 110(11):1892–1899.
- Mima, T., Simpkins, N., Oluwatimilehin, T., and Hallett, M. (1999). Force level modulates human cortical oscillatory activities. *Neuroscience Letters*, 275(2):77–80.
- Mima, T., Toma, K., Koshy, B., and Hallett, M. (2001). Coherence between cortical and muscular activities after subcortical stroke. *Stroke*, 32(11):2597–2601.
- Monti, R. J., Roy, R. R., and Edgerton, V. R. (2001). Role of motor unit structure in defining function. *Muscle & Nerve*, 24(7):848–866.
- Müller, K.-R., Anderson, C. W., and Birch, G. E. (2003). Linear and nonlinear methods for brain-computer interfaces. *IEEE Transactions on Neural Systems and Rehabilitation Engineering*, 11(2):165–169.
- Muthukumaraswamy, S. D. and Singh, K. D. (2011). A cautionary note on the interpretation of phase-locking estimates with concurrent changes in power. *Clinical Neurophysiology*, 122(11):2324–2325.

8. Bibliography

- Myers, L., Lowery, M., O'Malley, M., Vaughan, C., Heneghan, C., St Clair Gibson, A., Harley, Y., and Sreenivasan, R. (2003). Rectification and non-linear pre-processing of EMG signals for cortico-muscular analysis. *Journal of Neuroscience Methods*, 124(2):157–165.
- Negro, F., Keenan, K., and Farina, D. (2015). Power spectrum of the rectified EMG: when and why is rectification beneficial for identifying neural connectivity? *Journal of Neural Engineering*, 12(3):036008.
- Neto, O. P. and Christou, E. A. (2010). Rectification of the EMG signal impairs the identification of oscillatory input to the muscle. *Journal of Neurophysiology*, 103(2):1093–1103.
- Nolte, G., Bai, O., Wheaton, L., Mari, Z., Vorbach, S., and Hallett, M. (2004). Identifying true brain interaction from EEG data using the imaginary part of coherency. *Clinical Neurophysiology*, 115(10):2292–2307.
- Omlor, W., Patino, L., Hepp-Reymond, M.-C., and Kristeva, R. (2007). Gamma-range corticomuscular coherence during dynamic force output. *NeuroImage*, 34(3):1191–1198.
- Parra, L., Alvino, C., Tang, A., Pearlmutter, B., Yeung, N., Osman, A., and Sajda, P. (2002). Linear spatial integration for single-trial detection in encephalography. *NeuroImage*, 17(1):223–230.
- Patino, L., Omlor, W., Chakarov, V., Hepp-Reymond, M.-C., and Kristeva, R. (2008). Absence of gamma-range corticomuscular coherence during dynamic force in a deaf-ferented patient. *Journal of Neurophysiology*, 99(4):1906–1916.
- Pearson, K. (1901). On lines and planes of closest fit to systems of points in space. *Philosophical Magazine Series 6*, 2(11):559–572.
- Perez, M. A., Lundbye-Jensen, J., and Nielsen, J. B. (2006). Changes in corticospinal drive to spinal motoneurons following visuo-motor skill learning in humans. *The Journal of Physiology*, 573(3):843–855.
- Pfurtscheller, G., Stancák Jr., A., and Neuper, C. (1996). Post-movement beta synchronization. a correlate of an idling motor area? *Electroencephalography and Clinical Neurophysiology*, 98(4):281–293.

8. Bibliography

- Pohja, M. and Salenius, S. (2003). Modulation of cortex-muscle oscillatory interaction by ischaemia-induced deafferentation. *Neuroreport*, 14(3):321–324.
- Pohja, M., Salenius, S., and Hari, R. (2005). Reproducibility of cortex-muscle coherence. *NeuroImage*, 26(3):764–770.
- Raethjen, J., Lindemann, M., Dümpelmann, M., Wenzelburger, R., Stolze, H., Pfister, G., Elger, C. E., Timmer, J., and Deuschl, G. (2002). Corticomuscular coherence in the 6-15 hz band: is the cortex involved in the generation of physiologic tremor? *Experimental Brain Research*, 142(1):32–40.
- Raethjen, J., Muthuraman, M., Kostka, A., Nahrwold, M., Hellriegel, H., Lorenz, D., and Deuschl, G. (2013). Corticomuscular coherence in asymptomatic first-degree relatives of patients with essential tremor. *Movement Disorders*, 28(5):679–682.
- Ramoser, H., Müller-Gerking, J., and Pfurtscheller, G. (2000). Optimal Spatial Filtering of Single Trial EEG During Imagined Hand Movement. *IEEE Transactions on Rehabilitation Engineering*, 8(4):441.
- Rathore, S. S., Hinn, A. R., Cooper, L. S., Tyroler, H. A., and Rosamond, W. D. (2002). Characterization of incident stroke signs and symptoms: findings from the atherosclerosis risk in communities study. *Stroke*, 33(11):2718–2721.
- Riddle, C., Baker, M. R., and Baker, S. N. (2004). The effect of carbamazepine on human corticomuscular coherence. *NeuroImage*, 22(1):333–340.
- Riddle, C. N. and Baker, S. N. (2005). Manipulation of peripheral neural feedback loops alters human corticomuscular coherence. *The Journal of Physiology*, 566(2):625–639.
- Riddle, C. N. and Baker, S. N. (2006). Digit displacement, not object compliance, underlies task dependent modulations in human corticomuscular coherence. *NeuroImage*, 33(2):618–627.
- Rijntjes, M. (2006). Mechanisms of recovery in stroke patients with hemiparesis or aphasia: new insights, old questions and the meaning of therapies. *Current opinion in neurology*, 19(1):76–83.
- Rizzolatti, G. and Luppino, G. (2001). The Cortical Motor System. *Neuron*, 31(6):889–901.

8. Bibliography

- Rosenblum, M., Pikovsky, A., Kurths, J., Sch" afer, C., and Tass, P. A. (2001). Chapter 9 phase synchronization: From theory to data analysis. In Moss, F. and Gielen, S., editors, *Handbook of Biological Physics*, volume 4 of *Neuro-Informatics and Neural Modelling*, pages 279–321. North-Holland.
- Rossiter, H. E., Eaves, C., Davis, E., Boudrias, M.-H., Park, C.-h., Farmer, S., Barnes, G., Litvak, V., and Ward, N. S. (2013). Changes in the location of cortico-muscular coherence following stroke. *NeuroImage: Clinical*, 2:50–55.
- Sacchet, M. D., Sitaram, R., Braun, C., Birbaumer, N., and Fetz, E. (2012). Volitional control of neuromagnetic coherence. *Frontiers in Neuroprosthetics*, 6:189.
- Safri, N. M., Murayama, N., Hayashida, Y., and Igasaki, T. (2007). Effects of concurrent visual tasks on cortico-muscular synchronization in humans. *Brain Research*, 1155:81–92.
- Safri, N. M., Murayama, N., Igasaki, T., and Hayashida, Y. (2006). Effects of visual stimulation on cortico-spinal coherence during isometric hand contraction in humans. *International Journal of Psychophysiology*, 61(2):288–293.
- Salenius, S., Portin, K., Kajola, M., Salmelin, R., and Hari, R. (1997). Cortical control of human motoneuron firing during isometric contraction. *Journal of Neurophysiology*, 77(6):3401–3405.
- Salenius, S., Salmelin, R., Neuper, C., Pfurtscheller, G., and Hari, R. (1996). Human cortical 40 hz rhythm is closely related to EMG rhythmicity. *Neuroscience Letters*, 213(2):75–78.
- Sannelli, C., Dickhaus, T., Halder, S., Hammer, E.-M., Müller, K.-R., and Blankertz, B. (2010). On optimal channel configurations for SMR-based brain-computer interfaces. *Brain Topography*, 23(2):186–193.
- Sağlam, M., Matsunaga, K., Murayama, N., Hayashida, Y., Huang, Y.-Z., and Nakanishi, R. (2008). Parallel inhibition of cortico-muscular synchronization and cortico-spinal excitability by theta burst TMS in humans. *Clinical Neurophysiology*, 119(12):2829–2838.
- Schnitzler, A., Salenius, S., Salmelin, R., Jousmäki, V., and Hari, R. (1997). Involvement of Primary Motor Cortex in Motor Imagery: A Neuromagnetic Study. *NeuroImage*, 6(3):201–208.

8. Bibliography

- Schoffelen, J.-M., Oostenveld, R., and Fries, P. (2005). Neuronal coherence as a mechanism of effective corticospinal interaction. *Science*, 308(5718):111–113.
- Schoffelen, J.-M., Poort, J., Oostenveld, R., and Fries, P. (2011). Selective movement preparation is subserved by selective increases in corticomuscular gamma-band coherence. *The Journal of Neuroscience*, 31(18):6750–6758.
- Shenoy, P., Krauledat, M., Blankertz, B., Rao, R. P. N., and Müller, K.-R. (2006). Towards adaptive classification for BCI. *Journal of Neural Engineering*, 3(1):R13.
- Sherlin, L. H., Arns, M., Lubar, J., Heinrich, H., Kerson, C., Strehl, U., and Serman, M. B. (2011). Neurofeedback and basic learning theory: Implications for research and practice. *Journal of Neurotherapy*, 15(4):292–304.
- Siemionow, V., Sahgal, V., and Yue, G. H. (2010). Single-trial EEG-EMG coherence analysis reveals muscle fatigue-related progressive alterations in corticomuscular coupling. *IEEE Transactions on Neural Systems and Rehabilitation Engineering*, 18(2):97–106.
- Steg, C. v. d., Daffertshofer, A., Stegeman, D. F., and Boonstra, T. W. (2014). High-density surface electromyography improves the identification of oscillatory synaptic inputs to motoneurons. *Journal of Applied Physiology*, 116(10):1263–1271.
- Stegeman, D. F., van de Ven, W. J. M., van Elswijk, G. A., Oostenveld, R., and Kleine, B. U. (2010). The alpha-motoneuron pool as transmitter of rhythmicities in cortical motor drive. *Clinical Neurophysiology*, 121(10):1633–1642.
- Tecchio, F., Porcaro, C., Zappasodi, F., Pesenti, A., Ercolani, M., and Rossini, P. M. (2006). Cortical short-term fatigue effects assessed via rhythmic brain-muscle coherence. *Experimental Brain Research*, 174(1):144–151.
- Tibshirani, R. (1996). Regression Shrinkage and Selection via the Lasso. *Journal of the Royal Statistical Society. Series B (Methodological)*, 58(1):267–288.
- Tomioka, R., Dornhege, G., Nolte, G., Blankertz, B., Aihara, K., and Müller, K.-R. (2006). Spectrally weighted common spatial pattern algorithm for single trial EEG classification. *Dept. Math. Eng., Univ. Tokyo, Tokyo, Japan*, Tech. Report 40.
- Ushiyama, J., Katsu, M., Masakado, Y., Kimura, A., Liu, M., and Ushiba, J. (2011a). Muscle fatigue-induced enhancement of corticomuscular coherence following sustained submaximal isometric contraction of the tibialis anterior muscle. *Journal of Applied Physiology*, 110(5):1233–1240.

8. Bibliography

- Ushiyama, J., Suzuki, T., Masakado, Y., Hase, K., Kimura, A., Liu, M., and Ushiba, J. (2011b). Between-subject variance in the magnitude of corticomuscular coherence during tonic isometric contraction of the tibialis anterior muscle in healthy young adults. *Journal of Neurophysiology*, 106(3):1379–1388.
- Varela, F., Lachaux, J.-P., Rodriguez, E., and Martinerie, J. (2001). The brainweb: Phase synchronization and large-scale integration. *Nature Reviews Neuroscience*, 2(4):229–239.
- Vidaurre, C., Sannelli, C., Müller, K.-R., and Blankertz, B. (2010). Machine-Learning-Based Coadaptive Calibration for Brain-Computer Interfaces. *Neural Computation*, 23(3):791–816.
- von Carlowitz-Ghori, K., Bayraktaroglu, Z., Hohlefeld, F. U., Losch, F., Curio, G., and Nikulin, V. V. (2014). Corticomuscular coherence in acute and chronic stroke. *Clinical Neurophysiology*, 125(6):1182–1191.
- von Carlowitz-Ghori, K., Bayraktaroglu, Z., Waterstraat, G., Curio, G., and Nikulin, V. V. (2015). Voluntary control of corticomuscular coherence through neurofeedback: A proof-of-principle study in healthy subjects. *Neuroscience*, 290:243–254.
- von Carlowitz-Ghori, K. M. B., Hohlefeld, F. U., Bayraktaroglu, Z., Curio, G., and Nikulin, V. V. (2011). Effect of complete stimulus predictability on p3 and n2 components: an electroencephalographic study. *Neuroreport*, 22(9):459–463.
- Ward, N. J., Farmer, S. F., Berthouze, L., and Halliday, D. M. (2013). Rectification of EMG in low force contractions improves detection of motor unit coherence in the beta-frequency band. *Journal of Neurophysiology*, 110(8):1744–1750.
- Welch, P. (1967). The use of fast fourier transform for the estimation of power spectra: A method based on time averaging over short, modified periodograms. *IEEE Transactions on Audio and Electroacoustics*, 15:70–73.
- Witte, M., Patino, L., Andrykiewicz, A., Hepp-Reymond, M.-C., and Kristeva, R. (2007). Modulation of human corticomuscular beta-range coherence with low-level static forces. *The European journal of neuroscience*, 26(12):3564–3570.
- Womelsdorf, T., Schoffelen, J.-M., Oostenveld, R., Singer, W., Desimone, R., Engel, A. K., and Fries, P. (2007). Modulation of neuronal interactions through neuronal synchronization. *Science*, 316(5831):1609–1612.

8. Bibliography

Yang, Q., Fang, Y., Sun, C.-K., Siemionow, V., Ranganathan, V. K., Khoshknabi, D., Davis, M. P., Walsh, D., Sahgal, V., and Yue, G. H. (2009). Weakening of functional corticomuscular coupling during muscle fatigue. *Brain Research*, 1250:101–112.

Acronyms

- AP** action potential.
- APB** abductor pollicis brevis.
- BCI** brain-computer interface.
- CMC** corticomuscular coherence.
- CV** coefficient of variation.
- EEG** electroencephalography.
- EMG** electromyography.
- ERD** event-related desynchronization.
- GABA** gamma aminobutyric acid.
- LFP** local field potential.
- MEG** magnetoencephalography.
- MU** motor unit.
- MUAP** motor unit action potential.
- MVC** maximum voluntary contraction.
- PCA** principal component analysis.
- PTN** pyramidal tract neurons.
- R-CMC** regression corticomuscular coherence.

Acronyms

RSP relative spectral power.

SD standard deviation.

SEM standard error of the mean.

SI phase synchronization index.

SNR signal-to-noise ratio.

List of Figures

1.1. Coherence spectrum	1
1.2. Objectives	4
2.1. Pyramidal decussation and the formation of the corticospinal tract in the spinal cord	9
2.2. EMG signal during voluntary muscle contraction	10
2.3. Frequency bands of the EEG signal	11
2.4. Coherence of two oscillatory signals	13
2.5. Distribution of phase difference between EEG and EMG processes	14
2.6. Amplitude and phase of signals	16
2.7. Local synchronization	16
2.8. Amplitude envelope of an analytic signal	17
2.9. Ascending and descending pathways possibly mediating CMC	20
2.10. Effect of rectification on EMG power spectrum	24
2.11. Rectification of an amplitude-modulated signal	25
2.12. PCA procedure	27
2.13. PCA on EEG signals	28
2.14. Laplacian spatial filter	29
2.15. Spatial filters and patterns	30
2.16. Multiple linear regression	31
2.17. Collinearity	33
3.1. R-CMC method	35
4.1. Amplitude dynamics in corticomuscular interactions	50
4.2. Uncorrelated amplitude envelopes	50
7.1. Relation of the papers to each other	92

List of Figures

A.1. Experimental setup	111
A.2. Isometric contraction	112
A.3. EMG recording from the APB muscle	112

Experimental setup A

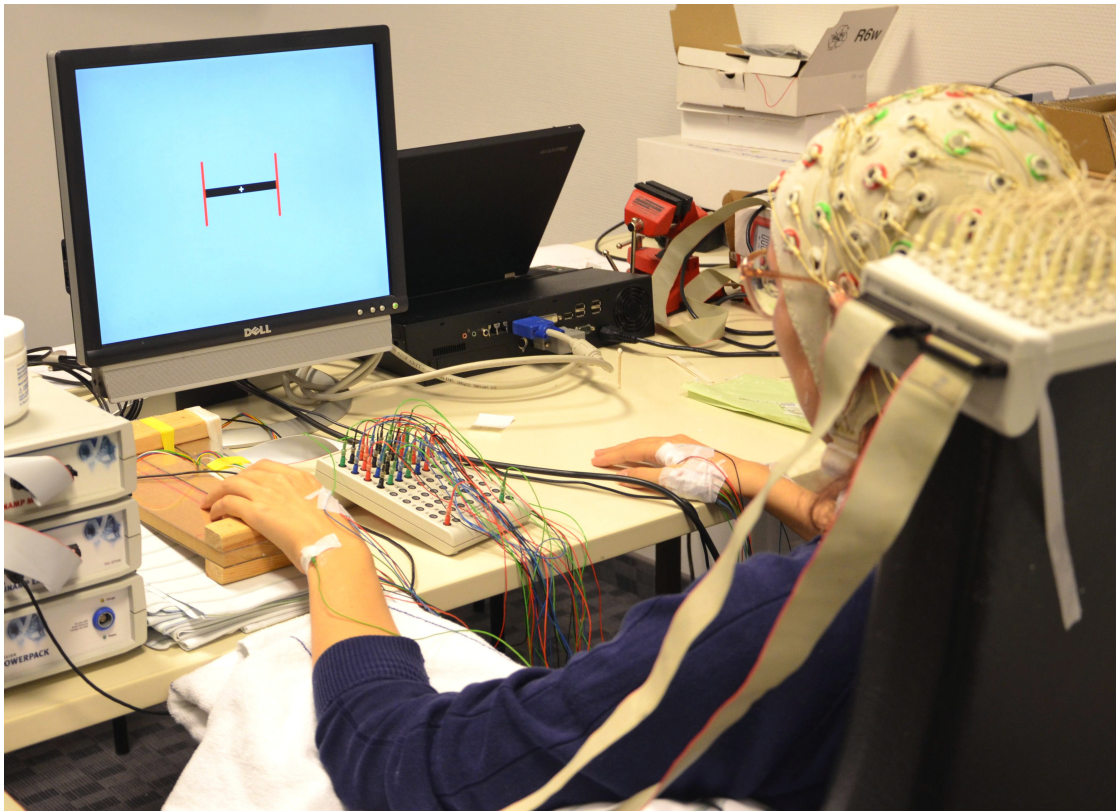


Figure A.1.: Experimental setup which only slightly varied between the studies. Subjects were measured in a comfortable sitting position except for stroke patients in the acute phase (see Chapter 5) who were measured in bed.

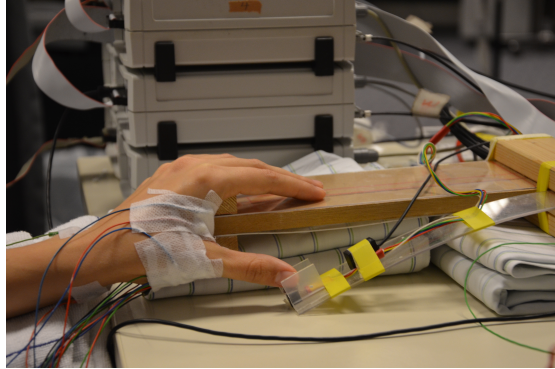


Figure A.2.: All subjects performed an isometric contraction following a movement. The task required them to press the lever of the apparatus down with their (right or left) thumb and then hold.

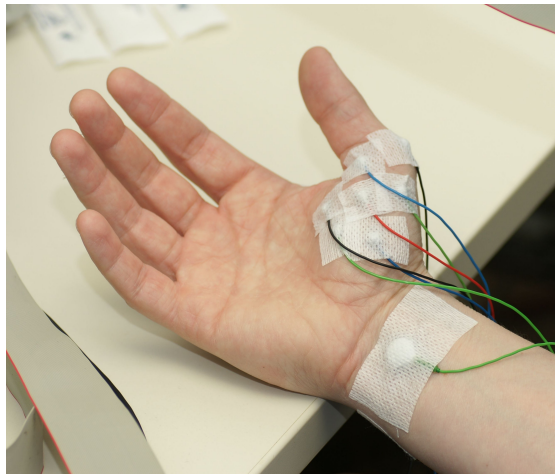


Figure A.3.: EMG was recorded from the abductor pollicis brevis (APB) muscle. The number of electrodes varied between the studies.